Soliton Excitations in Open Systems using GPGPU Supercomputing

André L. Almeida
Mestrado Integrado em Engenharia Física
Departamento de Física e Astronomia
2018

Orientador
Professor Doutor Ariel Guerreiro, Faculdade de Ciências

Coorientador
Dr. Nuno Azevedo Silva, Faculdade de Ciências

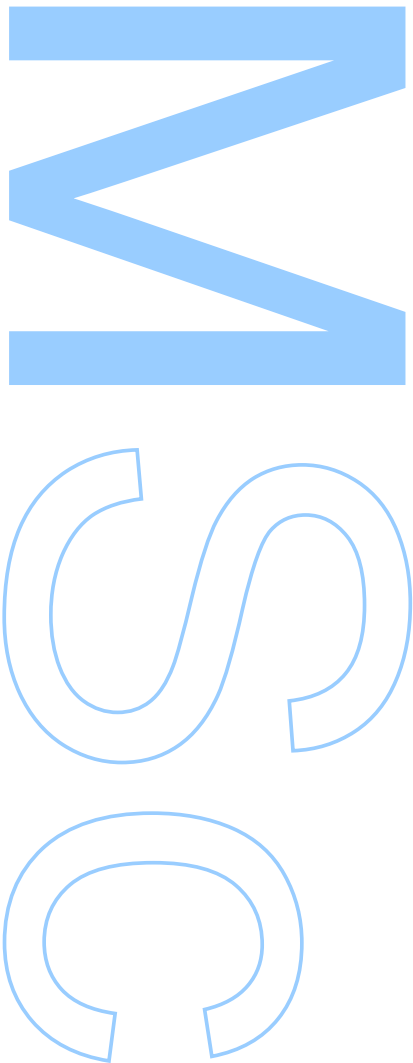

U.PORTO

FACULDADE DE CIÊNCIAS
UNIVERSIDADE DO PORTO

Todas as correções determinadas pelo júri, e só essas, foram efetuadas.

O Presidente do Júri,

Porto, _____/_____/_____

UNIVERSIDADE DO PORTO

MASTERS THESIS

Soliton Excitations in Open Systems using GPGPU Supercomputing

Author:
André ALMEIDA

Supervisor:
Professor Doutor Ariel GUERREIRO

Co-supervisor:
Dr. Nuno Azevedo SILVA

A thesis submitted in fulfilment of the requirements
for the degree of Master of Science

at the

Faculdade de Ciências
Departamento de Física e Astronomia

November 2018

$$0.99^{365} = 0.0026 \qquad 1.01^{365} = 37.8$$

" Start by doing what's necessary; then do what's possible; and suddenly you are doing the impossible. "

Francis Of Assisi

Acknowledgements

First and foremost I would like to thank my supervisor Professor Doctor Ariel Guerreiro and co-supervisor Nuno Silva for all of their work, motivation and inspiration throughout the past year. It has been a fantastic roller coaster between knowledge, experiences and personal development, and for that I am truly grateful.

Everyone that was able to extract a few good laughs from me, that with small actions performed as true heroes, making hours pass as fast as seconds. To both Tiagos, Simão, Margarida and Ludgero. Also to Juliana, Ana and Alexandra for their friendship and joyful moments.

I cannot stand out how important were those occasions of distraction provided by various books accompanied with a night coffee by Mr. Luís, also known as the best waiter ever. I also appreciate a less orthodox collective known as the City of Porto and every soul that planed and constructed it, and also everybody that walked this city and went away with a new *mark* on their mind.

It is with extreme gratitude that I acknowledge and thank Fábio, Cláudia and Paulo for their friendship, who every weekend, coffee or night out were able to send my mind to someplace far far away. To many others that guided me through younger years and, somehow, inspired me to be the person I am.

I also wish to thank my family for every opportunity, support and second of joy that they spent through all these years. My father Fernando, my mother Isabel and my little evil sister Sónia. I hope that the course I have been walking is able to give you a honored feeling.

Lastly, I want to specially express my gratitude to my girlfriend Beatriz for the encouragement, friendship, love and support in all good and even not so good moments. Without every talk, laughing and moment that we shared this whole journey would not be possible at all. At least not without maintaining my mental sanity.

UNIVERSIDADE DO PORTO

Abstract

Faculdade de Ciências

Departamento de Física e Astronomia

Master of Science

Soliton Excitations in Open Systems using GPGPU Supercomputing

by André ALMEIDA

This thesis investigates the stability of nonlinear excitations in open optical systems modeled by the Complex Ginzburg Landau Equation (CGLE) when influenced by effects such as dissipation and gain, using numerical simulations. This equation constitutes an extension of the notorious Generalized Nonlinear Schödinger Equation commonly used in optics to describe the propagation of light in nonlinear optical media, but its application extends well beyond this domain into fields such as Bose-Einstein Condensates and other Many-body Systems.

In particular, we have developed a numerical solver of the *CGLE* based on *GPGPU* Supercomputing and considered two complementary problems, namely the stability of dissipative solitons and the formation of Rogue-Waves. We have shown the possibility of obtaining stable Soliton-like solutions of the *CGLE*, called Dissipative Solitons and describing the propagation of light in atomic gases prepared by external coherent electromagnetic fields to exhibit strong nonlinear effects. These excitations extend the conventional notion of Soliton resulting from a balance between nonlinear effects and diffraction or dispersion, to include a second balance between gain and loss, and thus constitutes a more realistic description.

We have also applied the solver to explore the role of noise in the generation of Rogue-Waves governed by the *CGLE* and obtained surprising and counter-intuitive results, namely they suggest that the spectrum of these nonlinear waves is somewhat independent of the initial noise content of the signal and that the presence of strong noise has an inhibiting effect on the formation of Rogue-Waves.

UNIVERSIDADE DO PORTO

Resumo

Faculdade de Ciências

Departamento de Física e Astronomia

Mestre de Ciência

Excitações Solitónicas em Sistemas Abertos com Supercomputação GPGPU

por André ALMEIDA

Esta tese assenta na investigação de excitações nãolineares estáveis em sistemas óticos abertos descritos pela Equação Complexa Cúbica-Quintica de Ginzburg-Landau (*CGLE*), quando influenciada por vários efeitos. Estes efeitos podem ser dissipação e ganho, usando simulação numérica. Esta é uma extensão à célebre Equação de Schrödinger Nãolinear Generalizada usada frequentemente em ótica e capaz de descrever a propagação de luz em meios óticos nãolineares. Além disso, a sua aplicação alcança outros domínios como Condensados de Bose-Einstein e sistemas *many-body*, entre outros.

Em particular, fomos capazes de desenvolver um *solver* numérico da *CGLE* baseado em Supercomputação *GPGPU* e consideramos dois grandes problemas, sendo esses a estabilidade de Solitões Dissipativos e a formação de Rogue-Waves. Demonstramos a possibilidade de obter soluções Solitónicas estáveis à *CGLE* conhecidos como *Dissipative Solitons* que descrevem a propagação de luz em gases atómicos previamente preparados a partir de feixes electromagnéticos coerentes, de forma a exibirem nãolinearidades. Estas excitações extendem-se além da notação Solitónica resultantes de um balanço entre efeitos nãolineares e difração ou dispersão, passando a incluir também equilíbrio entre perdas e ganhos. Por estes motivos esta é uma melhor descrição que mais se assemelha a sistemas reais.

Além disso também aplicamos o nosso *solver* de forma a explorar o papel que o ruído tem na formação de Rogue-Waves em sistemas descritos pela *CGLE*. Em consequência obtivemos resultados surpreendentes e contra-intuitivos que sugerem que o espetro destas excitações nãolineares é de certa forma independente do ruído inicial e que a presença de maiores oscilações aleatórias tem um efeito inibidor na formação de Rogue-Waves.

Contents

List of Figures

List of Tables

Abbreviations

NLSE	Nonlinear Schrödinger Equation
GNLSE	Generalized Nonlinear Schrödinger Equation
CW	Continuous Wave
CGLE	Complex Cubic-Quintic Ginzburg-Landau Equation
GPGPU	General-Purpose Graphics Processing Unit
GPU	Graphics Processing Unit
CPU	Central Processing Unit
SVEA	Slow Varying Envelope Approximation
GVD	Group Velocity Dispersion
BS	Bright Soliton
TS	Temporal Soliton
SS	Spatial Soliton
API	Application Programming Interface
SSFM	Split-Step Fourier Method
FFT	Fast Fourier Transform
MBS	Maxwell-Bloch System
RW	Rogue-Wave
MI	Modulation Instability
PDF	Probabilistic Distribution Functions

In memory of

both my grandfathers. . .

Chapter 1

Introduction

1.1 State of the Art

Many phenomena in Nature are described by a nonlinear theory due to some nonlinear interactions, excitations or feedback [4–7]. In such cases we usually try to consider the larger amount of effects but discard some in the form of simplifications. Some of these are commonly related to losses and/or gain, which means that we turn out studying ideal isolated systems that neither gain nor lose energy[8]. We left out the realistic description of the phenomenon under study. However, when we introduce such effects that were overlooked many known results become inaccurate and require a revaluation of their validity[8]. This is the main problem under the scope of this thesis: we desire to understand how the results of nonlinear physics adapt in situations of open dissipative systems subject to many different gain and loss mechanisms, either linear and nonlinear. We start by focusing in the Nonlinear Schrödinger Equation which is an effective equation that describes many *idealized* systems[9] to then introduce higher nonlinear effects and terms related to non-Hamiltonian effects, in a more general model usually known as the Complex Cubic-Quintic Ginzburg-Landau Equation[10, 11].

Moreover, the course of this thesis follows an interesting path towards the specific problem of stability *vs* instability. In the former we evaluate the well known Soliton solutions that are nonlinear excitations with a very specific shape and proprieties, for example the collision of two solitons apparent to have no interaction between the involved excitations[12]. Furthermore, the case of instability is also interesting where we have nonlinear activity in the form of Rogue-Waves[13]. In the context of Optics, these are very short optical pulses that appear from nowhere with enormous amplitude and quickly

disappear leaving no trace behind. These excitations have a very short life-time when compared to the background time-scale[14]. We are interested in study both these opposite extremes in this thesis.

In order to develop insight about the mentioned cases we apply a methodology based in simulations since experimental observations of both these effects is notoriously difficult and the study of some statistical characteristics is important. Because Rogue-Waves are so short[15] we need to simulate with very high resolution in order to detect the maximum of detail about its behavior. Also this is an highly complex problem that needs to be simulated in a substantial scale with many concurrent effects. Since we are interested in statistical analysis we require the largest amount of data possible to be generated in the shortest amount of time. With this in mind we decided to develop a *GPGPU* Supercomputing solver based in Graphics Cards. This became a nuclear part of this thesis due its complexity.

Soliton solutions are well known in the field of Nonlinear Physics, namely Nonlinear Optics, since they appear in various systems described by the Nonlinear Schrödinger Equation[16]. The family of Solitons is immense with many shapes, characteristics and proprieties neither this is the first time that Solitons are considered in open dissipative systems[17, 18]. An interesting case of these nonlinear excitations are known as Auto-Solitons, that are capable of maintain their shape in open systems[12]. However, in dissipative situations there is an available interesting situation where the balance of the various concurrent effects such as nonlinearities and dispersion/diffraction, and gain with losses provide a mean to stationary propagation. There is also a constant interaction between the various terms and the dual nature here presented is characteristic of unstable equilibrium and we must be very careful in order to maintain the Solitonic solution balanced[11].

On the other hand of the *stability spectrum* are the Rogue-Waves with their chaotic aspect and appearance in nonlinear dissipative systems also described by the Complex Cubic-Quintic Ginzburg-Landau Equation[19, 20]. These are very mysterious phenomena since they occur mystifyingly and we yet unknown all activation mechanisms as well how nonlinearities, dissipation and sources operate and recombine to result in such spiky excitation[21]. We hope to develop some insight regarding this subject and evaluate how the conditions of the optical system can influence the behavior of Rogue-Waves. Moreover, there are some indications that the noise of the background can influence the propagation proprieties and we aspire to study this problem, namely how the random

background probabilistic distribution function and amplitude influences the proprieties of such system.

1.2 Structure of the Thesis

This thesis is organized in 6 chapters. The following Chapter presents the fundamental of nonlinear optics and its development towards the topics that elucidates in the previous section. From Linear Optics to the Nonlinear Schrödinger Equation with a development of both Slow Varying Envelope Approximation and Paraxial Approximation, followed then by the Constants of Motion of such systems. The limitations of the *NLSE* are presented and provided an efficient development to the Complex Cubic-Quintic Ginzburg-Landau Equation.

Later on in Chapter 3 we present a brief history of computing power and how it has evolved throughout the years. The main steps considered when developing our *GPGPU* Supercomputing solver are provided followed by its characterization of *SpeedUp*s compared to a high-end CPU, as well a physical testbed to evaluate the outputs and compare them to expected results and to the literature.

Chapter 4 describes the application of our solver to a very complex nonlinear atomic system that allows dissipative Bright Solitons to propagate with equilibrium. Whether if the nonlinearities are able to balance the dispersion effects and the limitations capable of destroying this steady propagation are shown with simulations and compared to known dissipative Bright Dissipative Solitonic solution. Lastly we shortly study the conditions of stability of both the Dissipative Soliton and of the background.

Finally, Chapter 5 presents analytical Breathers that are solution to the *NLSE* and/or *CGLE*, followed by the exploration of Rogue-Waves in nonlinear materials. We then develop two very interesting computational experiments to evaluate how the noise input signal affects the long run proprieties. We explored both the impact of the random background probabilistic distribution function and its initial amplitude.

Chapter 6 provides some conclusion and possible future work to follow the very promising hot topics of this thesis.

1.3 Outputs

During the course of this masters, the author has contributed to the scientific community with 1 *submitted article ;* 1 *inproceedings conference paper ;* 9 *oral presentations, of which 3 as speaker ;* 21 *poster presentations, of which* 6 *as first author (*2 *of them internationally).*

The list of works as a result of this masters is:

- Submitted Article

- Nuno A. Silva, A. L. Almeida, and A. Guerreiro (2018), *"Slow-light dissipative solitons in an atomic medium in a waveguide assisted by an incoherent pumping field"*. Physical Review A. - [*submitted*].

- Inproceedings Conference Article

- Silva, N. A., Almeida, A. L., Costa, J. C., Gomes, M., Alves, R. A., & Guerreiro, A. (2017, August). *Dissipative solitons in 4-level atomic optical systems*. In Third International Conference on Applications of Optics and Photonics (Vol. 10453, p. 104531C). International Society for Optics and Photonics.

- Talk Presentations

- A. L. Almeida; *"GPGPU Super-simulations observing Rogue Waves in a dissipative nonlinear optical medium"*, FISICA 2018, Sociedade Portuguesa da Física, Covilhã, Portugal, (2018)

- A. L. Almeida; *"Solving Dissipative Nonlinear Schrödinger Equation and predicting Rogue-Waves with GPGPU supercomputing"*, CAP Talk Series 2018, UP-SPIE Student Chapter, Porto, Portugal, (2018)

- A. L. Almeida, Tiago D. Ferreira, Inês S. Madureira, André Pereira, Nuno A. Silva, Ariel Guerreiro; *"Solving Dissipative Nonlinear Schrödinger Equation with GPGPU supercomputing"*, Encontro Nacional de Estudantes de Física 2018, Porto, Portugal, (2018)

- N. A. Silva, A. Almeida, André A. Pereira, I. Madureira, T. Ferreira ,A. Guerreiro; *"Tunable optical analogues using quantum optical systems"*, Nanoscale Quantum Optics Conference and MC Meeting, Prague, (February 2018).

- N. A. Silva, A. Almeida, André A. Pereira, I. Madureira, T. Ferreira, A. Guerreiro; *"Superfluidity of light in quantum optical systems"*, Nanoscale Quantum Optics - ESR Workshop COST Action MP1403, Braga, Portugal (September 2018).

- Tiago D. Ferreira, A. Almeida, André M. Pereira, I. Madureira, Nuno. A. Silva, A. Guerreiro; *"Using GPGPU supercomputing for Solving the Schrödinger-Newton equation"*, Encontro Nacional de Estudantes de Física 2018, Porto, (2018).

- Tiago D. Ferreira, A. Almeida, André M. Pereira, I. Madureira, Nuno. A. Silva, A. Guerreiro; *"The Schrödinger-Newton Equation: An Application for Studying Self-Defocusing Nematic Liquid Crystals Photon-Fluids"*, CAP Talk Series 2018, UP-SPIE Student Chapter, Porto, (2018).

- Inês S. Madureira, A. Pereira, Tiago Ferreira, André Almeida, N. A. Silva, A. Guerreiro; *"Towards using artificial intelligence in quantum physics"*, Encontro Nacional de Estudantes de Física 2018, Porto, (2018).

- André M. Pereira, I. Madureira, T. Ferreira, A. Almeida, N. A. Silva, A. Guerreiro; *"Nonlinear Fourier Transforms for the Analysis of Nonlinear Systems"*, Encontro Nacional de Estudantes de Física 2018, Porto, (2018).

• Poster Presentations

- A. L. Almeida, T. D. Ferreira, Nuno A. Silva, I. Madureira, A. Pereira, A. Guerreiro; *Dissipative Complex Cubic-Quintic Ginzburg-Landau Equation in Nonlinear Dissipative Propagation Phenomena*, FISICA 2018, Sociedade Portuguesa da Física, Covilhã, Portugal, (2018)

- A. L. Almeida, Nuno A. Silva, Tiago D. Ferreira, I. Madureira, A. Pereira, A. Guerreiro; *Predicting Unpredictable Extreme Events in Dissipative Nonlinear Optical Media with GPGPU Supercomputing*, XVI Jorge André Swieca School on Non linear and Quantum Optics, São Paulo, Brazil, (2018)

- A. L. Almeida, Nuno A. Silva, Tiago D. Ferreira, Inês S. Madureira, André Pereira, Ariel Guerreiro; *Rogue-Waves Counts as Noise Amplitude in Nonlinear Optical Propagation with GPGPU Super-simulations*, 3ª Jornadas em Engenharia Física, Física, Física Médica e Astronomia 2018, Porto, (2018)

- A. L. Almeida, Tiago D. Ferreira, Inês S. Madureira, André Pereira, Nuno A. Silva, Ariel Guerreiro; *Numerical Simulations of Photonic Crystals Bandgap in a 2D Dielectric Rectangular Grid*, Encontro Nacional de Estudantes de Física 2018, Porto, Portugal, (2018)

- A. L. Almeida, Nuno A. Silva, T. D. Ferreira, I. Madureira, A. Pereira, A. Guerreiro; *Exploring Dissipative Nonlinear optical media with GPGPU supercomputing*, Nanoscale Quantum Optics Conference and MC Meeting, Prague, Czech Republic (2018)

- A. L. Almeida, Alexandra R. S. Ferreira, João S. Cabaço, José L. Santos, Luís Coelho, José M.M.M. de Almeida; *Quantificação de Biodiesel em Combustível Diesel Mineral usando sensores de Fibra Óptica*, 26º Encontro Ibérico para o Ensino da Física, Braga, Portugal (2016)

- Tiago D. Ferreira, A. Almeida, André M. Pereira, I. Madureira, Nuno. A. Silva, A. Guerreiro; *"A Multidimensional Solver of the Schrödinger-Newton Equation based on GPGPU Supercomputing"*, FISICA 2018, Sociedade Portuguesa da Física, Covilhã, Portugal, (2018)

- Tiago D. Ferreira, A. Almeida, André M. Pereira, I. Madureira, Nuno. A. Silva, A. Guerreiro; *"Metallic Nanorings as Light Orbiting Resonator Devices"*, FISICA 2018, Sociedade Portuguesa da Física, Covilhã, Portugal, (2018)

- Tiago D. Ferreira, A. Almeida, André M. Pereira, I. Madureira, Nuno. A. Silva, A. Guerreiro; *"Small Excitations Dispersion Relation of Self-Defocusing Nematic Liquid Crystals Photon-Fluid"*, 3ª Jornadas em Engenharia Física, Física, Física Médica e Astronomia 2018, Porto, (2018)

- Tiago D. Ferreira, A. Almeida, André M. Pereira, I. Madureira, Nuno. A. Silva, A. Guerreiro; *"The LORD of Rings: Light Orbiting Resonating Devices"*, Encontro Nacional de Estudantes de Física 2018, Porto, Portugal, (2018)

- Tiago D. Ferreira, A. Almeida, André M. Pereira, I. Madureira, Nuno. A. Silva, A. Guerreiro; *"Solving the Schrödinger-Newton equation with GPGPU supercomputing"*; Nanoscale Quantum Optics Conference and MC Meeting, Prague, (2018)

- Nuno A. Silva, T.D. Ferreira, André L. Almeida, André Pereira, Inês S. Madureira, Ariel Guerreiro *"Tunable light fluids using quantum atomic optical systems"*, FISICA 2018, Sociedade Portuguesa da Física, Covilhã, Portugal, (2018)

- Inês S. Madureira, Tiago D. Ferreira, André L. Almeida, André A. M. Pereira, N. A. Silva, A. Guerreiro; *"Artificial Intelligence Applied to Quantum Mechanics"*, FISICA 2018, Sociedade Portuguesa da Física, Covilhã, Portugal, (2018)

- Inês S. Madureira, Tiago D. Ferreira, André L. Almeida, André A. M. Pereira, N. A. Silva, A. Guerreiro; *"Improving solvers for non-linear problems with high-dimensionality"*, FISICA 2018, Sociedade Portuguesa da Física, Covilhã, Portugal, (2018)

- Inês S. Madureira, Tiago D. Ferreira, André L. Almeida, André A. M. Pereira, N. A. Silva, A. Guerreiro; *"Solving Non-Linear Quantum Problems through a Convolutional Neural Network"*, 3ª Jornadas em Engenharia Física, Física, Física Médica e Astronomia 2018, Porto, (2018)

- Inês S. Madureira, A. Pereira, Tiago Ferreira, André Almeida, N. A. Silva, A. Guerreiro; *"Transparent boundary conditions: solving scattering problems in your computer"*, Encontro Nacional de Estudantes de Física 2018, Porto, Portugal, (2018)

- André A. Pereira, I. Madureira, T. Ferreira, A. Almeida, N. A. Silva, A. Guerreiro; *"NFT: a Nonlinear Signal Analysis Tool"*, 1st meeting on MOFsENSing, Porto, 2018

- André A. Pereira, I. Madureira, T. Ferreira, A. Almeida, N. A. Silva, A. Guerreiro; *"Nonlinear Fourier Transform for Rogue Ocean Waves"*, 3ª Jornadas em Engenharia Física, Física, Física Médica e Astronomia 2018, Porto, (2018)

- André A. Pereira, I. Madureira, T. Ferreira, A. Almeida, N. A. Silva, A. Guerreiro; *"Nonlinear Fourier Transform"*, FISICA 2018, Sociedade Portuguesa da Física, Covilhã, Portugal, (2018)

- André A. Pereira, I. Madureira, T. Ferreira, A. Almeida, N. A. Silva, A. Guerreiro; *"Ocean waves and solitons"*, FISICA 2018, Sociedade Portuguesa da Física, Covilhã, Portugal, (2018)

- André A. Pereira, I. Madureira, T. Ferreira, A. Almeida, N. A. Silva, A. Guerreiro; *"Determining the Ground State of Helium Atoms with Numerical Hatree-Fock Methods"*, Encontro Nacional de Estudantes de Física 2018, Porto, Portugal, (2018)

The author of this thesis also attended the following conferences:

- *FÍSICA2018 – 21ª Conferência Nacional de Física e 28º Encontro Ibérico para o Ensino da Física* from Sociedade Portuguesa Da Física at the Faculty of Health Sciences of University Beira Interior, Covilhã, Portugal (August 29th to September 1st, 2018).

- *Future of Computing 2018* from Parque de Ciência e Tecnologia da U.Porto – UPTEC at the Faculty of Fine Arts of University of Porto, Porto, Portugal (June 25th to 29th, 2018).

- *School: Introduction to Quantum Technologies* from the Physics of Information and Quantum Technologies Group at the Instituto de Telecomunicações of University of Aveiro, Aveiro, Portugal (November 25th, 2017).

- *FÍSICA2016 – 20ª Conferência Nacional de Física e 26º Encontro Ibérico para o Ensino da Física* from Sociedade Portuguesa Da Física at the Campus de Gualtar of University of Minho, Braga, Portugal (September 8th to 10th, 2016).

And was awarded scholarships and financial support to attend the following conferences:

- *São Paulo School of Advanced Science 2018* from the University of São Paulo at Instituto de Pesquisas Energéticas e Nucleares, São Paulo, Brazil (July 23th to 27th, 2018).

- *XVI Jorge André Swieca School on Non linear and Quantum Optics* from Center for Lasers and Applications at IPEN, São Paulo, Brazil (July 16th to 21th, 2018).

Chapter 2

Complex Ginzburg-Landau Equation in Optics

In the previous Chapter we discussed how nonlinear effects are important and slowly taking more and more part of our day to day experience. In this chapter we provide some important insight knowledge to understand the importance and applications of Nonlinear Optics, and also some important relations with the physical proprieties of media. We will then proceed by describe the simplest case with the Nonlinear Schrödinger Equation and then develop towards both Temporal (with the Slow Varying Envelope Approximation) and Spatial (with the Paraxial Approximation) cases. In these non-dissipative systems we present the Conserved Quantities and other Constants of Motion.

Solitons are an important solution in Nonlinear Optics and we desire to better understand what they are, their characteristics and proprieties as well how they apply in the context of this thesis. Latter we briefly discuss the limitations of the Nonlinear Schrödinger Equation to introduce the Complex Cubic-Quintic Ginzburg-Landau Equation and the new physics it has to offer, such as the description of real systems in perfect balance between dispersion/diffraction and nonlinearities, and gain with losses.

These studies of the State of the Art are important to accompany the future work presented in later chapters such as the high-end *GPGPU* simulations and to Extreme Events of Rogue-Waves.

2.1 Introduction

The development of the laser in 1960 by T. Maiman [22] and the improvements that followed constitute an important moment in the field of optics and, to some extent, it represents the birth of Nonlinear optics. Nonlinear Optics studies the interaction between light and matter when the medium responds in a manner that is nonlinearly proportional to the optical amplitude and phase, typically for very large intensities. Today, the light emitted by a laser is not only sufficiently intense to produce a dramatic optical response in the matter but and perhaps, more importantly, it has the spectral purity, temporal and spatial coherence necessary to control to an extreme degree the nonlinear interaction between light and matter [23]. Indeed, if only intensity was sufficient to induce the plethora of known nonlinear optical effects in matter, it would suffice to focus sunlight on a nonlinear crystal to observe super-continuum generation. Instead, after some critical intensity, the crystal just melts away.

Light from some of the early Continuous Wave (*CW*) lasers, such as the *He-Ne* laser is characterized by a strong spectral purity, specifically by having an emission spectrum with very well defined wavelengths, that can be tunned around specific absorption lines of the atoms that constitute the matter. This promotes a resonant interaction between the atoms and the laser beam, allowing them to exchange energy very efficiently and resulting in a strong coupling between them. This is also true with more recent lasers having continuous and broad emission spectra, such as ultrashort pulsed lasers. This is justified by the second propriety of laser light, namely coherence, which describes the capability of waves to interfere and form patterns and results from the existence of a well defined relationship of the phase of light at different points of space, moments of time and even between wavelengths. When coherent light shines on matter with wavelengths close to atomic transitions, coherence can be transmitted and stored in the state of matter, such that when the atom re-emits light it can still interfere with the initial incident wave.

Modern Nonlinear Optics results therefore from this complex dance between light and matter, where sufficiently intense and coherent light exchange energy, momentum and coherence. One of the most simple nonlinear phenomenon is the Optical Kerr Effect [1], where the excited polarization of the medium changes in a nonlinear manner under the influence of an applied electric field, which can be interpreted as an induced change in the refractive index of the medium [24], but more complicated effects can also arise. The type of nonlinear effects strongly depends on the type of coherence exhibited by light at play

in a given experiment. Wave mixing processes are very influenced by temporal coherence and their occurrence is determined by the phase difference accumulated by light as it is absorbed and re-emitted by matter, which must necessarily interfere constructively for the process to be efficient and is described by the notorious *phase matching conditions* [1].

The significance of the *phase matching conditions* is quintessential since it establishes at a fundamental level a relation between coherence and energy-momentum conservation in wave mixing processes. Similar relations between coherence interactions and conservation laws can be found throughout many other topics and subfields of nonlinear optics, as we shall discuss later on.

Spatial coherence can also result in intensity nonlinear effects, such as self-focusing of optical beams, which when combined with the natural diffraction of the beam can lead to self-guiding, with the beam creating its own waveguide via Kerr lensing as it propagates in a medium.

Although intensity, spectral purity, and coherence are important ingredients for nonlinear effects to occur, real materials also support phenomena that degrade them, such as loses and decoherence and necessarily impact on nonlinear effects. The role and consequences of these phenomena are not yet fully explored in the literature, not only because they add another degree of complexity in the understanding of light-matter interactions, but also because the nonlinear phenomenology when they are sufficiently weak to be neglected is so rich that they have not yet captured the main attention of the scientific community.

Indeed, the analysis of nonlinear effects has been primordially focused on two main regimes. For very weak light intensities or when resonant coherent interactions between light and matter are scarce, a linear description of optical systems is usually sufficient to provide a good insight and prediction of the phenomenon under analysis. However, when the nonlinear nature of the problem can compete or even surpass the linear effects, an extension of the linear models must be made. Then, we can typically employ one of three available approaches: perturbative nonlinear optics, where the polarization effect is treated as series expansion; extreme nonlinear optics, in which is a complete description of the medium is employed; and ultra extreme nonlinear optics, where we usually only considered in cases to analyze vacuum nonlinear effects under very intense fields.

2.2 Nonlinear Response of Optical Media

Nonlinear Optics is a description of the physical behavior of light in some medium and how the optical proprieties alter by the presence of a light field. Those effects are known from far back before nonlinear optics but when some individual materials are under a very intense field, we observe the presence of a change due to the light itself, and such effects can be either temporary or permanent depending on miscellaneous factors. The beginning of Nonlinear Optics is usually associated with the experiment of Franken *et. al.* [25] who reported in 1961 the generation of a laser output signal at the frequency twice of the input signal. This occurred only one year after the development of the Ruby Laser.

The knowledge of Classical Electromagnetism is completely depicted by the famous Maxwell equations. These equations in the formulation of the International System of Units (*SI*) are

$$\nabla \cdot \mathbf{E} = \frac{\rho}{\varepsilon_0} \tag{2.1a}$$

$$\nabla \cdot \mathbf{B} = 0 \tag{2.1b}$$

$$\nabla \times \mathbf{E} = -\frac{\partial \mathbf{B}}{\partial t} \tag{2.1c}$$

$$\nabla \times \mathbf{B} = \mu_0 \left(\mathbf{J} + \varepsilon_0 \frac{\partial \mathbf{E}}{\partial t} \right). \tag{2.1d}$$

From this set of equations we can develop to the optical wave propagation equation with just a few physical considerations and mathematical manipulation (see Appendix A)

$$\nabla^2 \mathbf{E} - \frac{1}{c^2} \frac{\partial^2 \mathbf{E}}{\partial t^2} = \frac{1}{\varepsilon_0 c^2} \frac{\partial^2 \mathbf{P}}{\partial t^2}, \tag{2.2}$$

where c is the speed of light in the vacuum and ε_0 is the vacuum permittivity. The induced polarization $\mathbf{P}$ can be better understood if we separate it in two simple terms.

$$\mathbf{P}(\mathbf{r}, t) = \mathbf{P}_L(\mathbf{r}, t) + \mathbf{P}_{NL}(\mathbf{r}, t), \tag{2.3}$$

where $\mathbf{P}_L$ is the linear term and $\mathbf{P}_{NL}$ describes the nonlinear response. The origins of the optical response of a medium can be traced to the atomic constituents, namely the *charged* fundamental particles that compose the atoms and that make up matter. As light shines on these charges, electromagnetic forces push them out of their equilibrium state.

If we consider a classical description of the reaction of these particles to the electromagnetic field, we typically conceptualize the charges as oscillators that are pushed out of their equilibrium position into an oscillatory motion. As these oscillate, they produce microscopic currents and work like small antennas that in turn emit a secondary electromagnetic field. This feedback process between the field and the charges that compose matter at a microscopic level results in the effective nonlinear phenomena experienced at a macroscopic level.

This classical image and intuition of the interactions between light and matter holds in part in the quantum description. At a quantum level, the state of the charged particles is no longer described in terms of their motion, but rather by a wave function and its associated probability distribution of finding a particle in a given point of space. In this case, the action of the electromagnetic field is to distort these wave functions and probabilistic distributions. But like in the classical model, the end result is a variation in time of the charge distribution at a microscopic level, resulting in small electric currents that ultimately lead to the emission of the secondary electromagnetic field.

The polarization field $\mathbf{P}$ is but the mathematical expression of this secondary field in the macroscopic Maxwell Equations. Depending on the nature of the materials, the polarization can relate in different ways to the applied electric field $\mathbf{E}$, but ultimately that dependency is determined by the dynamic feedback process between light and matter that occur at a microscopic level. These processes can be quite rich in diversity and yield a wide range of optical macroscopic proprieties.

For example, if the wavelength of the applied electromagnetic field does not coincide with any of the absorption lines of the material, the wave function of the electrons (which accounts for most of the optical response in ordinary materials) undergoes only a very small but fast distortion. In these cases, the optical response is very weak but quite instantaneous, and effects like absorption are almost absent.

On the other hand, when the electromagnetic field is resonant or nearly resonant with the absorption lines of the material, it can produce electronic transitions to higher energy states with potentially larger lifetimes. In these cases, the optical response can be larger but slower. Moreover, the electronic dynamics during resonant interactions can be much more complex, involving strong dissipative processes for example, or even the interplay between atomic states. This complexity produces a myriad of macroscopic Optical effects

from dispersion to absorption. Indeed, near electronic resonances the plethora of optical phenomena is very diverse and stimulating for scientific and curious minds.

Typically, strong nonlinear effects occur when, at a quantum level, electronic transitions involve more than one photon. The simplest example concerns two-photon absorption that occurs when the transition between two electronic levels requires the energy of not one but two photons. Then, as the electron decays, it can emit a single photon with twice the energy of the incoming one, resulting in a wave mixing process of frequency duplication.

In the laboratory, the strong dependency of the light-matter interaction on the microscopic photon-electron dynamics, and ultimately, on the proximity between the spectrum of an optical beam to the absorption line of a material, can be used to control and tune the effective optical proprieties of the material. For example, a combination of finely tuned optical beams can produce giant nonlinearities (*e.g.* giant Kerr effect [26]), almost cancels absorption (*e.g.* electromagnetically induced transparency [6]), and even decreases the velocity of propagation of light (*e.g. slow light* [27]). Despite the powerful control of the optical proprieties of materials that can be achieved with modern optical techniques, nature does not allow all this without a price. The different optical proprieties and phenomena are interconnected: dispersion usually implies absorption [28], strong nonlinearities usually must be generated by extra beams [29], just to mention a few cases. Hence, it is not always possible to have idealized experimental conditions and in general realistic situations all optical phenomena are present and affecting each other.

Despite the complexity of the microscopic phenomena that determine the optical macroscopic proprieties of a medium, the macroscopic description of the results of such effects is relatively simples. This description is given using a constitutive relation that determines the polarization $\mathbf{P}$ in terms of the applied electric field $\mathbf{E}$. The expression for the constitutive relations can be mathematically plenteous as the media can exhibit a wide diversity of behaviors, from nonlocal and non instantaneous response, typically involving spatial and temporal convolutions by some functions describing the optical response, known as susceptibilities. Such susceptibilities express the optical proprieties of the media and can be scalar functions or even tensors, for anisotropic media.

To clarify how this works, we consider a simple example of an isotropic medium with a Kerr type nonlinear response, neglecting nonlocal and memory effects. The constitutive relations can be written as

$$\vec{P}_L = \varepsilon_0 \chi^{(1)} \vec{E} \qquad \vec{P}_{NL} = \varepsilon_0 \chi^{(3)} |E|^2 \vec{E}, \tag{2.4}$$

where the index $i = x, y, z$, according to some decomposition of the electric field vector along a cartesian coordinate system[1].

In many situations, $\mathbf{P_{NL}}$ can be treated as a small perturbation when compared to $\mathbf{P_L}$ because the resulting changes in the refractive index are typically very small changes ($\Delta n/n < 10^{-6}$) for electric fields up to $10^8 V/cm$. To obtain the effective wave function for this type of nonlinearity, we now assume that the electric field corresponds to a monochromatic plane wave polarized along the x-direction, given by

$$\mathbf{E}(\mathbf{r}, t) = \frac{1}{2} \left[E(\mathbf{r}, t) \exp(-i\omega_0 t) + c.c. \right] \hat{\mathbf{x}}, \tag{2.5}$$

where ω_0 is the carrier frequency, $\hat{\mathbf{x}}$ is the polarization unit vector that determines the direction of the polarization, and $\mathbf{E}(\mathbf{r}, t)$ is the envelope amplitude of the electric field, which is assumed to vary much slower than the carrier wave.

Substituting equation (2.5) in equation (2.2), we identify that the nonlinear polarization couplings components oscillates with frequency ω_0 and $3\omega_0$. Each term in the nonlinear polarization describes a different wave mixing process that at a quantum level is usually associated with the destruction and production of photons with different energies and momenta. The terms that oscillate with $3\omega_0$ are much faster and during the cycle of the wave produce very small effects, and can be neglected. This simplification is equivalent to introducing the notorious phase-matching conditions, which translate the conservation conditions for wave mixing process. In fact, neglecting the terms that oscillate with $3\omega_0$ is equivalent to impose the conservation of energy at a quantum level between the photons absorbed and emitted.

As a result, and after neglecting the fast terms, the nonlinear polarization can be written as

$$P_{NL}(\mathbf{r}, t) \approx \varepsilon_0 \varepsilon_{NL} E(\mathbf{r}, t) \tag{2.6}$$

with

[1] The index convention is linked to the dielectric constant tensor and x, y, z are the directions of the *principal dielectric axis*, following the *repeated suffix convention*

$$\varepsilon_{NL} = \frac{3}{4}\chi^{(3)}|E\left(\mathbf{r},t\right)|^2. \tag{2.7}$$

This expression has an interesting interpretation since it implies that under these conditions the nonlinear effects result in an effective dielectric constant which is dependent on the intensity of the electric field, say

$$\varepsilon = 1 + \chi^{(1)} + \varepsilon_{NL} \tag{2.8}$$

$$\varepsilon = 1 + \chi^{(1)} + \tfrac{3}{4}\chi^{(3)}|E\left(\mathbf{r},t\right)|^2. \tag{2.9}$$

Notice that so far we have been working with a monochromatic field, which is equivalent to say that this relation is valid for a specific frequency of the electromagnetic spectrum. Generalizing for an arbitrary frequency, we get

$$\tilde{\varepsilon} = 1 + \tilde{\chi}^{(1)}\left(\omega\right) + \tilde{\varepsilon}_{NL}\left(\omega\right), \tag{2.10}$$

where the tilde denotes the Fourier Transform of the function under it. This dielectric constant is used to define the refractive index $\tilde{n}$ and absorption coefficient $\tilde{\alpha}$, which also are intensity dependent.

$$\tilde{n} = n_0 + n_2|E|^2, \qquad \tilde{\alpha} = \alpha_0 + \alpha_2|E|^2. \tag{2.11}$$

Curiously, the linear refractive index n_0 and the absorption coefficient α_0 are related to the real and imaginary parts of $\tilde{\chi}^{(1)}$. Furthermore, the nonlinear coefficient n_2 and the nonlinear two-photon absorption α_2 are

$$n_2 = \frac{3}{8n}\Re\left[\chi^{(3)}\right], \qquad \alpha_2 = \frac{3\omega_0}{4nc}\Im\left[\chi^{(3)}\right], \tag{2.12}$$

where $\Re$ and $\Im$ are the real and imaginary parts, respectively.

Higher-order nonlinear effects can be included in a phenomenological manner by using $\tilde{n} = n_0 + n_{nl}\left(I\right)$ in place of equation (2.11), where $n_{nl}\left(I\right)$ represents the nonlinear part of the refractive index that depends on the beam intensity $I = |E|^2$. This can be a way to introduce the Complex Cubic-Quintic Ginzburg-Landau Equation (*CGLE*), by considering $\tilde{n}$ to have a dependence on $I^2 = |E|^4$.

2.3 Nonlinear Schrödinger Equation

The previous section presented the basic approach to describe the optical response of nonlinear media using a perturbative technique. According to this formalism, for a coherent optical pulse with a central carrier frequency, the polarization can be decomposed into several terms, each corresponding to a contribution to the polarization proportional to a specific power of the field amplitude. Also, the nonlinear susceptibilities of these terms are typically calculated considering the central carrying frequency of the pulse. This is, of course, an approximation, as most materials are characterized by strong linear and nonlinear dispersion, especially for frequencies near atomic absorption lines. Therefore, it is sometimes necessary to include corrections corresponding to higher order dispersion terms. The Generalized Nonlinear Schrödinger equation (*GNLSE*) is a recent topic of research that has gained some attention in the last decades since it is capable of presenting higher nonlinearities than the *NLSE*. It presents the difficulty that it is usually non-integrable and there are not many models available to study the additional physics it brings [30].

In the following sections, we show how the simplifications of the description of the response of the media can be used to derive an effective model for the optical propagation and many nonlinear effects in terms of the envelope of the optical beams. These effective models can be classified into two main classes: Temporal signals, corresponding to the propagation dynamics of a pulse of light, and Spatial signals, corresponding to the propagation of *CW* beam. Each of these cases follow different approaches although the resulting set of equations share great similarities, indeed, we shall see how in both cases the propagation of the optical field is described by a specific form of the *NLSE*.

2.3.1 Temporal Signals and the Slow Varying Envelope Approximation

The effective model for the propagation of an optical pulse in a nonlinear material is derived from the Wave Equation (2.2) when we consider that the electric field can be written as a combination of three contributions

$$E(\mathbf{r},t) = A(Z,t)\,F(X,Y)\exp(i\beta_0 Z), \tag{2.13}$$

where the first term $A(Z,t)$ describes the pulse profile along the propagation direction at a given time t, $F(X,Y)$ corresponds to the transverse field distribution, and the last

term is the carrier wave. Note that the time dependence of $A(Z,t)$ allows the inclusion in the model of the chromatic dispersion of the material that results in the propagation at different speeds of the various spectral components of the pulse.

It is also important to notice that the expression for $F(X,Y)$ is obtained *ex-ante* as the solution for the spatial optical modes of the field and often corresponds to the Gaussian fundamental spatial mode. Therefore, the objective is to derive an equation for the pulse profile $A(Z,t)$, which is achieved by considering the *SVEA*. This approximation considers the cases where the profile of the pulse varies much slower than the time scale of the oscillations of the monochromatic carrier and where the duration of the pulse contains several optical cycles.

To include effects associated with the chromatic dispersion of the material it is often convenient to work in the Fourier domain, where the Fourier Transform of $A(Z,t)$ is represented by $\tilde{A}(Z,\omega)$ and has been shown to satisfy [31]

$$\frac{\partial \tilde{A}}{\partial Z} = i\left[\beta(\omega) + \Delta\beta - \beta_0\right]\tilde{A}, \tag{2.14}$$

where $\beta(\omega) = k_0 n(\omega)$ is the propagation constant of the pulse, which already includes the linear dispersion effects via its dependency on $n(\omega)$, β_0 is the propagation constant for the carrier frequency and the $\Delta\beta$ corresponds to the nonlinear dispersion, which is basically an intensity dependent contribution to the dispersion of the pulse.

The propagation constant $\beta(\omega)$ is often considered as a Taylor Series expansion around the carrier frequency ω_0

$$\beta(\omega) = \beta_0 + (\omega - \omega_0)\beta_1 + \frac{1}{2}(\omega - \omega_0)^2\beta_2 + \mathcal{O}\left(\omega^3\right), \tag{2.15}$$

with the factor $\beta_m = d^m\beta/d\omega^m$ at $\omega = \omega_0$. Each of the terms of this expansion corresponds to a specific dispersion order of the medium and the coefficients $\beta_m = d^m\beta/d\omega^m$ are typically determined experimentally. The *SVEA* implies that $|\partial_z^2\tilde{A}| \ll |\partial_z\tilde{A}|$, which in the Fourier space translated into assuming that the spectral width of the pulse is much smaller than the value of the carrier, i.e. $\Delta\omega \ll \omega_0$. In other words, the pulse has a relatively narrow spectrum and basically, the refractive index perceived by each spectral component of the pulse is very close to the value corresponding to the carrier frequency ω_0. Under these conditions, we only need to take into account the first terms in equation (2.15). Indeed most authors consider the dispersion only up to the third order.

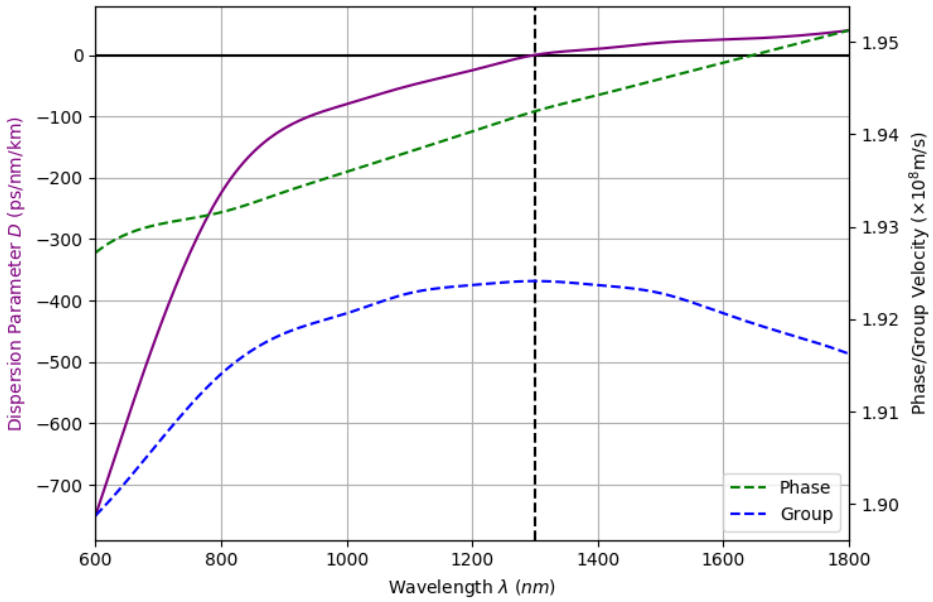

FIGURE 2.1: Group time delay dispersion characteristic of fused silica (solid line). The *phase* and *group* velocities (plotted against the right-hand axis) are shown dotted. This is a chromatic dispersion of an optical fiber used nowadays in communications. The dispersion parameter D is plotted against the left-hand axis, as color indicated. Data adapted from [1].

Substituting equation (2.15) in (2.14) and taking the Inverse Fourier transform we obtain

$$\frac{\partial A}{\partial Z} + \beta_1 \frac{\partial A}{\partial t} + i\frac{\beta_2}{2}\frac{\partial^2 A}{\partial t^2} = i\gamma|A|^2 A, \tag{2.16}$$

where the nonlinear term on the right hand side of this equation is obtained as the Fourier Transform of the term in equation (2.14) describing the nonlinear dispersion.

The group velocity of the pulse v_g is given by $v_g = 1/\beta_1$, where as factor β_2 is associated to the group velocity dispersion parameter (*GVD*).

Equation (2.16) can be further reduced to a $(1+1)$-dimensional *NLSE* by applying the variable transformation described in reference [32], resulting in

$$i\frac{\partial u}{\partial z} - \frac{s}{2}\frac{\partial^2 u}{\partial \tau^2} \pm |u|^2 u = 0, \tag{2.17}$$

where $s = sign(\beta_2) = \pm 1$ stands for the sign of the *GVD* parameter, which can be positive or negative depending on whether the material exhibits normal or anomalous dispersion - figure 2.1.

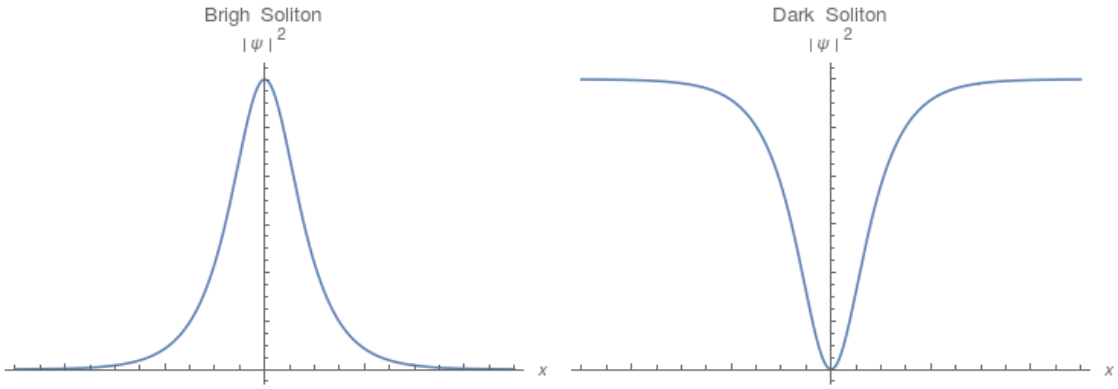

FIGURE 2.2: *Left:* Representation of a Bright Soliton solution, described by an Hyperbolic Secant which is a wave packet of frequencies. *Right:* Representation of a Dark Soliton solution, described by an Hyperbolic Tangent, known for its amplitude drop on a constant background.

Equation (2.17) is formally identical to the notorious Schrödinger Equation of Quantum Mechanics but with a nonlinear potential and where the temporal and spatial coordinates are exchanged. For this reason, this equation has been named as the Nonlinear Schrödinger Equation (*NLSE*) and constitutes one of the most fundamentals equation in Nonlinear Optics. This equation describes the propagation of an optical pulse in a material supporting a Kerr nonlinearity. Again the signal of the Kerr nonlinear term is determined by the characteristics of the material and can be positive in silica optical fibers or negative in semi-conducting waveguides, for example.

The *NLSE* is most famous for being able to support a rich plethora of nonlinear excitations, often named as Solitons. The sign of the *GVD* plays an important role in determining the nature and proprieties of this nonlinear excitations. For example with positive or normal *GVD* (corresponding to $s = +1$) the material can support Dark Temporal Solitons, whereas with negative or anomalous *GVD* (corresponding to $s = -1$) the medium supports Bright Temporal Solitons, as illustrated in figure 2.2

2.3.2 Spatial Signals and the Paraxial Approximation

When instead of temporal signals, such as optical pulses, we consider spatial signals such as CW beams the *SVEA* cannot be applied. Then, a different approximation must be used to obtain an effective propagation equation that describes the intensity profile of the beam. In these cases, we consider that the electric field can be described as a combination of two contributions

$$E(\mathbf{r},t) = A(\mathbf{r}) \exp(i\beta_0 Z), \tag{2.18}$$

where $A(\mathbf{r})$ describes the spatial distribution of the amplitude of the beam, and the second contribution is analogous to the carrier wave and describes the quick oscillations of the electric field along the propagation axis Z. Also, $\beta_0 = k_0 n_0 = 2\pi n_0/\lambda$ is the propagation constant in term of the optical wavelength $\lambda = 2\pi c/\omega_0$.

The Paraxial Approximation corresponds to assuming that the envelope function $A(\mathbf{r})$ varies with Z on a scale much larger than the wavelength λ, such that the second derivative $\partial^2 A/\partial Z^2$ can be neglected when compared to the first derivative $\partial A/\partial Z$. Then, the function $A(\mathbf{r})$ can be shown to follow the nonlinear parabolic equation given by

$$2i\beta_0 \frac{\partial A}{\partial Z} + \left(\frac{\partial^2 A}{\partial X^2} + \frac{\partial^2 A}{\partial Y^2}\right) + 2\beta_0 k_0 n_{nl}(I) A = 0. \tag{2.19}$$

It should be noticed that this equation adequately describes both diffracted and nonlinear effects. Also, in the absence of nonlinear effects, the equation simplifies to the well known paraxial equation [33] studied in the context of scalar diffraction theory [34].

It is useful to introduce some new dimensionless variables to scale the equation (2.19) to a simple form, say

$$x = X/w_0 \qquad y = Y/w_0 \qquad z = Z/L_d \qquad u = (k_0|n_2|L_d)^{1/2} A, \tag{2.20}$$

where w_0 is a transverse scaling parameter related to the input beam width - beam waist - and $L_d = \beta_0 w_0^2$ is the diffraction length - also identified in the literature as the Rayleigh range. In terms of these new variables, equation (2.19) takes now the form of a usual $(2+1)$-dimensionless *NLSE*.

$$i\frac{\partial u}{\partial z} + \frac{1}{2}\left(\frac{\partial^2 u}{\partial x^2} + \frac{\partial^2 u}{\partial y^2}\right) + s|u|^2 u = 0, \tag{2.21}$$

where the choice of the sign corresponds to the sign of the nonlinear parameter n_2. For example, self-focusing media are characterized by a positive nonlinear refractive index and $s = +1$, whereas self-defocussing media has a negative nonlinear refractive index ($n_2 < 0$) and $s = -1$.

To clarify notation, we should notice that equation (2.21) was identified as being a $(2+1)$-dimensional where 2 refers to the number of transverse dimension in the *NLSE*

and $+1$ corresponds to the propagation along z. Notice that this *NLSE* is almost identical to the one derived in the previous section for a temporal signal, but now instead of having a combination of temporal and spatial coordinates, the current *NLSE* is expressed only in term of spatial coordinates. This interchange between spatial and temporal coordinates allows to establish a connection between the solutions of both *NLSE*s, specially in terms of the nonlinear excitations supported by them. Indeed, the temporal Solitons sustained by equation (2.17) have a direct correspondence to Spatial Solitons obtained as solutions of equation (2.21), and *vice-versa*. This is a curious expression of the space and time symmetry in optics.

The dimensionality of equation (2.21) depends on the nature of the problem. For example, when considering a narrow slab of some nonlinear media that works as a planar waveguide, the optical field is strongly confined in one spatial dimension (for example x) and it is possible to drop the dependency on $\partial^2 u/\partial y^2$ since the beam can only propagate along the x coordinate. This approximation must be done carefully since it strongly depends on the waveguide dimensions that must only support a finite number of spatial modes. In this case, the electric field can be written as

$$E\left(\mathbf{r},t\right)=A\left(x,z\right)B\left(y\right)\exp\left(i\beta_0 z\right), \tag{2.22}$$

which after some appropriate manipulations the equation for $A\left(x,z\right)$ is

$$i\frac{\partial u}{\partial z}+\frac{1}{2}\frac{\partial^2 u}{\partial x^2}\pm|u|^2u=0, \tag{2.23}$$

where $u\left(x,z\right)$ is a rescaled version of $A\left(x,z\right)$. This *NLSE* equation is refereed to as being $(1+1)$-dimensional and is the simplest form of the *NLSE*.

Another example are optical fibers that are often designed to support a single fundamental mode.

2.3.3 Conserved Quantities and other Constants of Motion

One of the challenges of studying physical systems described by nonlinear equations is that most of the standard methods used to find solutions for linear equations do not apply. Although for some specific cases, such as the Nonlinear Schrödinger Equation, there are specific techniques that allow to obtain solutions (*e.g.* Inverse Scattering Method

[35]), this is not usually the case. Instead, only approximate solutions can be obtained, either analytically, or resorting to numerical methods.

The lack of exact solutions for nonlinear equations is critical when trying to validate the results of numerical methods since one does not have a reference against which to compare and verify whether the method converged, or even to check if the solution is stable. In these cases, we need to adopt a different approach and use conservation laws that are supported by the nonlinear equations.

The conservation laws of most nonlinear equations fall in one of two categories: *(i)* the first type is a consequence of the symmetries of the physical system under analysis, and are identified using the variational formalism via the applications of the Noether's Theorem [36], and *(ii)* the second type does not depend on the existence of special types of symmetries but are usually a special feature of integrable nonlinear equations.

In this thesis we shall make use of the first type of conservation laws. Their derivation is quite cumbersome and falls out of the scope of the thesis, but can be found in many references [30, 32, 37].

In particular, many of the nonlinear equations that are similar to the Nonlinear Schrödinger Equation preserve the following quantities

$$E = \int_{-\infty}^{+\infty} u^* \left(i\partial_x\right) u dx \tag{2.24}$$

$$N = \int_{-\infty}^{+\infty} |u|^2 dx \tag{2.25}$$

$$P = \int_{-\infty}^{+\infty} \frac{1}{2} \left(u\partial_x u^* - u^*\partial_x u\right) dx, \tag{2.26}$$

corresponding respectively to the energy, norm of mass of the solution, and momentum. The conservation of the norm or mass of the solution is a direct result of the invariance of the equation under changes in the global phase of the solution. The conservation of the energy results from the invariance of the equation under changes in the origin of time (translation in time), while the conservation of momentum expresses the invariance of the system under spatial translations.

In some cases it is even possible for the solution to conserve some generalized momenta. Many nonlinear equations similar to the *NLSE* satisfy these conservation laws, but this is not always the case. Then, and alternatively, it is possible to derive equations for the variation of the associated quantities [9, 37]

$$\frac{dN}{dt} = i\int_{-\infty}^{+\infty}\left(uR^* - u^*R\right)dx \tag{2.27}$$

$$\frac{dP}{dt} = -i\int_{-\infty}^{+\infty}\left(\partial_x uR^* + \partial_x u^*R\right)dx \tag{2.28}$$

$$\frac{dI_1}{dt} = iDP + i\int_{-\infty}^{+\infty} x\left(uR^* - u^*R\right)dx \tag{2.29}$$

with D, P, and R arbitrary functions of the amplitude pulse under study [9]. The importance of equations from (2.24) to (2.29) will become obvious in the following chapter as to test the numerical methods developed during this thesis.

2.4 Soliton Solutions

In the early years of the 19*th* century the naval engineer James Scott Russell made the first observation of a very uniform accumulation of water in a boat canal that was capable to propagate for many kilometers without any losses in amplitude and with constant width. This was a very strange phenomenon at the time because no known description of hydrodynamics could explain how such a single wave propagates with those proprieties [38]. The initial description of the engineer James Russell was of a wave in a steady state that [39]

> *"rolled forward with great velocity, assuming a form of a large solitary elevation (...) which continued its course along the channel apparently without change of form or diminution of speed."*

Similar phenomena was latter also observed in Biology, Oceanography, Medicine and Social Behavior [8, 32, 40–44].

The phenomenon was then called as *Wave of Translation*. Only later in 1965 the Soliton term appeared to reflect the particle-like nature of nonlinear excitations that continued intact even after collision in a medium with linear optical proprieties (see figure 2.3). The literature then started not to distinguish between the two terms and *Soliton* is now used instead of *Wave of Translation* although they are not exactly defined in the same way.

Because of this ambiguity, there are many types of Solitons, depending on the specific nonlinear equation and leading to intense studies to better understand how they influence and could be used to describe some physical effects.

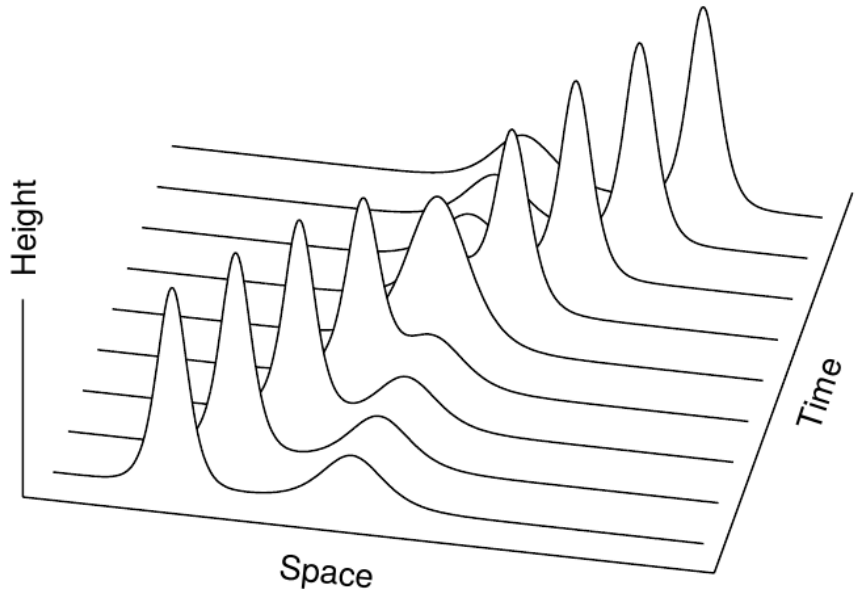

FIGURE 2.3: Two Spatial Solitons colliding in a linear medium: A larger and faster pulse overtakes a smaller and slower one. The two Solitons emerge from the collision with their identities intact. The wave height profile is shown for several times, representing a propagation. Figure adapted from [2]

In the context of Nonlinear Optics, Solitonic solutions are classified into two main categories: Spatial Solitons or Temporal Solitons, depending on the axis where the confinement of the light takes place. A Temporal Soliton represents an optical wave package that maintains its shape whereas a Spatial Soliton represents a *CW* beam that is confined in the directions transverse to the direction of propagation [45].

2.4.1 Temporal Solitons

Temporal Solitons are light wave packages or pulses with a finite duration that maintains their shape as they propagate in a nonlinear medium, and typically are obtained as solutions of the *NLSE*

$$i\frac{\partial u}{\partial z} - \frac{s}{2}\frac{\partial^2 u}{\partial \tau^2} \pm |u|^2 u = 0, \tag{2.30}$$

as studied in section 2.3.1.

As a result, a Temporal Soliton (*TS*) has a wide spectrum, containing several frequencies that must propagate with the same phase velocity, such that their relative phase is preserved and the pulse as a whole conserves the envelope shape.

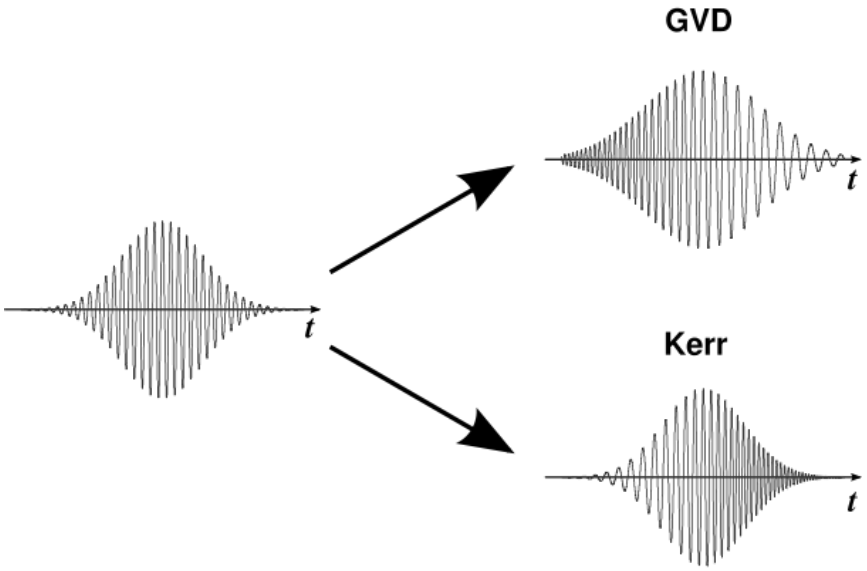

FIGURE 2.4: Representation of an initial carrier pulse with temporal modulation shaped by a Gaussian, as it propagates through a medium with (*right-top*) dominant anomalous dispersion and (*right-bottom*) dominant Kerr effect or the case where normal dispersion is present.

For a general pulse in an arbitrary medium this is no longer the case due to the presence of dispersion. In this case, after some propagation distance L the pulse duration typically widens by a factor of

$$\Delta\tau \approx DL\Delta\lambda, \tag{2.31}$$

where $\Delta\lambda$ is the wavelength bandwidth and D is the dispersion parameter [46, 47].

Another effect that accompanies the widening in pulse duration is the expansion of the pulse chirp as some frequencies traveling with higher velocity tend to accumulate in the front of the pulse, while others traveling slower tend to accumulate in the back of the pulse. Such effect is the result of normal dispersion and the carrier frequency changes throughout the time.

In fiber optics communication, this is a very big problem because along some hundred or thousands of kilometers the optical signal can change and even become imperceivable by the receiver. Nowadays this is overcome with the use of combinations of different optical fibers with opposing dispersion that compensate each other.

Temporal Solitons can avoid the widening of pulse duration introduced by dispersion by compensating it via nonlinear effects. Indeed, as the pulse propagates in a medium

that supports Kerr effect, it produces a modulation of the effective refractive index proportional to the shape of the envelope of the pulse. As a result, parts of the pulse will travel faster than others (see figure 2.4). The special aspect of a *TS* is that the shape of the pulse is such that it compensates the dispersive effects and the resulting chirp exactly. In a *TS* the slower frequencies tend to accumulate in regions of the pulse where the Kerr effect increases the refractive index. The extra component of refractive index introduced by the Kerr effect exactly compensates the velocity differential produced by dispersion and as a result all frequencies keep their relative phase and the shape of the pulse remains unchanged.

In general, one distinguishes between Bright and Dark Solitons. Bright Solitons are formed in media with anomalous dispersion and positive Kerr effect. They constitute a heap of optical intensity [48, 49]. The most commonly known Temporal Bright Soliton, are given by

$$u\left(t,x\right)=A_1\text{sech}\left(t\right)\text{e}^{ix}. \tag{2.32}$$

On the other hand, a Dark Soliton occurs in media with normal dispersion and negative Kerr effect. In this case the Soliton is formed within a region of uniform optical intensity as a local reduction of the light intensity. A well known general Dark Soliton solution is given by

$$u\left(\tau,x\right)=A_2\text{tanh}\left(\tau\right)\text{e}^{ix}. \tag{2.33}$$

Today there is a large number of known Temporal Solitonic solutions which depend on the type of nonlinear effects supported by the medium.

Moreover, there are solutions of equation (2.30) that are stable and predictable but not static. Such results are known as Breathers and introduce a new dynamic in the field of nonlinear propagation. They are very important since many nonlinear systems can accommodate such solutions to observe new phenomena that are unattainable in idleness propagation. This is latter explored in better detail in Chapter 5.

2.4.2 Spatial Solitons

Spatial Solitons (*SS*) are analogous to Temporal Solitons but they are governed by the *NLSE* (or more generalized form of this equation [50, 51])

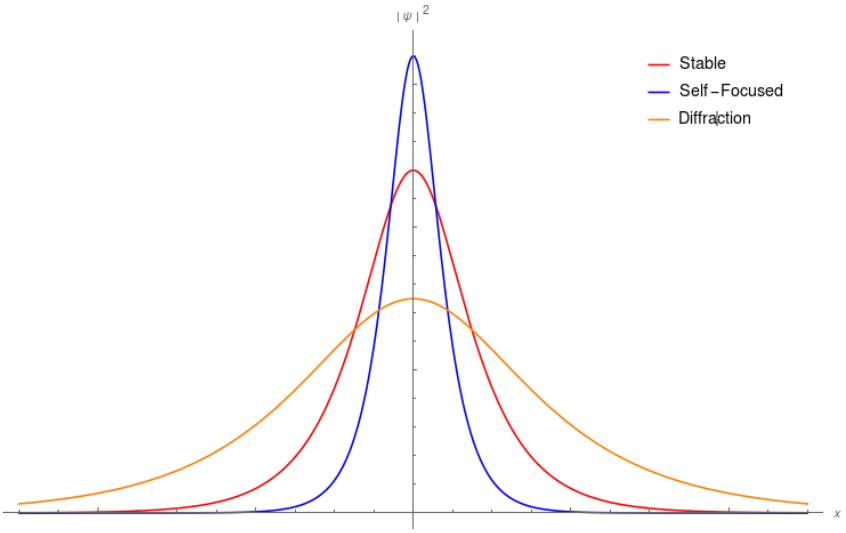

FIGURE 2.5: Transverse section cut of a Soliton propagating in a nonlinear $\chi^{(3)}$ medium. Since this effect requires some parameters to be balanced, the same input Soliton can have distinct outcomes, being a self-focused, diffracted or stable one.

$$i\frac{\partial u}{\partial z} + \frac{1}{2}\frac{\partial^2 u}{\partial x^2} \pm |u|^2 u = 0, \tag{2.34}$$

obtained in section 2.3.2. Unlike *TS*, which are pulses of light, *SS* occur in *CW* beams when the intensity profile of the beam remains unchanged as it propagates. Whereas a *TS* result from a balance between nonlinear effects and dispersion, *SS* result from a balance between nonlinearities and diffraction.

Diffraction is the innate tendency of a beam to spread (diffract) as it propagates in empty space or in an inhomogeneous medium. As a result, the intensity profile of the beam varies. This is a recurrent effect in Gaussian beam Optics, since all Gaussian beams must have a focal plane where the waist is minimal [1]. The effects of diffraction can be overcome in linear optics when using special *self-diffraction* solutions of the wave equation, such as Bessel beams, and can even be beneficial to remove local perturbations in the intensity profile due to *self-healing* proprieties [52, 53].

Another example of diffraction compensation in linear optics can be found in optical fibers and other waveguides. Such structures have a refractive index profile in the plane transverse to the beam propagation that compensates diffraction with refraction.

In 1964, Chiao *et. al.* [54] discovered that a similar effect can be produced solely by nonlinear effects if they lead to a change in the refractive index of the medium that becomes higher in the central region of the beam. In essence, an optical beam can create its own waveguide and be trapped by this *self-focusing* phenomenon. Experimentally the

input beam diffracts at low power, where the nonlinearities do not have enough magnitude to rival the broadening of the pulse. When the intensity of the input peak is enough to provide a strong *self-focusing* effect and thus compensates the natural diffraction of the medium, the shape of the pulse propagates unchanged (see figure 2.5). In some sense, the nonlinear effects produce a concave lens that tends to induce a continuous phase-change on the wavefront. We can calculate how this affects the wave front by considering the local phase

$$\phi(x,y) = k_0 n L(x,y), \tag{2.35}$$

where $L(x,y)$ describes the contributions of each space position to the overall phase-change $\phi(x,y)$. The $L(x,y)$ function dictates how and in what way the effect occurs. For example, in a convex lens, we have a function that induces a higher phase-advance in the outer limits of the beam.

Just as in Temporal Solitons, in the *SS* we can have a balance between the Kerr Lens effect (that will try to narrow the beam) and the Diffraction Effect (that naturally tries to spread it into a larger cross section). Just note that this balance is very sensitive and only occurs in specific cases where diffraction and *self-focusing* compensates each other exactly - figure 2.6.

This phenomenon is described by the *NLSE*

$$i\partial_z u + \frac{1}{2}\partial_x^2 u + N^2|u|^2 u = 0 \tag{2.36}$$

which is a variation of (2.23). In the equation presented we introduce $N = L_d/L_{nl}$, with L_d being the typical length from which the effects of diffraction are no longer negligible and similarly for L_{nl} with nonlinear effects. Furthermore, in some sense the parameter N^2 is a measurement of the how one is compared to the other.

Interestingly, we can gain very important understanding from this parameter. If $N \ll 1$ we can discard the nonlinear part of the equation because $L_d \ll L_{nl}$ and equation (2.36) becomes a simple wave equation. On the other hand, if $N \gg 1$ the nonlinear effects are dominant over the diffraction, resulting in the focusing of the propagation profile. When the two effects balance each other, we can achieve a stable long propagation without any change in the profile, as shown in figure 2.6 where the bottom example is for a system with $N \approx 1$.

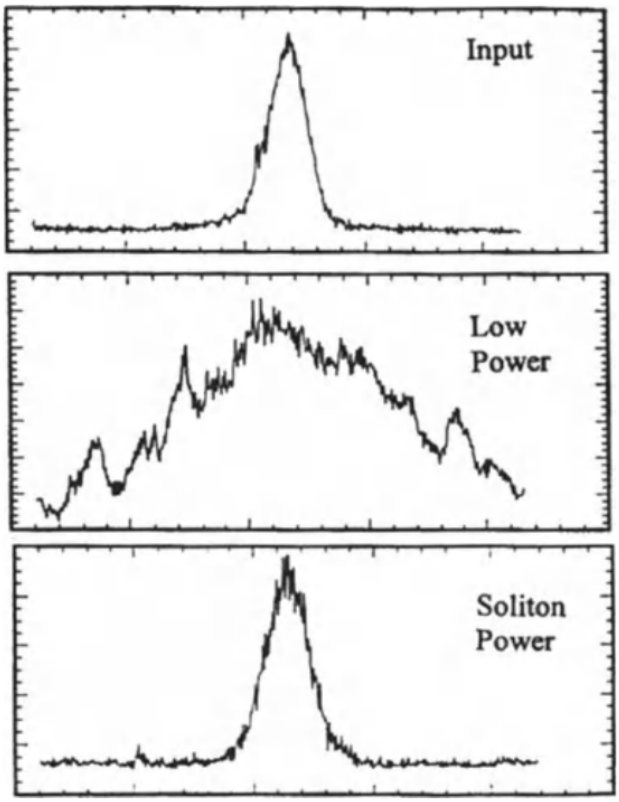

FIGURE 2.6: The spatial beam power profile along the x-axis of some input beam (*top*), when the output waveguide requires different stability power (and beam diffracts or collapse, *middle*) and when provided the *soliton* power (no diffraction, *bottom*), and balanced propagation can been achieved. Image adapted from [3]

To conclude this brief description of *spatial Solitons* can be understand by means of a lens analogy [55]. Diffraction creates a curved wavefront similar to that produced by a concave lens and as a consequence spreads the beam to a wider region of space. On the other hand, the index gradient created by the *self-focusing* effect acts as a convex lens that tries to focus the beam towards its center and the Kerr nonlinear effect acts somehow in this manner. The stable propagation emanates from the effects of both *lenses* canceling each other [54]. Of course there are some quirks that must be addressed, but in general, it is a good analogy and we are explaining a nonlinear phenomenon resourcing to linear optics.

2.5 Open Dissipative Systems

2.5.1 Limitations of the NLSE

Although the scalar *NLSE* previously presented is valid for both Temporal and Spatial wave propagation, it is derived on the basis of quite general assumptions and some important limitations emanate. For instance, presumptions about the dissipative (or diffractive) effects and the nonlinear proprieties of physical systems may be enough for most regular applications, it fails in a number of cases. The presented derivation of the *NLSE* assumes that the nonlinear effects are of non-resonant nature and that the most important ones are described by the envelope of the optical field at the fundamental frequency ω_0 propagating with wavenumber $k = n(\omega_0)\,\omega/_0 c$. All higher-order harmonics are assumed to be too weak to modify the field evolution at the fundamental frequency governed by the *NLSE*.

However, there are some important applications where resonant effects must be evaluated, leading to various frequencies generation within the medium, disturbing the propagation proprieties due to the coupling to some other optical modes when *phase-matching conditions* are satisfied. For example, three-wave mixing occurs when strong interactions between some frequency ω_1 and ω_2 is present, leading to an output frequency $\omega = \omega_1 + \omega_2$ as long as phase match occurs with $\Delta k = k - (k_1 + k_2) = 0$. This kind of three-wave mixing is possible in a medium for which the lowest-order nonlinearity is quadratic and governed by the second-order susceptibility $\chi^{(2)}$. However, and since we are working under the assumption that the medium is isotropic this is not a problem to consider under the scope of this thesis.

Still, an important limitation of the *NLSE* is related to Spatial Solitons formed in the presence of non-Kerr nonlinearities. The conditions for stable spatial solutions for the *NLSE* strongly depends to the $(D+1)$-dimensional problem. In the mentioned conditions we have $D = 1$, furthermore we require the quintic nonlinearity to induce a completer description of the system, such as collapse. The occurrence of the beam collapse indicates that the primary *NLSE* should be corrected by taking into account higher-order effects related to dispersion or the non-paraxial nature of the beam propagation.

Another important aspect to consider is the case of non-conservative real systems where gain or losses are present. The presented *NLSE* is not capable of accounting for such phenomena since there are no terms that resembles unstable effects. For that, we

have to consider a new physical description by taking advantage of the one already presented and considering complex factors. This situation recovers the Constants of Motion of section 2.3.3, where such complex terms impact the change of these Conserved Quantities. This is important, since any system can be considered an open one up to some extent. Also, interaction between gain and losses, even of different orders of dependence to the optical field, can interplay with one another and provide interesting new phenomena.

2.5.2 Complex Cubic-Quintic Ginzburg-Landau Equation

In the previous sections of this thesis, we examined how nonlinear systems that are described by the *NLSE* are identified and intended to better understand what is the physics underling it. Note that these are cases where equilibrium is considered to be present and we have not treated situations where loss or gain are involved or even other types of filtering. Likewise, neither we extended our mathematical perturbative description above $\chi^{(3)}$ order nor we assumed that it was enough. Well, in fact for most of the situations it is but the introduction of new terms can provide a better understanding or even unveil new phenomena that was suppressed by the absence of the one describing it.

Moreover, we start with the expansion of the perturbative approach and introduce an higher field sensitive term associated to the amplitude with a $\chi^{(5)}$ dependence [2] together with $|\psi|^4\psi$. Thenceforth we extend the interpretation of the susceptibilities factors and allow them to be complex quantities. Recalling the meaning of such consideration from section 2.2 this provides conditions to describe a system that is not in equilibrium with the surrounding and is associated with *open systems*. Likewise, the constants of motion are altered by such complex terms either with gain or losses.

This type of description is observed not only in optics but also in many phenomena such as Bose-Einstein Condensates [3] [56] and Superconductivity [4] [57]. We can evaluate such optical systems provided that we are in a perturbative regime and thus it is useful to rewind and write an abstract equation of a problem resorting to this perturbative approach

[2] Since we are dealing with centrosymmetric optical materials we can always discard $\chi^{(even)}$. This is because the tensor describing such materials do not provide conditions to the polarization having the same direction for the optical field A and an opposite one $-A$. This is equivalent to say that the polarization function requires a component in E^{even} in its Taylor expansion. Because of symmetry reasons, this is not possible if the lattice is centrosymmetric.

[3] For Bose-Einsteins condensates it is widely used the *Gross–Pitaevskii* Equation.

[4] In Superconductivity the nonlinear equation mostly used is the *Ginzburg–Landau Equation*.

$$-i\partial_t\psi = \left[\sum_{h,j} A'_{h,j}\partial^h_{x_j} - \sum_m \tilde{q}_m|\phi_m|^m - \sum_n \tilde{p}_n V_n\right]\psi, \tag{2.37}$$

where ψ represents any abstract field parameter, $A'_{h,j}$ a complex function and x_j are the basis coordinates. We assume any dependent order field so that we have $\phi_m(\psi)$. The set of $\tilde{q}_m$ are seen as complex ones that provide a real and imaginary component and this is also the case for all $\tilde{p}_n$. However, the set of functions V_n are identified as independent of ψ. Considering a limited expansion of the summations with $h \leq 2$ and $j = 1$ we face a $(1+1)$-dimensional equation known as the Complex Cubic-Quintic Ginzburg-Landau Equation (*CGLE*) that is represented as

$$i\partial_t\psi + \zeta\partial_x^2\psi + \lambda\partial_x\psi + \alpha\psi + \eta|\psi|^2\psi + \nu|\psi|^4\psi + = i\beta\partial_x^2\psi + i\sigma\partial_x\psi + i\delta\psi + i\varepsilon|\psi|^2\psi + i\mu|\psi|^4\psi \tag{2.38a}$$

$$i\partial_t\psi + (\zeta - i\beta)\,\partial_x^2\psi + (\lambda - i\sigma)\,\partial_x\psi + (\alpha - i\gamma)\,\psi + (\eta - i\varepsilon)\,|\psi|^2\psi + (\nu - i\mu)\,|\psi|^4\psi = 0 \tag{2.38b}$$

where each factor in equation 2.38b has a physical meaning associated and presented in order to understand the physical contribution of each term; ζ is the real term of the Kinetic energy of the particle/phenomenon described by the equation, λ resembles the first order dispersion term, resulting in changes of the group velocity; α describes the linear relation to the field offset in energy levels; η represent either a negative or positive nonlinear Kerr effect, leading to second order events; and ν describes the saturation of non linear refractive index, if negative. The imaginary term have associated β as a measure of spectral filtering or linear parabolic gain effects; σ that correlates to losses of first order, revealing spacial behavior with temporal decay; γ is the linear gain-loss coefficient and has a huge impact on the stability of solutions; ε is a non-linear gain that for stable Soliton-solutions balances between the effect of γ and ε in order to critically maintain stability; and finally μ, when negative, has a direct relationship to the saturation level on the non-linear gain.

Complex nonlinear dissipative systems are nowadays subject of very broad interest [58] and represents a way to establish a bridge between the theory and the experiment by considering dissipative (real) systems. In such cases, the Solitonic structure can be preserved if appropriate gain matches linear and nonlinear losses. Optical Solitons are a form that preserves self-confined dissipative structures that can be described by the Complex Cubic-Quintic Ginzburg–Landau equations (*CGLE*) [43].

These are nonintegrable systems describing real structures and can only be solved

numerically. However, an approximate analytical approach is needed in order to guide simulations and to avoid tedious numerical computations necessary to determine the stability domain point by point. Indeed, the stability criteria for dissipative one-, two-, and three-dimensional Solitons must be established and confirmed by exhaustive numerical simulations [18].

With a good representation of the initial state of the system, if we have the intention to time-propagate the system state it can be done numerically with the use of simulation models by applying some numerical method. We proceeded by means of a Time-Evolution Operator system in a dissipative nonlinear system.

The *CGLE* is a very important and one of the most used nonlinear equations in physics and requires a big commitment and knowledge in numerical methods to achieve solutions. We now that stable solutions do exist but a stability analysis must be performed to understand how and what parameters play an important part and which have little to no effect in the output characteristics of the signal.

2.6 Conclusion

In conclusion, in this chapter we examined a few elements of the world of nonlinear optics starting with the simple Kerr Lens effect. A more complete area of optics is presented accounting some of the nonlinear responses of the medium to an intense optical field and physical knowledge is explored to provide some level of intuition to the reader.

We evaluated both temporal and spatial propagation events with the help of the *NLSE* with two important approximations: Slow Varying Envelope Approximation and Paraxial Approximation. How the nonlinear susceptibilities are related to the refraction index and absorption changes was investigated and mathematical relations to these consequences were presented. The Constants of Motion and respective moments were presented.

Solitons are an important phenomenon that will play a critical role in the scope of this thesis and, as we saw, are present in many areas of science, from Biology to Medicine. They are an odd effect that occurs in nature known to be very intense and consisted through propagation if special conditions are provided. Spatial and Temporal Solitons exist in different situations and are very sensitive to nonlinear effects of the medium.

We presented the limitations of the *NLSE* and deduced a perturbative extension of it known as the *CGLE*. For that, we introduced the notion of a complex factor that behaves as an exchanger of energy capable to change the constants of movement that usually are

perpetual. Note that this is only an extension to the perturbation approach to nonlinear optics (*GNLSE*) and is not capable to describe consistently the physics when going beyond its intrinsic limit. Nevertheless, the *CGLE* provides an intense extension to the *NLSE* where new phenomena and atomic systems can be described and studied.

This chapter provided the knowledge required to better understand all the cases that will be presented as well as supply the ability to understand any computational method employed and interpret its results.

Chapter 3

Physical Model and Code Development

In this chapter, we start by providing some awareness about the evolution of programming and how the origins of computational physics are related to Supercomputing, both in *GPGPU* and in *CPU*. The explanation about important points that must be addressed when programming is presented and how it can influence the total outcome.

The following provides Physical Model to implement in order to solve the type of problem discussed in the previous Chapter, namely the *CGLE*. The approach here used is based in a perturbative analysis to quintic order and complex factors controlling each term in the mathematical description with the well documented Symmetric Split-Step Fourier Method. Once the model is described we implemented it in two programming languages, the first one oriented to *CPU* and the other in a platform able to run in *GPGPU* Supercomputing.

The implementation of the code was very important and lead to very interesting results, with increasing quality both in resolution and in runtimes, since the hardware where it is implemented is heavily directionalized to intense calculations. We tested the solver validity against some results that have already been published in the literature to evaluate if it behaves as expected.

3.1 Introduction

The development of a physical model describing a system with a methodology easy to implement in some programming language is very important since in the last decades

simulations have been one of the most growing areas in physics and engineering. Using the huge amount of available resources of nowadays computers such as processing unit and memory, we can instruct them to execute simple but targeted calculations following some criterion to produce the desired output.

The development of models that resemble complex operations of calculations was a hot topic in the second half of the past century, and newly developed numerical models led to one of the most powerful tools available in solving difficult and repetitive arithmetics, such as matrix multiplication and Fourier Transforms. The main hardware component of such tool is the Central Processing Units (*CPU*). The Central Processing Unit (*CPU*) Architecture represents the way these devices are built and for many years the solo way to increase performance was to enlarge the clock speed at which the operations were performed. The downside of such an approach was that it consumed too much energy from the power outlet resulting in a intense heating of the unit very quickly. Intending to reduce thermals of the chip while increasing computer power, manufacturers invested big amounts of financial resources to find a solution.

Numerical models are not capable of providing the same important information as the physical counterpart, however it is efficient to supply results even when analytical solutions are not available and this is why the study of *computational physics* has gained so much attention: we can achieve solutions of systems that are no soluble with mathematical expression. Because of this a new field in natural sciences denominated of *computational* appeared, and Physics was no exception with many bright minds committed to developing models that mirrors some physical phenomena.

With the appearance of personal computers growing after early 1990, the two main computer *CPU* suppliers were Intel (the main inventor of x86 [1]) alongside with AMD [59].

Intel research team introduced a solution that used 2 processing units on a single *CPU* in 2004, being at the time a complete revolution on computer muscle *vs* power consumption. The chip was called *Celeron Dual-Core* [60, 61], presenting for the first time the notion of *multicore*. Nowadays, personal computers can easily have 8 cores or more.

$$S_l = \frac{1}{(1-p) + \frac{p}{s}}. \tag{3.1}$$

[1] Architecture x86 was designed by Intel and AMD in 1978. This is the working table of any modern operating system since they are all based on x86 protocols. Only Intel and AMD can build CPUs for the usuals operating systems today used [59].

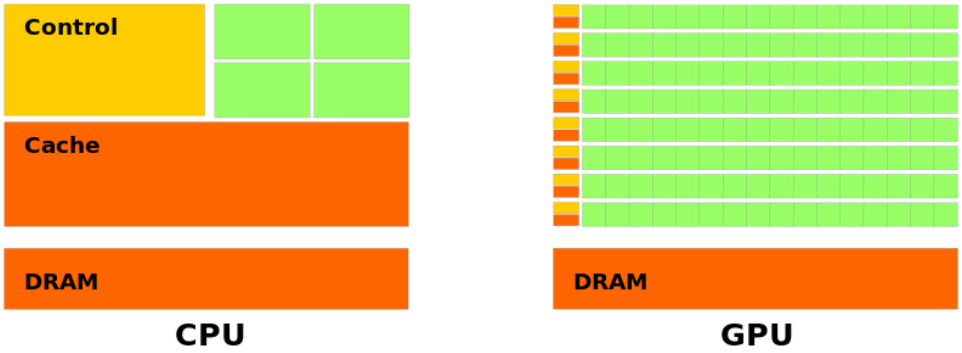

FIGURE 3.1: Comparison of main architecture of a *CPU* and *GPU*. As one can see, *CPU* has fewer core-count but more cache and better generalized purpose units. On the other hand, a *GPU* has hundreds time more cores but they are specialized on a determined kind of tasks.

Equation (3.1) states the Amdahl's law as the mathematical statement of the above mentioned. It quantifies the maximum speedup $S_l(s)$ of an algorithm by how much can be parallelized s versus the portion of code p that does not benefits from more threads, with the programming language to be very important. Some simply does not allow good performance on multi-thread while in some cases it is even impossible. Another way of improving the speedup is by increasing the available resources of the machine. Gustafson's law quantifies the maximum theoretical acceleration one can expect, based on resources and Amdahl's law [62].

Parallel computing was, in the beginning, looked upon as an *exotic* pursuit and typically got compartmentalized as a specialty within the field of computer science is only available to those who became specialized and with large amounts of financial resources. This perception has changed in profound ways in recent years. The importance of parallel programming in the computing world today and the increasingly large role it will play in the years to come is evident.

One way to implement optimal multi-thread code is by using *OpenCL*. It is a framework to run programs in multiple platforms and provides a standard interface for parallel computing. The great advantage is that it allows one programming code (in $C++$) to run in *CPU* (multi-thread) or *GPU*. However, *GPU*s usage used to be in rendering graphics and provide video output to the user to interact with. This has been modernized in the past decades.

*GPGPU*s, also known as General-Purpose Graphics Processing Unit or solely *GPU*, are specialized electronic devices that do the same distinct math over and over again but the advantage of the *CPU* is on making various types of tasks while a *GPU* is heavily

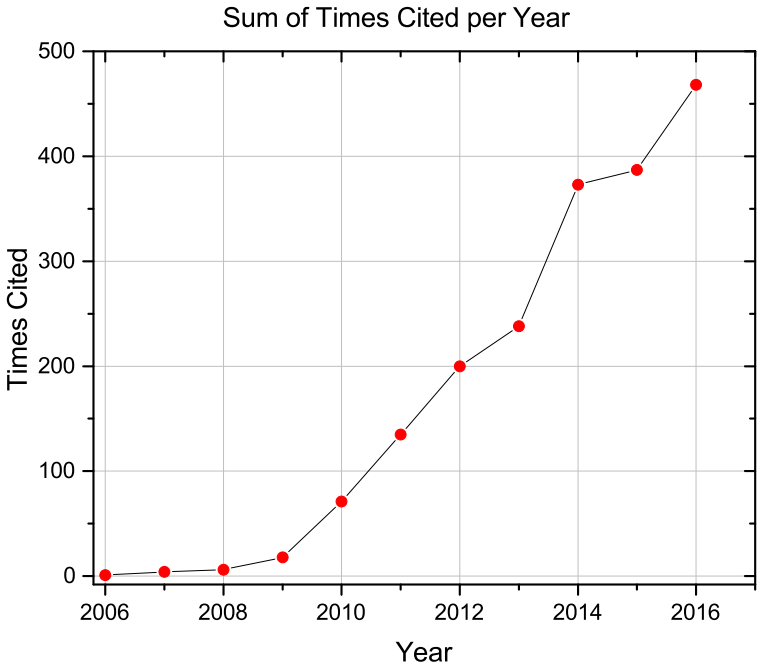

FIGURE 3.2: Number of citations on the area of *GPGPU Simulation* through the years. Data exported from Web of Science on November 2017.

individual on the type of workload to perform (see figure 3.1). Also, because of specific calculations to render graphics, these units are more directionalized and small, allowing more population density in the same area, when compared to a *CPU*.

The release of *GPU*s that possessed programmable pipelines attracted many researchers to the possibility of using graphics hardware for more than simply *OpenGL* rendering. Because standard graphics Application Programming Interface (*API*s) at the time were the only way to interact with a *GPU*, any attempt to perform arbitrary computations on a *GPU* would be very complicated. Because of this, researchers explored general-purpose computation by trying to make their problems appear to the *GPU* to be traditional rendering[2].

This process may appear simple but the knowledge needed to program the *GPU*s had to be enormous and to facilitate this process, as a strategy try to set the commercial standard of *GPU* programing language *NVIDIA* deployed a *GPU* with built-in *CUDA*

[2]Early *GPU*s were designed to produce a color for every pixel on the screen, completely controlled by the programmer. Researchers considered that the input *colors* could actually be any data and the results would be handed back to the *GPU* as the final pixel *color*. This data could be read back by the researchers, and the *GPU* would never be the wiser. The *GPU* was being tricked into performing non-rendering tasks by making those appear as if they were. This trickery was an incredible way to deceive electronics, almost an artistic way of humans in controlling machines.

Architecture. The number of people with the ability to program these *GPU* core kernels is nowadays growing and manufacturers have released many *API*s to this kind of work. A interesting evidence of this is the number of annual citations on articles related with *GPGPU* simulations (figure 3.2). Others *API*s are now available that provide general-purpose computational tools such as *OpenCL*.

Parallel computing can provide great optimization with cheap resources if we are willing to pass the doors to lower-level programming. For that, we must first study and develop a model that can take advantage of high-density matrix multiplication and Fast Fourier Transform ($\mathcal{FFT}$) that *GPGPU* are optimized for.

3.2 The Symmetric Split-Step Fourier Method

The *CGLE* presented in section 2.5.2 constitutes an extension of the *GNLSE* which includes not only the unitary evolution typical of a wave function of a quantum system, but also nonlinearity processes that are typically found when describing statistical processes. Despite the fundamental difference of the numerical methods developed for solving the *GNLSE*, it can be adapted to address the *CGLE*.

In particular, both equations are second-order nonlinear parabolic partial equations, for which there is a multitude of numerical methods, including the Crank-Nicolson implicit scheme and pseudo-spectral methods [63], which were originally developed to address second order linear parabolic partial equations, such as the Heat Equation. These methods basically convert partial differential equations into algebraic equations that can be integrated numerically in a computer via some process of discretization.

However, the existence of nonlinear terms affects the stability conditions of these method, and many times it is necessary to use other more robust approaches, typically relying on the split of the integration step into several *substeps*. Perhaps the most popular splitting method is the Strang-Splitting algorithm, which is a second order method [31]. The idea of these methods is that the differential equation can be written as

$$\partial_t \psi = \hat{\mathcal{L}}\psi, \tag{3.2}$$

where the operator $\hat{\mathcal{L}}$ is some nonlinear differential operator that only contains derivatives on spatial coordinates. The purpose of the method is to identify a splitting of the operator $\hat{\mathcal{L}}$, into two other operators, say

$$\hat{\mathcal{L}} = \hat{A} + \hat{B} \tag{3.3}$$

and decompose the integration step into the following steps

$$\partial_t \phi_1 = \hat{A}\phi_1, \text{ with t}\in [t, t + \Delta t/2] \text{ and } \phi_1(t) = \psi(t) \tag{3.4}$$

$$\partial_t \phi_2 = \hat{B}\phi_2, \text{ with t}\in [t, t + \Delta t] \text{ and } \phi_2(t) = \phi_1(t + \Delta t/2) \tag{3.5}$$

$$\partial_t \phi_3 = \hat{A}\phi_3, \text{ with t}\in [t + \Delta t/2, t + \Delta t] \text{ and } \phi_3(t + \Delta t/2) = \psi_2(t + \Delta t), \tag{3.6}$$

where Δt is the integration step.

The challenge of the splitting methods is to find a particular combination of operators $\hat{A}$ and $\hat{B}$ (*i.e.* a splitting of $\hat{\mathcal{L}}$) that balances low numerical error with speed in calculation and other numerical requirements, such as memory consumption. In the case of the *GNLSE*, the most common splitting is provided by $\hat{A} = {}^{i}/_{2}\partial_x^2$ and $\hat{B}$ containing the remaining terms of $\hat{\mathcal{L}}$, typically responsible for the nonlinear dynamics.

The integration of each *substep* of the splitting algorithm can resort to a variety of specific numerical methods, that can include the Runge-Kutta family [64] and Crank-Nicolson [65]. In the past years however, the pseudo-spectral methods have established themselves as the standard for these applications. In particular, one combination of the splitting methods with pseudo-spectral methods based on the Fast Fourier Transform (*FFT*) known as Symmetric Split-Step Fourier Method (*SSFM*) is the most commonly used.

This method takes advantage of the relative speed and numeric economy of the *FFT*, and uses it to calculate the spatial derivatives of ψ using the Fourier Transform of ψ. In practice, this performs the integration of the first and last *substeps* of the splitting method in the direct space, whereas the second step is performed in the Fourier space.

The idea of adapting the *SSFM* to tackle the *CGLE* is based on this approach. Notice that for the *CGLE*, the operator $\hat{\mathcal{L}}$ is now

$$\hat{\mathcal{L}} = -i\mathbf{H} = -i\left(\mathbf{D}'\partial_x^2 + \mathbf{K}'\partial_x + \mathbf{C}'|\psi|^2 + \mathbf{Q}'|\psi|^4 + \mathbf{L}'\right). \tag{3.7}$$

Then, using the same criteria adopted for the *GNLSE*, an appropriate splitting is

$$\hat{A} = \mathbf{D}'\partial_x^2 + \mathbf{K}'\partial_x \tag{3.8}$$

$$\hat{B} = \mathbf{C}'|\psi|^2 + \mathbf{Q}'|\psi|^4 + \mathbf{L}', \tag{3.9}$$

where the operator $\hat{A}$ contains the terms of $\hat{\mathcal{L}}$ that have derivatives on the spatial coordinates, whereas $\hat{B}$ contains the remaining terms. This takes advantage of a well known propriety of the Fourier transform, where the derivative can be calculated by a simple multiplication,

$$\mathcal{F}\left[f^{(n)}(x)\right](k) = (2\pi ik)^n \mathcal{F}\left[f(x)\right](k). \tag{3.10}$$

The combination of these exhibited terms can be summarized in the following scheme

$$\tilde{\psi}(t,\mathbf{k}) = \mathcal{F}\left[\psi(t,\mathbf{r})\right] \tag{3.11}$$

$$\psi(t+\Delta t/2,\mathbf{r}) = \mathcal{F}^{-1}\left[\exp\left(-i\Delta t\tfrac{\hat{A}}{2}\right)\tilde{\psi}(t,\mathbf{k})\right] \tag{3.12}$$

$$\psi^{NL}(t+\Delta t/2,\mathbf{r}) = \exp\left(-i\Delta t\hat{B}\right)\psi(t+\Delta t/2,\mathbf{r}) \tag{3.13}$$

$$\tilde{\psi}^{NL}(t+\Delta t/2,\mathbf{k}) = \mathcal{F}\left[\psi^{NL}(t+\Delta t/2,\mathbf{r})\right] \tag{3.14}$$

$$\psi(t+\Delta t,\mathbf{r}) = \mathcal{F}^{-1}\left[\exp\left(-i\Delta t\tfrac{\hat{A}}{2}\right)\tilde{\psi}^{NL}(\Delta t+\Delta t/2,\mathbf{k})\right] \tag{3.15}$$

where $\mathcal{F}$ and $\mathcal{F}^{-1}$ represent the Fourier and Inverse Fourier transform, respectively.

It should be noticed that it is not convenient to perform a single integration step at a time but to attach the last and first *substeps* of two consecutive steps (see figure 3.3). This method satisfies a propriety known as *First Same As Last* [66] that allows to concatenate the *substeps* involving the operator $\hat{A}$, say

$$\psi(t+2\Delta t,\mathbf{r}) = \exp\left(\frac{\Delta t}{2}\hat{A}\right)\exp\left(\Delta t\hat{B}\right)\exp\left(\Delta t\hat{A}\right)\exp\left(\Delta t\hat{B}\right)\exp\left(\frac{\Delta t}{2}\hat{A}\right)\psi(t,\mathbf{r}). \tag{3.16}$$

This procedure allows to exempt from doing two Fourier transforms, which reduces the execution time and numerical errors.

3.2.1 Implementation

The *SSFM* is a well known method of solving the *GNLSE*, which has been tested extensively and validated in terms of Numerical Analysis. However, and to our knowledge, it is commonly used to solve the *CGLE* and only a few examples can be found in the Literature [67]. As mentioned previously, the dissipative nature of the *CGLE* and the balance of losses and gain introduce new features for which this numerical method has not been fully tested. As a result, the implementation of the solver of the *CGLE* was done in two

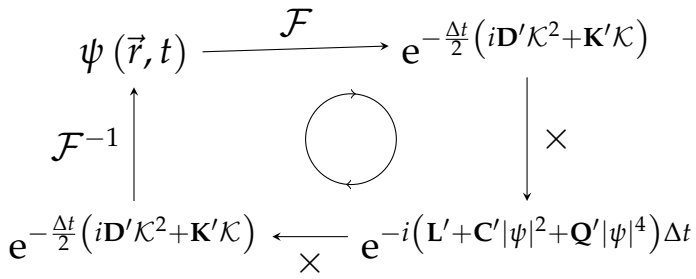

FIGURE 3.3: Graphical representation of the principle of Symmetric Split Step Fourier Method applied to a field provides a way to recursively calculate the condition of the function at time $t + \Delta t$ knowing its previous state at t.

steps: (i) the first focused on the validation of the *SSFM* as adequate for solving the *CGLE*, which involved the quick implementation of the algorithm in Python, and (ii) the second more concerned with performance, which involved a second implementation that could run on *CPU* and that was written in a combination of *C++* and *ArrayFire*.

The use of Python in the first step of development was justified because this is an *opensource* language that includes numerical packages, such as *NumPy* and *SciPy*, that have been extensively tested. Furthermore, it is a high-level programming language that favors quick development and debugging, thus reducing development time. The main disadvantage is that this language does not make full use of the computing power available on the *GPU*, which results in a poor performance and low runtimes.

In the second step of development, the algorithms were adapted to make use of the parallelism and computing power of *GPU*. This implied that the code had to be rewritten using a language such as *C++* combined with the package *ArrayFire*, which includes the implementation of some fundamental numerical methods to run on *GPU*. Since the *ArrayFire* includes numerical packages written in either CUDA or OpenCL, the code can run not only in *NVIDIA GPU*s (that support both *CUDA* and *OpenCL*) but also other *GPGPU*s (which typically only run *OpenCL*). This allows a strong portability of the code over different hardware without compromising on efficiency.

The final solver has shown great stability, with a strong decrease in runtime, while allowing to tackle larger problems. Furthermore, one advantage of being written in *ArrayFire* and *C++* is that, although development having the *GPU* in mind, the same code can be compiled to run on CPU. This allows to fully determine the *SpeedUp* and performance improvement of *GPGPU* Supercomputing versus *CPU* in the case of the solver of the *GCLE*.

Designation	CPU	RAM	GPU	GDDR SDRAM
Laptop 1	i7-4720HQ	8GB	Radeon R9 M256	4GB
Laptop 2	i7-4700MQ	12GB	GForce 840M	2GB
Desktop	Ryzen 1700	16GB	GTX 1060	6GB
Workstation	i7-4930K	64GB	GTX Titan	6GB

TABLE 3.1: List of specifications of the Hardware used to benchmark the newly developed *GPGPU* Supercomputing solver.

3.2.2 Computational Performance and Benchmarks

This section presents the analysis of the computational performance of the solver of the *CGLE* and to verify the advantages of *GPU* computing against the single-thread CPU equivalent. This was done by running the same physical problem on different platforms, with specific hardware budgets ramping from low-end laptop to an high-end desktop, and running the solver in both *CPU*s and *GPU*s, as well as, using implementations based both in *CUDA* and *OpenCL*.

The specifications of the computers used are presented in table 3.1.

The computers equipped with *NVIDIA GPU*s where used to run the code in versions based both on *CUDA* and *OpenCL*, whereas non-NVIDIA only run the code in the *open-source OpenCL*. Also the code ran on the *Workstation* was compiled to tun on the *CPU*. *"Laptop 1"* was equipped with an Intel i7-4720HQ, 8GB of DDR3 RAM, and a Radeon R9 M256 GPU with 4GB of GDDR5; *"Laptop 2"* was equipped with an Intel i7-4700MQ, 12GB of DDR3 RAM, and a GForce 840M GPU with 2GB of GDDR3; the *"Desktop"* was equipped with an AMD Ryzen 1700, 16GB of DDR4 RAM, and a GTX 1060 GPU with 6GB of GDDR5; and lastly the *"Workstation"* was equipped with an Intel i7-4930K, 64GB of DDR3 RAM, and a GTX Titan GPU with 6GB of GDDR5.

The numerical tests considered the simulations of physical systems with different sizes and consisted in measuring the elapsed time during each simulation. The results are shown in figure 3.4 and 3.5 as *SpeedUp* factors of the simulations in different platforms and for different versions relative to the *CPU* version. The results for single-thread show that for small physical systems with smaller number of grid points, there is no benefit in using *GPU*s since the *CPU* cores are significantly faster. However, as the number of grid points of the simulations increases, the *CPU* performance decays considerably and all the *GPU*s outperform the *CPU*.

Furthermore, *CUDA* seams to run better in higher-end cards but *OpenCL* is very capable of follow the competitor's results. With the *GTX Titan* using *CUDA* framework we

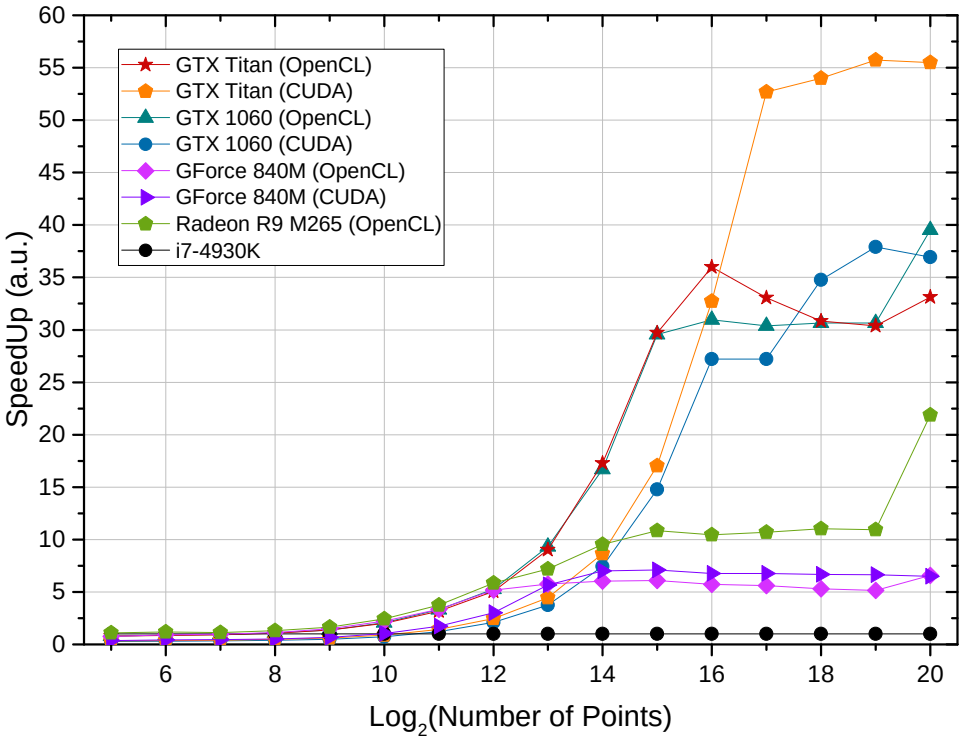

FIGURE 3.4: Results of the tests performed to the *GPGPU* solver in single core processing to compare *SpeedUp* against the resolution of the system. The various used hardwares are indicated in the legend with the respective framework. Results are relative to the *CPU* performance.

achieved a saturation *SpeedUp* at around 55 which means that, for example, the simulation code can run in slightly over 2 days in this hardware while in a *CPU* it would take 3 and a half months.

For single processing, there is an evident exponential growth of *SpeedUp* being very notorious for resolutions above 2^{14} following then for some saturation level. There is a separation of 3 major groups of results: low end laptop at $\approx$ 8, medium range desktop with $\approx$ 32 and later is the workstation *CUDA* line with the highest diminution of runtime, being $\approx$ 55 faster. Note the interesting detail that *CUDA* and *OpenCL* have little differences for most of the used hardware with exception of *GTX Titan*. This is a result of the very high core-count of *CUDA* units and its capability at large amounts of operations.

This shows that *GPGPU*s can provide very accurate and yet extremely fast results when compared with a workstation *CPU* with an associated cost of hardware very different, where most of cheap laptops today in the market are already equipped with such *GPGPU*s capable to run almost 10 times faster.

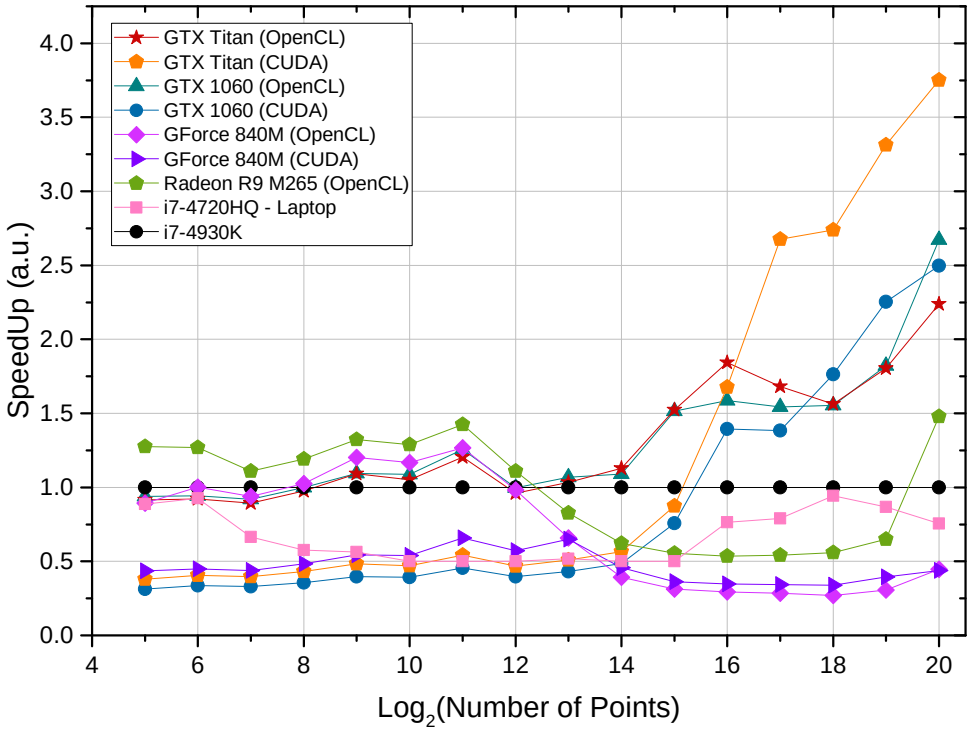

FIGURE 3.5: Results of the tests performed to the *GPGPU* solver in multi core processing to compare *SpeedUp* against the resolution of the system. The various used hardwares are indicated in the legend with the respective framework used. Results are relative to the *CPU* performance.

In case of multi-thread , the results of figure 3.5 show that low-end *GPGPU*s have an hard time to compete with such workstation *CPU*. For resolutions higher than 2^{12} both laptop *GPU*s (*GForce 840M* and *Radeon R9*) and *CPU* (*i7-4720HQ*) show longer runtimes than the high-end *CPU*. On the other hand we have desktop and workstation *GPU*s that for high resolutions show a very good *SpeedUp*, capable of reaching a maximum 3.7. The desktop units have a top *SpeedUp* of ≈ 2.7 with *OpenCL*.

Moreover, *CUDA* is less efficient in *CPU* and *GPU* for lower resolutions (bellow 2^{16}) in all hardware. However, the *OpenCl* framework does not provide any advantage in *GPGPU* at high resolutions, where *CUDA* scales very well. It is also very interesting the comparison of the workstation *CPU* (*Intel i7-4930K*) and the laptop one (*Intel i7-4720HQ*). For higher resolutions, there is a small decreasing performance of the laptop one but it was expected an higher discrepancy. The main difference is that the *4930K* alone costs more than the whole laptop where the *4720HQ* is inserted.

We expect the single core to take more time to provide results because the clock speed plays an important role if it saturates and latency starts to become crucial, resulting in

slow calculation being performed. Yet multiple core results are very interesting and allow a rapid observation of the dynamical behavior of highly nonlinear system. Also, single core outputs have higher numerical accuracy and are better suited for small transient effects of more demanding applications, all of it with the cost of higher runtime. Nevertheless, in both cases there is a resolution band where the *GPGPU*s tools outperform the usual *CPU* programming times.

3.3 Results and Applications to the Solver

We must first address what are single and multiple core operations and what are the differences between each other. A single core operation is known as

> *the use of a single processing block of the Central Processing Unit to sequentially perform the instructed operations;*

and the case of multi core processing is a dramatic change in the way that the tasks are organized by

> *computing multiple operations independent of each other and preform various instructions at the same time, being capable to reduce the latency of results.*

In the previous section we did observe the results against single processing increased performance when using *GPGPU* instead of *CPU*. It is important to note the small to null difference in low-resolutions problems. We observe results starting to be significant at higher resolutions as the *Intel i7-4930K* is not capable to accompany all *GPGPU*s performance. Note that all three laptop *GPU*s configurations have similar efficiency (GForce 840M *CUDA/OpenCL* and the Radeon R9 M256 *OpenCl*).

For single processing, there is an evident exponential growth of *SpeedUp* being very notorious for resolutions above 2^{14} following then by some saturation level. There is a separation of 3 major groups of results: low end laptop at ≈ 8, medium range desktop with ≈ 32 and later is the workstation *CUDA* line with the highest diminution of runtime, being ≈ 55 faster. Note the interesting detail that *CUDA* and *OpenCL* have little differences for most of the used hardware with exception of *GTX Titan*. This is a result of the very high core-count of *CUDA* units and its capability at large amounts of operations. This shows that programs that run with *GPGPU*s can provide very accurate and yet extremely fast results when compared with a workstation *CPU* with an associated cost of

hardware very different, where most of cheap laptops today in the market are already equipped with *GPGPU*s capable to run almost 10 times faster.

While observing the calculated plot for multiple-core programing we observe that the outcome is not very different. *OpenCL* is much more efficient than the *CPU* and *CUDA* for lower resolutions (bellow 2^{16}) independently of the hardware. However, the *CUDA* framework does not provide any advantage in any *GPGPU* and performed worst than the *CPU*. It is also remarkable the comparison of the workstation *CPU* (*Intel i7-4930K*) and the laptop one (*Intel i7-4720HQ*). For higher resolutions, there is a decreasing performance of the laptop but for low ones, they walk hand-to-hand. The main difference is that the *4930K* alone costs more than the whole laptop where the *4720HQ* is inserted.

We expect the single core to take more time to provide results than multi-core, this because the parallel work is an important component. However in such cases there is higher heat generation and it can saturates to the point where latency starts to become crucial, resulting in slow calculation being performed. Yet multiple core results are very interesting and allow a rapid observation of the dynamical behavior of such highly non-linear system. For final results, the single core outputs have higher finesse and are better suited for small transient effects of more demanding applications, all of it with the cost of higher runtime. Nevertheless, in both cases there is a resolution band where the *GPGPU*s tools outperform the usual *CPU* programming times.

This computational implementation of the *SSFM* in *GPGPU* allows to quickly simulate the dynamics of any real system with dispersion, nonlinearities, losses, and gain. It is ready for atomic gases or mediums with very high nonlinear behavior when a light pulse propagates. Recent studies with nanoparticles [10] show that we can control the nonlinear response of the host by changing their density and size. There is also the possibility to study a nonlinear medium response to a random signal which in recent years have become very interesting with Rogue-Waves observation [68].

3.3.1 Analysis of Physical Simulations

The tests described in the previous section were designed to evaluate the computational performance of solver in different platforms and running different software implementations. This section focuses on the tests used to validate the physical results provided by the solver. This was done by simulating the propagation of a pulse of light in a medium described by the *CGLE* that has been well studied and characterized in the

Literature [67, 69, 70]. In particular, we considered the propagation of a laser pulse in a nonlinear medium with a cubic-quintic type of nonlinearity and subjected to loss and gain. Under these conditions the pulse can be described by the propagation equation corresponding to a temporal *CGLE*

$$i\partial_t\psi + (\zeta - i\beta)\,\partial_x^2\psi + (\lambda - i\sigma)\,\partial_x\psi + (\alpha - i\gamma)\,\psi + (\eta - i\varepsilon)\,|\psi|^2\psi + (\nu - i\mu)\,|\psi|^4\psi = 0. \tag{3.17}$$

This has been investigated in recent years, and much interest has been devoted to the identification of stability conditions of Bright Temporal Solitons in a medium with non-null $\chi^{(3)}$ and $\chi^{(5)}$ [67]. In our simulations we consider Soliton solutions of the form

$$q\,(z,t) = A\mathrm{sech}^{1+id}\left[V\left(z - \frac{t}{v}\right)\right]\exp\left[i\,(kt - \Omega z)\right], \tag{3.18}$$

which were used to determine the initial conditions of the simulation and correspond to an extension of the definition of a Bright Temporal Soliton, presented in equation (3.18). The values of A, d, V, v, k and Ω are chosen according to the stability conditions provided in [71].

$$B^2 = \frac{\gamma + \frac{\lambda^2}{4\beta}}{\beta d^2 - \beta + 2\zeta d} \qquad \Omega = \frac{\lambda}{2\beta} \tag{3.19}$$

$$k = B^2\left[\zeta\left(1 - d^2\right) + 2\beta d\right] - \zeta\Omega^2 \qquad \frac{1}{v} = \frac{\zeta}{\beta} \tag{3.20}$$

and

$$(\eta\beta - \zeta\varepsilon)d^2 + 3(\varepsilon\beta + \zeta\eta)d - 2(\eta\beta - \zeta\varepsilon) = 0. \tag{3.21}$$

Indeed, when these stability conditions are meet, the simulations show that the Soliton remains stable over large propagation distances (see figure 3.6) in accordance to the results of reference [71].

Furthermore, if we reduce the amplitudes of the Soliton while maintaining all other parameters then, we fall out of the stability conditions (see figure 3.7a). In this case, during propagation the wave-package broadens and its peak intensity further decreases, in a way similar to the pulse broadening process explained in Chapter 2, where the nonlinear effects were not sufficient to compensate the dispersion.

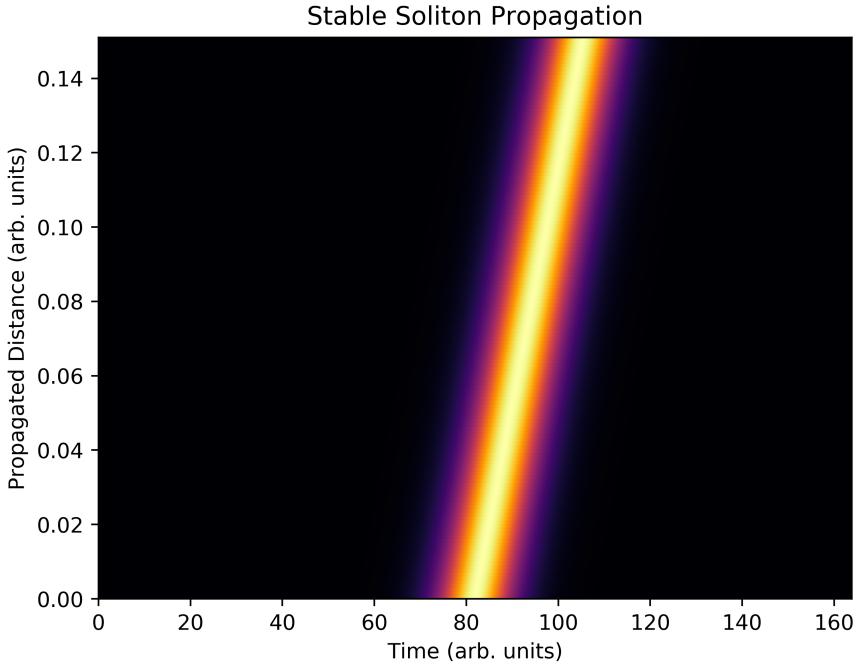

FIGURE 3.6: Simulated stable Bright Soliton in a dissipative Cubic-Quintic medium. We can observe an unchanged signal equally advancing, meaning that it has a linear phase.

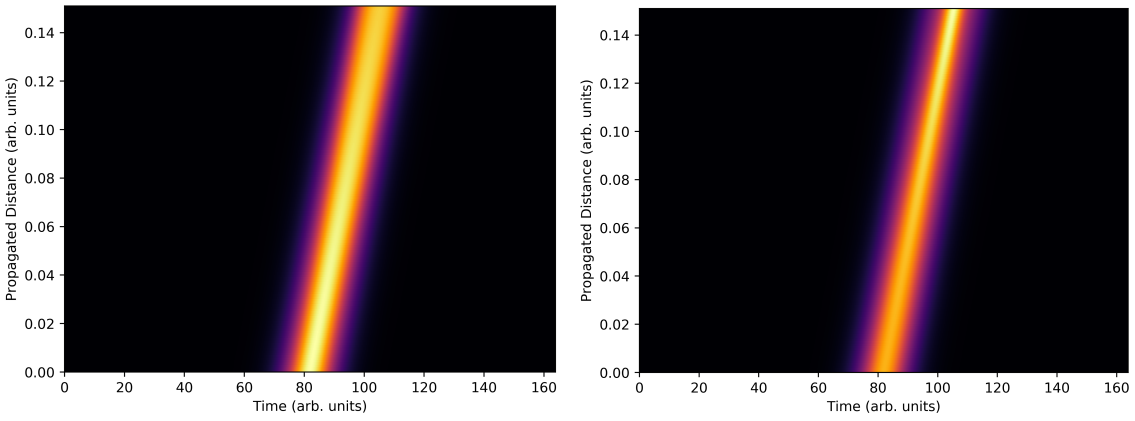

(A) (B)

FIGURE 3.7: In 3.7a the system has higher dispersive proprieties than the ones that ensure stability Solitonic propagation of the input signal and as it propagates the temporal pulse broadens. On the other hand figure 3.7b has an input intensity higher than the stability condition requires leading to an increasing of the Kerr lens effect and slowly deforming the signal.

In another simulation we increased the value of $\chi^{(5)}$ and thus enhanced the nonlinear compensation of dispersion beyond the stability conditions. As a result, the wave package experiences a nonlinear process of pulse compression (see figure 3.7b).

In these situations explored in figures 3.6, 3.7a and 3.7b are temporal analogues of the self-focusing regimes experienced by Spatial Solitons, as described in section 2.4.2. As expected, the solver not only reproduces the two unstable regimes but more importantly, is capable of simulating a stable Soliton with the parameters predicted by the analytical models. This indicates that numerical errors introduced by truncation or approximations intrinsic to the algorithms are sufficiently small and that the solver is well conditioned. Obviously, for the numerical parameters of the solver, such as integration step and spacial grid step, must be chosen to guarantee numerical stability and convergence.

3.4 Conclusions

In this Chapter we presented the theory, implementation and tests to a new *GPGPU* Supercomputing tool capable of providing faster results with higher resolution, compared to their counterpart in *CPU*. Such programming codes that use *GPGPU* cores are more complex. However they provide results with lower cost as a result of the endorsed optimization. We successfully implemented a library capable to solve numerically systems that are described by the Complex Cubic-Quintic Ginzburg-Landau Equation (*CGLE*) with very low runtimes.

The code was implemented in *C++* with *ArrayFire*, and so it is capable to run in almost every graphics card unit available in any computer, from laptops to workstations. This is an important achievement because now we can simulate a complex equation in virtually any machine, providing an high portability. The approach to benchmark the solver was dived in two manners; first against a single core hardware of a *CPU* in a workstation. We obtained a *SpeedUp* of around 55 using a *GTX Titan* with *CUDA* framework. When using mainstream desktop hardware we observed a good improvement, with 30 times less time required to simulate the propagation dynamics of such physical nonlinear light-matter interaction system; the other test-case we used to evaluate the solver was against multi-core *CPU*. Here the results are somewhat different in terms of scale, with a maximum SpeedUp of approximately 3.7. For low resolutions we found a separation of frameworks, with *CUDA* under-performing *OpenCL* and even the *Intel CPU*. Interestingly

and in contrary to the single-thread comparison, the *GPGPU*s of laptops cannot outperform the workstation *i7-4930K CPU*.

Once the code was constructed we tested its validity by comparing various runs of simulations to a known system. We simulated a stable Bright Dissipative Soliton in a cubic-quintic atomic gas to find the results to be in agreement with the literature. Also, changes in the parameters of the equation or the input signal have the expected outcome.

Chapter 4

Case Study 1: Nonlinear Temporal Dissipative Solitons

In the previous chapters we have introduced the *CGLE* and described the implementation and the features of a numerical tool developed using heterogeneous computing strategies such as *GPGPU* Supercomputing. However, while the solver is interesting *per se*, the problems that it is capable to tackle are what count the most. In these next two chapters we devote ourselves to the study of two distinct regimes that appear from the dual nonlinear/non-conservative nature of the *CGLE*. In this chapter, we explore how we can tame nature and the dissipative characteristics of real atomic optical media that are many times overlooked, to observe localized wave solutions, the so-called dissipative Solitons. Moreover, we discuss the opportunities that our code offer to tackle the problem of Rogue-Waves and the challenges of such problem, in order to provide numerically accurate results. These two cases are the opposite of each other, where in this Chapter stable propagation is seeked and in Chapter 5 we look for noise and breathing solutions. In both these cases the usage of our *GPGPU* Supercomputing solver is mandatory to achieve results with very high resolution in a relatively short amount of time.

4.1 Introduction

In Chapter 2 we outlined how the interaction between light and matter at the microscopic level influences the macroscopic optical properties. Remarkably, even though at a fundamental level these processes are described by the linear theory of quantum mechanics, the multiple feedback processes between light and matter results in an effective

change of the optical properties, not only of the linear refractive index but also of the nonlinear susceptibility [45]. Indeed, the exploration of these coherent optical effects associated with the atomic states of matter has been a topic of research in the last three decades, and its singular properties range from electromagnetic induced transparency [72] to slow-light [6], and light processing [53]. Also, and particularly interesting for the topic of this thesis, the quantum enhancing of the nonlinear response via a near-resonant interaction has motivated a lot of studies in nonlinear science, including the existence of Temporal [73] and Spatial Solitons [3], or even the realization of optical analogues [29]. Still, most of these studies often overlook the gain and dissipative properties, also characteristic of the near-resonance regime [11].

Indeed, the complexity of the microscopic interaction between light and matter does not express itself uniquely in a conservative way and in fact, not all the energy absorbed by matter is re-emitted into the electromagnetic field of light. Part of this energy is dissipated into other macroscopic mechanisms such as collision and eventually heat, resulting in optical losses [74]. Moreover, additional electromagnetic fields [71], pumping processes or even movement [49] that can modify the atomic populations, which in some cases can result into gain. To understand the mechanism and the role of these dissipative effects is a challenge of uttermost importance for real-life experiments and for the development of future technology. In the particular case of Soliton solutions, this perturbs the system to a state of non-equilibrium, making these self-localized solutions otherwise stable, unstable.

Remarkably, a class of solitary waves can still exist in some nonconservative systems. The solutions, often called dissipative Solitons or Auto-Solitons are a result from a double dynamical equilibrium achieved between not only the dispersion and nonlinearity - as the case for a conservative nonlinear optics system - but also between dissipation and gain mechanisms (see figure 4.1). The existence of Dissipative Solitons in optical systems is a topic of particular interest to the field of Lasers [7], contrary to what happens in the context of coherent media, where most of the field is still uncharted. The first work to consider this problem [71], predicted and analyzed the behavior of a family of solutions of Temporal Dissipative Solitons which propagate inside a hollow core photonic crystal fiber filled with a 3-level atomic system. This work constituted the main motivation for the results we present in this Chapter and which are part of the results of a publication recently prepared [75]. Still, the atomic system and settings we have used in our work has slightly different optical properties and tunable to an extent beyond that of the work [71]

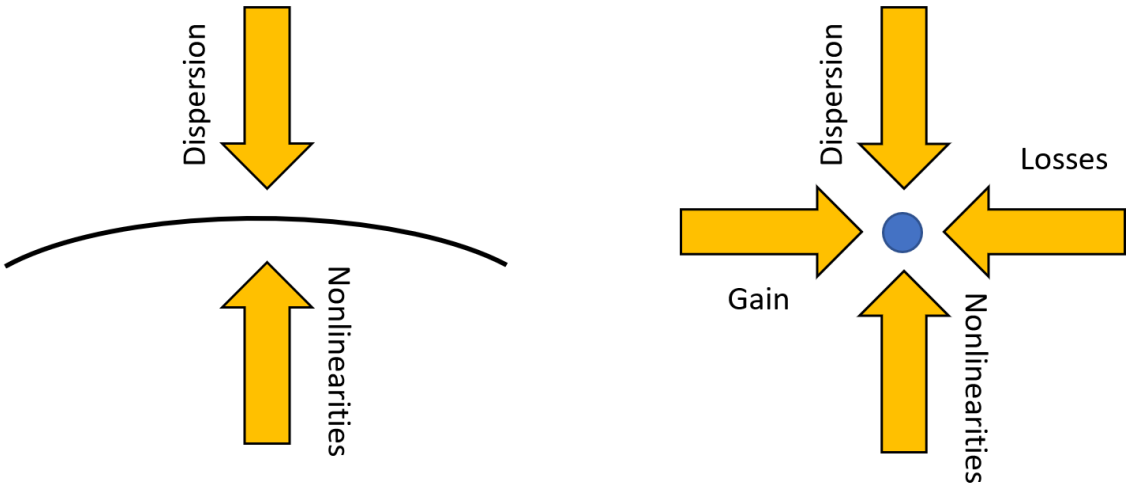

FIGURE 4.1: Qualitative representation of systems that lead to different families of solutions. In the left we have an Hamiltonian system that is balanced resulting in a family of Soliton solutions.However, in Dissipative systems, the double balance between various effects can lead to unstable behavior and only exists a fixed Soliton solution.

which allowed us to observe a different class of Dissipative Solitons.

4.2 Physical model

For now on, our problem of interest is the propagation of an optical pulse in a two dimensional waveguide with rectangular cross section, filled with a 4-level atomic system with$N$-type configuration, as represented schematically in figure 4.2. The optical pulse enters the media as a weak probe field $\boldsymbol{E}_p = \frac{\boldsymbol{e}_p}{2}\left[\mathcal{E}_p(r,t)\, e^{i\left(k_p z-\omega_p\right)t} + \text{c.c.}\right]$, which drives the transition $|1\rangle \rightarrow |3\rangle$ near-resonantly, with envelope function $\mathcal{E}_p(r,t)$ with center frequency ω_p, wave vector k_p and polarization vector $\boldsymbol{e}_p$. Moreover, the transition $|2\rangle \rightarrow |3\rangle$ also driven in near-resonance conditions by a continuous-wave strong control field $\boldsymbol{E}_c = \frac{\boldsymbol{e}_c}{2}\left[\mathcal{E}_c(r)\, e^{i(k_c z-\omega_c)t} + \text{c.c.}\right]$, with envelope function $\mathcal{E}_c(r)$, center frequency ω_c, wave vector k_c and polarization vector $\boldsymbol{e}_c$. Finally, an incoherent pumping mechanism drives the transition $|1\rangle \rightarrow |4\rangle$ in both ways. As discussed before in Chapter 2 and considering that the polarizations are orthogonal, $\boldsymbol{e}_p \cdot \boldsymbol{e}_c = 0$, the propagation of the probe beam can be described by a wave equation

$$\frac{\partial^2 \boldsymbol{E}_p}{\partial z^2} + \nabla_\perp^2 \boldsymbol{E}_p - \frac{1}{c^2}\frac{\partial^2 \boldsymbol{E}_p}{\partial t^2} = \frac{1}{\varepsilon_0 c^2}\frac{\partial^2 \boldsymbol{P}}{\partial t^2}. \tag{4.1}$$

where the polarization term

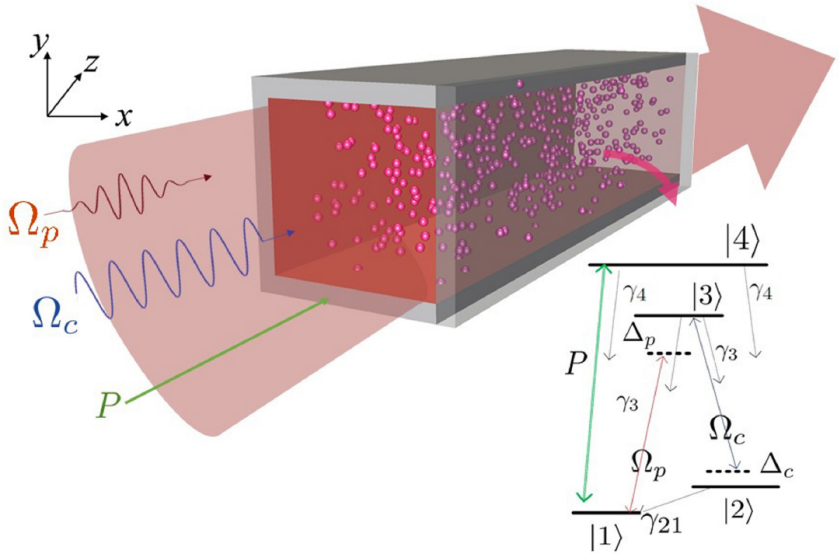

FIGURE 4.2: Representation of the physical system under study. A rectangular optical waveguide filled with a N-level energy scheme. Figure courtesy of Nuno A. Silva.

$$\boldsymbol{P} = \eta e^{i\left(k_p z - \omega_p t\right)} \boldsymbol{\mu}_{31} \rho_{31} + \text{c.c.}, \tag{4.2}$$

accounts for the optical response of the atomic media. In this definition, η stands for the atomic density, $\boldsymbol{\mu}_{ij}$ corresponds to the dipole moment of the transition $|i\rangle \rightarrow |j\rangle$ and ρ_{ij} are the matrix elements of the density matrix operator ρ. All the information about the average quantum state of the atoms in a specific region of space is contained in the density operator ρ and its time evolution is described by the Master Equation in the Lindblad form

$$\partial_t \rho = -\frac{i}{\hbar}\left[\hat{H}, \rho\right] - \frac{\hat{\Gamma}\left(\rho\right)}{2}, \tag{4.3}$$

where $\hat{\Gamma}$ is the Lindblad superoperator that accounts the relaxation and dephasing processes, and $\hat{H}$ is the Hamiltonian of the system. This equation constitutes the most general dynamical equation for the evolution of the density operator ρ when we neglect memory effects, which is an appropriate model for a gas in thermal equilibrium. Also, H is the Hamiltonian of the system given by

$$\hat{H} = \sum_{i=1}^{4} \hbar\omega_i \left|i\right\rangle - \frac{\hbar}{2}\left(\Omega_p e^{-i\omega_p t}\hat{\sigma}_{31} + \Omega_c e^{-i\omega_c t}\hat{\sigma}_{32} + \text{H.c.}\right), \tag{4.4}$$

where the Ω_i are the Rabi frequencies for the transitions defined as $\Omega_p = \mu_{31}E_p/\hbar$, $\Omega_c = \mu_{32}E_c/\hbar$ and $\hat{\sigma}_{ij} = \left|i\right\rangle\left\langle j\right|$ is the atomic projection operator. Under the rotating wave

approximation, we can derive the explicit form of the system of equations that arises from equation (4.3) [75].

$$\nabla^2\mathbf{E} - \frac{1}{c^2}\frac{\partial^2\mathbf{E}}{\partial t^2} = \frac{1}{\varepsilon_0 c^2}\frac{\partial^2\mathbf{P}}{\partial t^2}. \tag{4.5}$$

The combination of the wave equation (4.5) with the master equation (4.3) constitute the notorious Maxwell-Bloch system (*MBS*). In general, the interaction dynamics between the atoms and the field described by the *MBS* is complex, making it extremely difficult to be studied using analytic and numerical methods [76]. Instead, one often considers cases where the system has evolved into a quasi-equilibrium were the atomic state remains stationary. In these cases, it is possible to determine the matrix elements of the density matrix operator ρ_{ij} corresponding to the transition between atomic levels and express the macroscopic optical response in terms of the susceptibilities as previously discussed in Chapter 2 using perturbative methods. However, this approach is not valid for the case of pulsed fields, which feature a variation of the envelope in time, violating the steady-state approximation. In these cases, a more sophisticate approach needs to be employed, which is based on the perturbative multiple scale technique [71, 77].

Employing this multiple scale technique, as described in the paper [75], it can be obtained an effective $(1+1)$-dimensional model enclosing the dynamics of the *MBS* as

$$\begin{aligned} i\partial_z\psi + \zeta\partial_t^2\psi + \eta|\psi|^2\psi = \\ i\beta\partial_t^2\psi + \lambda\partial_t\psi + i\gamma\psi + i\varepsilon|\psi|^2\psi \end{aligned} \tag{4.6}$$

where ζ, η, β, λ, γ, and ε are effective parameters that can be obtained from the physical properties of the media. This model corresponds to the already introduced *CGLE*, with the left hand-side terms of the equation describing the usual dynamics of an envelope function in a nonlinear medium, while the extra terms in the right hand side account for the non-conservative phenomena. Also, each of the terms has it own interpretation in the context of optics, as discussed previously in Chapter 2, and for the atomic media under consideration, can be tuned to a great extent in the parameters space using experimentally tuned parameters of the system. This discussion fall out of the topic of the chapter, but more information is discussed in detail in the extended version of the paper [75].

4.3 Dissipative Soliton Solutions

If one considers the *CGLE* described by equation (4.6) without the non-conservative terms of the right hand side, it is straightforward to obtain a standard *NLSE* in a $(1+1)$-dimensional system. As mentioned before in Chapter 2, this conservative model can be applied to a wide range of fields in physics and in particular to optics, and one of its hallmarks is that it admits a family of stable localized wave solutions, the so-called Solitons. Moreover, Solitons can be either of the Bright (if $\zeta\eta = 1/2$) or Dark Solitons(if $\zeta\eta = -1/2$) depending on the signal of the dispersion and of the nonlinearity. However, if $\lambda \neq 0$, $\beta \neq 0$, $\varepsilon \neq 0$ or even $\gamma \neq 0$, these solutions are no-longer stable due to the dissipative properties of the system, and in the case of optics, due to the loss of energy of the electromagnetic field. Still, in some cases, it is possible to employ a semi-analytic and perturbative approach to find, within the typical class of Soliton solutions described in the following equation

$$\psi(z,t) = A\text{sech}^{1+id}\left[V\left(z - \frac{t}{v}\right)\right]\exp\left[i\left(kt - \Omega z\right)\right], \tag{4.7}$$

an equilibrium point in the parameters space [71]. However, the perturbative nature of this approach does not warrant that the solution is indeed a stable one.

Still, and as mentioned before, such systems can still admit a class of localized solutions called Dissipative Solitons, if additional equilibrium conditions between gain and loss are met. First proposed in a work by *Pereira and Stenflo* [78], the existence of this solutions is well reported in the literature, particularly in [11] and [79], for both the case of the cubic and the cubic-quintic *CGLE*. More recently, works by *Borhanian et. al.* [17] and *Facão et. al* [71] extended the class of solutions to include the imaginary part of the first order dispersion. The regions of parameters and their relation to the stability of these solutions is also well discussed within the references.

For the case we are considering, we need to use the ones proposed by Facão *et. al.* [71], which where already introduced in equation (4.7) and with the parameters

$$\begin{aligned} A &= \sqrt{\frac{3V^2 d\,(1+4\beta^2)}{2\,(2\eta\beta-\zeta\varepsilon)}} \\ V &= \sqrt{\frac{\gamma+\frac{\lambda^2}{4\beta}}{\beta d^2-\beta+\zeta d}} \\ \Omega &= -V^2\left[2\nu d-\frac{\zeta\left(d^2-1\right)}{2}\right]+\zeta d^2 \\ k &= -\frac{\lambda}{2\nu} \\ v &= \zeta\frac{2\nu}{\lambda}, \end{aligned} \tag{4.8}$$

and with the chirp parameter d equals to

$$(\eta\beta-\zeta\varepsilon)d^2+3(\varepsilon\beta+\zeta\eta)d-2(\eta\beta-\zeta\varepsilon)=0. \tag{4.9}$$

$$d=\frac{6(\varepsilon\beta+\zeta\eta)+\sqrt{6^2(\varepsilon\beta+\zeta\eta)^2-32(\eta\beta-\zeta\varepsilon)^2}}{4(\zeta\varepsilon-\eta\beta)}. \tag{4.10}$$

It can also be shown that the family of solutions is only stable [18] provided that the following conditions are met simultaneously

$$\beta > 0 \tag{4.11}$$

$$\gamma+\frac{\lambda^2}{4\beta} > 0 \tag{4.12}$$

$$\varepsilon > \frac{\beta\left(3\sqrt{1+4\beta^2}-1\right)}{4+18\beta^2}. \tag{4.13}$$

Unfortunately, it happens that the region of stability of the Soliton exactly coincide with the region of the instability for the background, $\gamma+\frac{\lambda^2}{4\beta}<0$. This was previously noted in other type of Dissipative Soliton solutions and means that the stability of the solution is limited by the growth rate of the background, which is significant at distances $z_{ins}\sim\left(\gamma+\frac{\lambda^2}{4\beta}\right)^{-1}$.

4.4 Simulations with *GPGPU*

At this point we have information about the medium, the type of solution, as well as the relations between the stable dissipative solution and the proprieties of that medium.

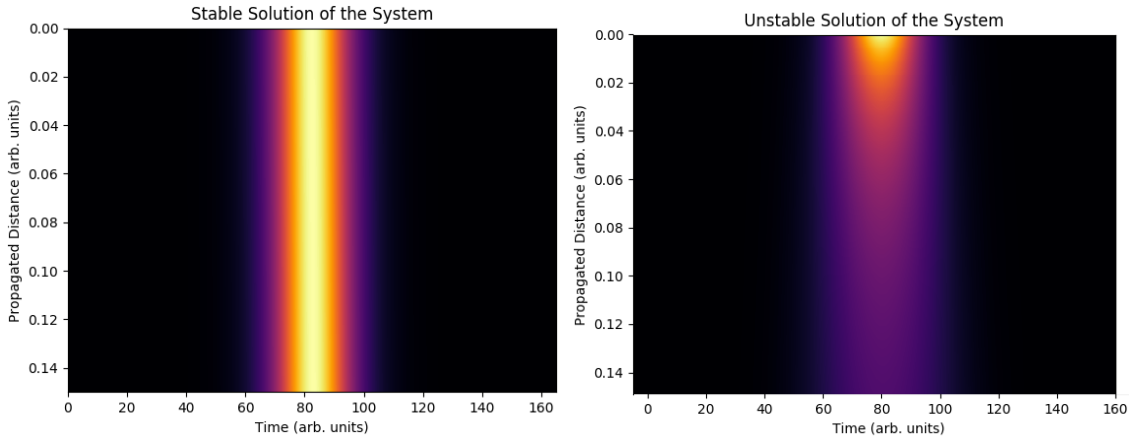

(A) (B)

FIGURE 4.3: *(A)* Stable propagation of a dissipative solitonic solution, and *(B)* is the result of the propagation of a simple sech Bright Soliton in a medium that does not support such solution.

With the developed solver mentioned in Chapter 3 we can simulate the propagation dynamics of the input signal. The case proposed in the previous section is a typical situation of dissipative nonlinear optics phenomena that requires our *GPGPU* solver to study its long-run proprieties.

For the 4-level atom atomic system considered here we have chosen appropriate experimental values to obtain the effective parameters to equation (3.17), $\zeta = -1/2$; $\beta = 3.5 \times 10^{-4}$; $\lambda = 1.10 \times 10^{-3}$; $\gamma = 2.46 \times 10^{-2}$; $\eta = 1.00$; $\varepsilon = -91.5$; $\nu = 2.00 \times 10^{2}$ and all the remaining ones $\sigma = \alpha = \mu = 0$. For this case the dissipative Solitons solution of equation (4.6) has parameters $A = 0.28$, $V = 0.087$, $\Omega = -0.128$ and chirp $d = 5.75$. Using this values we have performed numerical simulations with our *GPGPU* Supercomputing solver to investigate both qualitatively and quantitatively the nature of these solutions. For comparison purposes, we also show the results of a numerical simulation of typical sech-type Solitons (introduced in equation (2.32) of Chapter 2) with the previously enunciated parameters. The results of both simulations are presented in figures 4.3a and 4.3b. If we verify the observations previously made in this chapter regarding if a system is favorable to dissipative Solitons, we verify that it all comply within the condition $\eta\zeta = -1/2$ and $\gamma \neq 0$, so we are in a physical system that allows dissipative stable Solitonic solution in the form of Bright-Soliton, given by equation (4.7). Furthermore, the solution proper values must obey the set of condition presented in (4.8), (4.9) and (4.13).

Knowing this we can provide it to the solver and simply wait for the program to simulate the propagation dynamics of such an open dissipative system. This was done

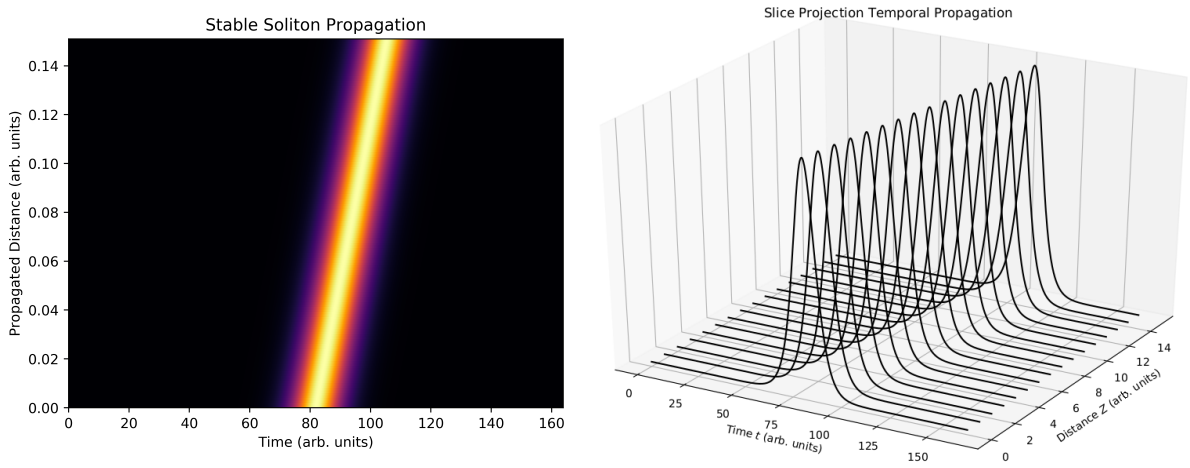

(A) (B)

FIGURE 4.4: *(A)* Result of the simulation data using the *GPGPU* solver with a *GTX Titan* and *CUDA*. The medium parameters are $\zeta = -1/2$; $\beta = 3.5 \times 10^{-4}$; $\lambda = 1.10 \times 10^{-3}$; $\gamma = 2.46 \times 10^{-2}$; $\eta = 1.00$; $\varepsilon = -91.5$; $\nu = 2.00 \times 10^{2}$ and all the remaining $\sigma = \alpha = \mu = 0$. *(B)* Sliced view of the propagation characteristics of the same system under study. We observe the same proprieties as before but now from a 3D projection.

and the result is presented in figure 4.4a.

In figure 4.4a is depicted the same data as in figure 4.4b but now in a *3D* projection of various steps along the simulated propagation distance. It is very interesting to observe the maximum amplitude and width conservation with the linear phase shift along the medium.

The outcome is interesting: we do have a medium with nonzero values of β, γ and ε heavily determining dissipative effects, and if the sign of each is positive, which is the case of the first two and the last one representing a quintic nonlinear gain because it is negative, remembering that the relation between ε and γ is critical to the formation of dissipative Solitons. We were able to have stable propagation of a pulse solution in a dissipative open-system as a result of temporal stability conditions and the balance of dispersion, nonlinearities, gain, and losses. It is also extraordinary the fact that a *GPGPU* solver was able to simulate such system dynamics in a reduced time scale when compared with others *CPU* programming techniques.

Also very curious is the fact that from the set of previously presented conditions that define the parameters to guarantee stable propagation, there is a duality nature that allows us to consider a change in one to represent a variation in the other. This allows us to tune the work in two aspects: if we know the type of desired solutions then the appropriate medium susceptibilities and dispersion must be adjusted, or the other way around;

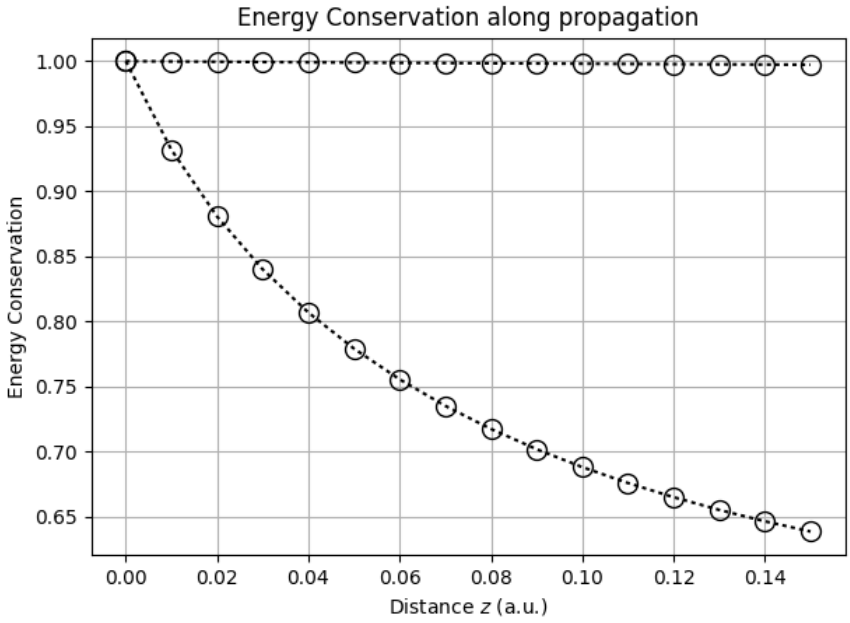

FIGURE 4.5: Results of energy conservation for the numerical evolution of a Soliton solution of the form of equation (2.32) (unstable) and of equation (4.7) (stable) in a medium described by equation (4.6).

if a specific medium is required we are able to compute the various parameters of the solution to ensure dissipative Solitons to flow unchanged.

As it can be seen the Dissipative Soliton solution preserves its shape, amplitude and main characteristics, contrary to what happens to the non-dissipative type Soliton. This is explicit in a conservation of energy

$$N(z) \equiv \frac{\int_{-\infty}^{+\infty} |\boldsymbol{E}_p(z,t)|^2 dt}{\int_{-\infty}^{+\infty} |\boldsymbol{E}_p(0,t)|^2 dt} \tag{4.14}$$

whose results are presented in figure 4.5. This allows us to confirm the type of solutions in Dissipative Solitons and that the loss of energy of Dissipative systems follows a decaying exponential behavior [80].

We studied how a stable dissipative Soliton propagates in a medium if the correct shape and constants are provided. However, if this is not the case the signal is no longer stable and this is what occurs for real system, since noise significantly affects physical effects that are so sensitive to small fluctuations. Since that the stability is limited by the background up to a significant distance

$$z_{ins} \approx \left(\gamma + \frac{\lambda}{4\beta}\right). \tag{4.15}$$

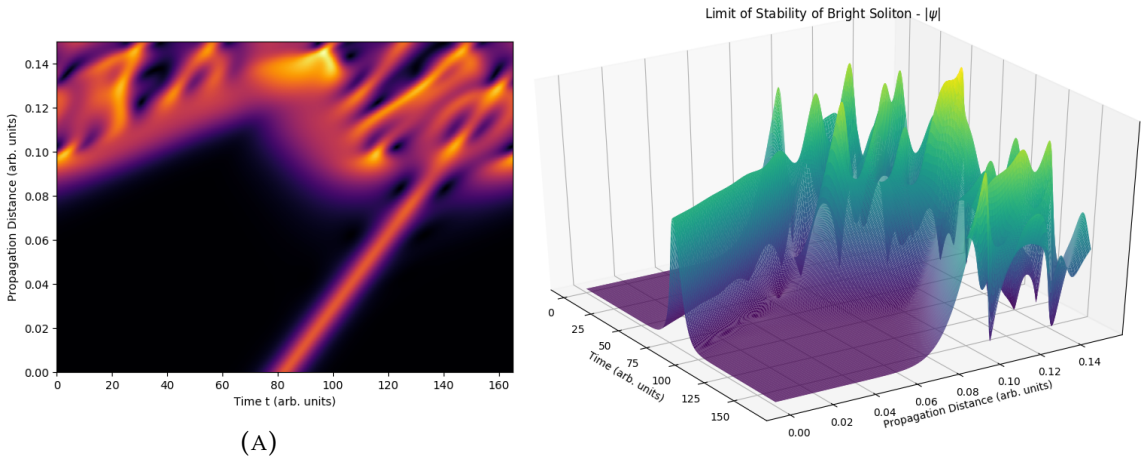

(A) (B)

FIGURE 4.6: Representation of the *GPGPU* Supercomputing simulation of a Soliton profile propagating in a medium that allows stable Dissipative Solutions but that is affected by background instability. In (A) we have the relative data plotted in a plane and in (B) the same output results but in a more intuitive *3D* projection representation.

With our *GPGPU* Supercomputing solver we can predict how such episodes can occur and what is the behavior along the propagation. For example, in figures 4.6a and 4.6b we have simulated a system that is affected by such effects, ultimately leading to its collapse. Also, since the condition of instability of the background is not met, we cannot have infinite stable background.

Observing in figure 4.6a that the input signal is similar to the stable one of figure 4.2, however after some characteristic propagation distance z_{ins} the background starts to be heavily unstable and ultimately affects the Dissipative Soliton leading to its collapse. The $3D$ projection of the same data in figure 4.6b allows us to intuitively notice how the low noise eventually leads to the destruction of the stable solution.

This system has the gain balanced with loses. In the profile analysis of figure 4.7 we can observe that there is a substantial difference in energy at the end in comparison with the input one. Curiously, the chaotic information provided by this simulation allows us to better understand the importance of small changes in the pulse shape and the dramatic effects it can lead to [28], so we must be aware that real systems must be very well designed and prepared.

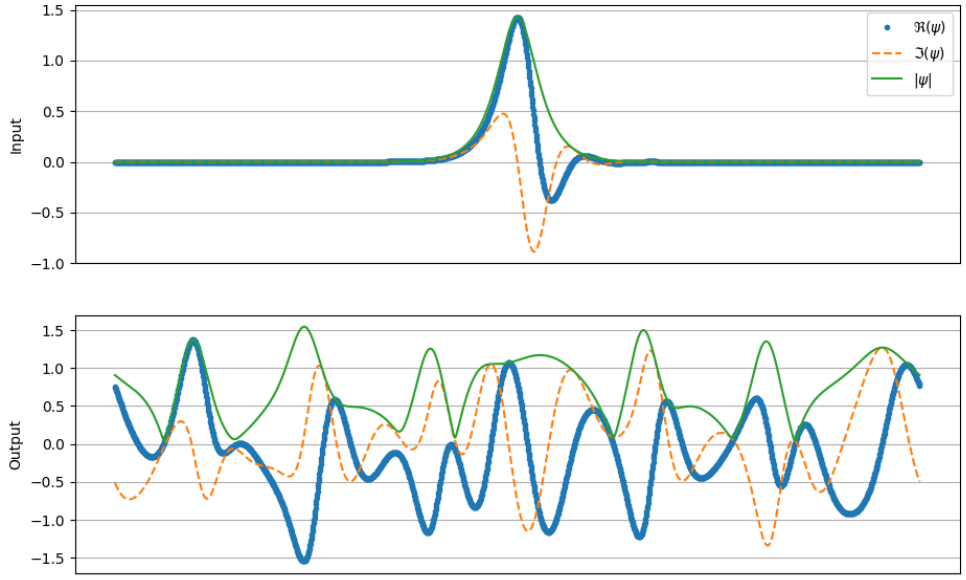

FIGURE 4.7: Comparison of the Optical Time Pulse profile signals at the input (above) of the medium and the result at the output (bellow). Both Real, Imaginary parts as well the modulus of ψ are represented.

4.5 Conclusion

In conclusion, we were able to study the dynamics of a nonlinear dissipative system to the propagation of an input signal modulated by a Dissipative Bright Soliton shape in a dissipative medium.

Based in the *SVEA* we described how Temporal Solitons are important in these quantum systems and developed a dissipative nonlinear atomic gas simulation experiment confined to a waveguide which requires the *CGLE* to completely describe the system and, since the *GPGPU* Supercomputing solver developed in the previous chapter is capable to simulate the dynamics of such configuration, we employed it to run various simulations to study how dissipative Solitons behave in such conditions.

We concluded that a dissipative medium can admit a specific pulse shape - Dissipative Bright Soliton - to propagate without any change in amplitude because of a spot-on balance between all the effects that the *CGLE* account and that are established in the form of a mathematical equation. Also, the fact that we can calculate these results in a fraction of the time that is required by *CPU* programming is mesmerizing. The influence of

the background noise is very important to determine the overall distance of stability and heavily determines conditions in experimental situations.

Chapter 5

Case Study 2: Rogue Waves

In the previous chapter we studied stable and balanced optical propagation with predictable steady-state long run optical behavior. However, the *CGLE* allows to study other complex and very interesting phenomena, such as Rogue-Waves, also known as Extreme Events which are very mysterious phenomena that has been studied in recent year. Various studies shown that it has some link to Solitonic Breathers and that only occurs in the presence of strong nonlinearities, both in Optical Physics but also in Oceanography [81]. While in the previous Chapter we observed solutions of the *CGLE* that are stable, here we present the other side of the picture, with unbalanced systems.

This phenomenon occurs without any warning nor signal and at the same speed it appears it then completely disappears leaving no trace behind. There is not yet a broadly accepted model capable to completely explain the origin. We hope to discuss some possible models capable to introduce some common ground. However, because Rogue-Waves are a newborn topic there is still a lack of complete uniformity in the literature, namely in Optics.

Provided the right conditions and input signal, in Nonlinear Optics we can achieve a state where the event will occur somewhere down the propagation path. Our *GPGPU* Supercomputing solver is capable to simulate these extreme nonlinear media and we hope to achieve these results. Furthermore, we are interested in study how the input noise provided in can impact the long run proprieties of the signal and if there is any dependence of these proprieties with the noise. Since we can simulate very large amount of datasets in a relatively fast way, we will dedicate strong efforts in order to try better understand this mysterious phenomenon and its statistical proprieties.

5.1 Introduction

The study of Rogue-Waves (*RW*) arise from the field of fluid dynamics and oceanography to investigate the origins and dynamics of very large surface waves that appear suddenly on the ocean. Several studies have established a relation between the emergence of *RW* and nonlinear phenomena [14, 15, 82] and excitations, such as Spiny Solitons [7, 21], however many aspects of this type of waves remain to be investigated. It is believed that they arise when waves traveling at different speeds momentarily overlap and interfere constructively at a given position and for a few brief instants. Other explanations suggests that *RW* arise from nonlinear instabilities that transfer energy between waves and concentrate it in one of them before redistributing it back to the original waves.

RW are not unique to oceanic waves. Many other systems support phenomena that resemble *RW*. This includes the *CGLE*, which as been used to study extensively the proprieties of *RW* via numerical simulations [20, 83]. It has been suggested that the emergency of *RW* in the *CGLE* may result from the nonlinear interaction of fluctuations or noise either, such as Modulation Instability (*MI*) [84–87]. To some extent, *RW* are the opposite of Dissipative Solitons. While Dissipative Solitons constitute a stable solution of the *CGLE* that result from a delicate balance between different dynamics (dispersion, nonlinear effects, gain and loss), *RW* appear to be the result and expression of instability, coincidence, randomness and nonlinear wave interaction.

Another aspect which distinguishes the Dissipative Solitons studied in the previous Chapter and the *RW* supported by the *CGLE* is that while the former considered media with focusing nonlinearities, the latter was only identified in media with defocusing nonlinearities. If rather than the more complex *CGLE* we consider the *NLSE*

$$i\frac{\partial\psi}{\partial\xi}+\frac{1}{2}\frac{\partial^2\psi}{\partial\tau^2}+N^2|\psi|^2\psi=0, \tag{5.1}$$

we find that defocusing media typically supports a multitude of Solitons solutions similar to the Dark Temporal Soliton studied in section 2.4.1, corresponding to localized depressions in optical intensity in an uniform background. Among these, one of the most well known solution is the Peregrine Soliton (see figure 5.1)

$$\psi\left(\xi,\tau\right)=\left[1-\frac{4\left(1+2i\xi\right)}{1+4\tau^2+4\xi^2}\right]\mathrm{e}^{i\xi}, \tag{5.2}$$

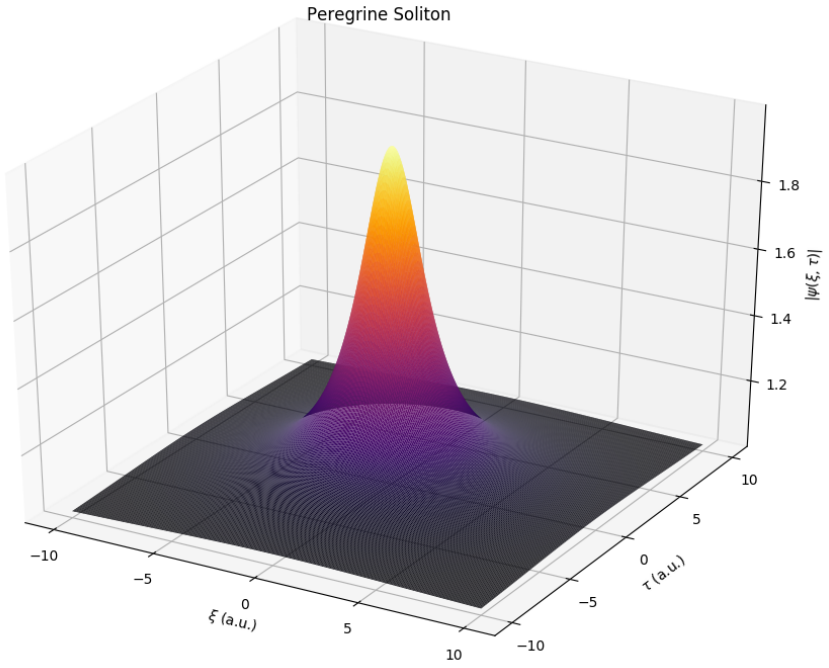

FIGURE 5.1: 3D representation of a Peregrine Soliton propagating on a stable constant background optical medium. Temporal and Spatial axis are set to arbitrary units.

which is characterized by a double spatio-temporal localization. In particular, it starts out as a weak oscillation on a continuous background and then develops a progressive increase in amplitude and a narrowing in temporal duration. After reaching a maximum of amplitude, this Soliton undergoes the reverse process and fades away into the background. This dynamics resemble qualitatively the proprieties of *RW*, which enticed the hypothesis of using them to explain or model *RW*.

Recent studies attempt to include higher-order nonlinearities and corrections, and in the process generalize and adapt the solutions from the *NLSE* into the *CGLE*. This is important because some phenomena can only be observed when considering the balance or unbalance between processes such as nonlinearities, dissipation, losses, etc.. This includes a solution of the $(1+1)$-dimensional *NLSE* known as the Akhmediev Breather [85, 88] which was proposed in 1986 and corresponds to a periodic revival of the Peregrine Soliton (see figure 5.2). The mathematical description of this solution is given by

$$\psi(\xi,\tau) = \left[\frac{(1-4a)\cosh(b\xi) + \sqrt{2a}\cos(\Omega\tau) + ib\sinh(b\xi)}{\sqrt{2a}\cos(\Omega\tau) - \cosh(b\xi)}\right] e^{i\xi} \tag{5.3}$$

where Ω is known as the dimensionless modulation frequency $a = \frac{1}{2}\left(1-\Omega^2/4\right)$, with $0 < a < 1/2$ determining the frequencies that experience gain and $b = \left[8a\left(1-2a\right)\right]^{1/2}$.

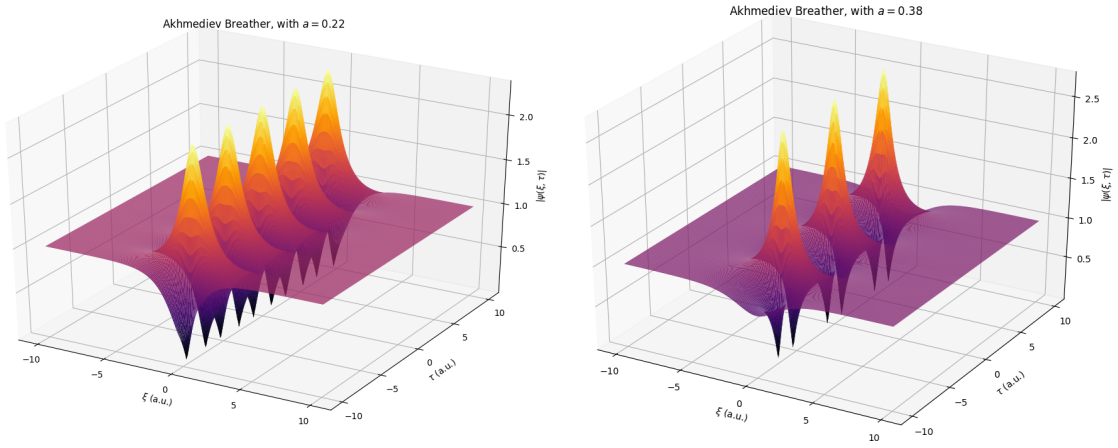

(A) (B)

FIGURE 5.2: Representation of two different states of Akhmediev Breathers in the same mesh dimensions when varying the parameter a from $a = 0.22$ - figure 5.2a - to $a = 0.38$ - figure 5.2b. This changes the spikes density by reducing the spatial width. There is also a small change in the temporal width.

The characteristics of the breather depends strongly on the modulation frequency a, which controls the temporal separation between Soliton revivals, as shown in figure 5.2.

Another family of analytical solutions of the *NLSE* that share similarities with *RW* are the complex Kuznetsov-Ma Breathers (*K-Mb*) [89], which are a form of nonlinear superposition of a Bright Soliton (*BS*) and a uniform background, corresponding to a plane wave. These breathers are different from the Akhmediev breathers that are driven solely by the *MI*. While the Akhmediev breathers that are driven solely by the *MI*, the *K-Mb* can results from the combination of *MI* and other processes [90]. The K-Mb can also be generalized as solutions of the *CGLE* [91], resulting in

$$\psi(\xi,\tau) = \left[s - \frac{2\left(b^2 - s^2\right)\cos(\gamma\tau) + i\gamma\sin(\gamma\tau)}{b\cosh\left(2\xi\sqrt{b^2 - s^2}\right) - s\cos(\gamma\tau)} \right] e^{is^2\tau} \tag{5.4}$$

were $\gamma = 2b\sqrt{b^2 - s^2}$. The parameter $b \geq s$ determines the initial shape of the nonlinear wave, while s is the background amplitude. We can observe two main terms in equation (5.4): the first is related to the uniform background, while the other describes the dynamical nature of the *BS* [92]. A first order Kuznetsov-Ma Breather is represented in figure 5.3

There is a curious relation between the *K-Mb* and the Bright Solitons discussed in section 2.4.1. If we consider the expression for the *K-Mb* [90, 91] and analyze the shape of the nonlinear wave at specific instants of time given by

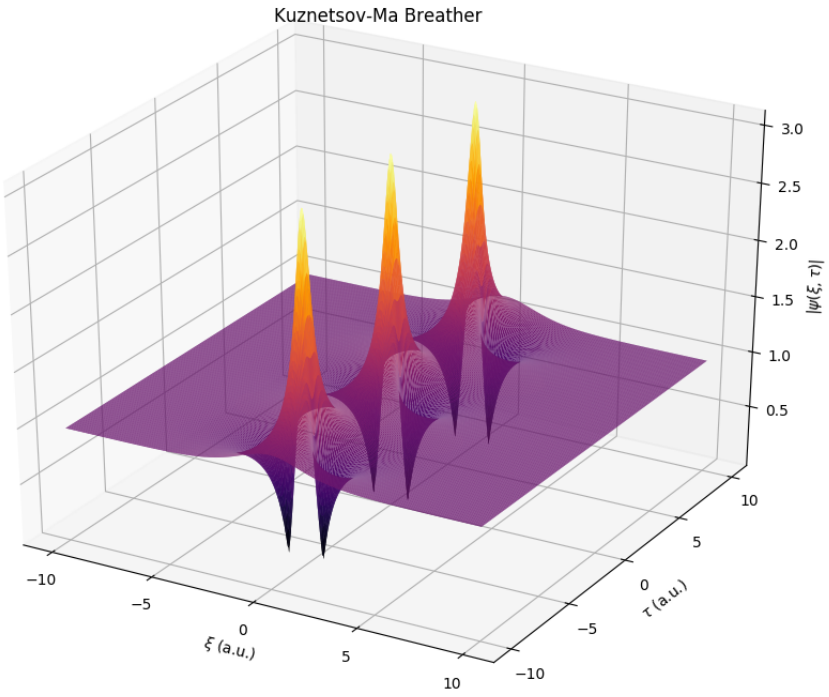

FIGURE 5.3: 3D Projection representation of a first-order Kuznetsov-Ma Breather, which is a breathing solution of the *NLSE*. The axis values are of arbitrary units.

$$\tau_p = \frac{\pi + 2n\pi}{4b\sqrt{b^2 - s^2}}, \tag{5.5}$$

where n is an integer, we identify by direct substitution the expression of a Bright Soliton

$$\psi\left(\xi, \tau_p\right) = \left[s - 2i \operatorname{sech}\left(2\sqrt{b^2 - s^2}\xi\right)\right] \mathrm{e}^{i\phi}, \tag{5.6}$$

such that $\phi = s^2 \frac{\pi}{4b\sqrt{b^2 - s^2}}$.

Also, numerous physical phenomena involve waves with two or more components (for example, to take into account different polarizations), which can exchange energy between themselves and have been recently shown to support *RW* [68]. These systems are described by vector Nonlinear Schrödinger Equation (*VNLSE*), which over recent years have been established as a paradigm of nonlinear systems with multiple degrees of freedom [93]. Another example is the Manakov System [94]

$$\partial_\tau v_1 + i\zeta v_1 = q_1 v_2 + q_2 v_3 \tag{5.7a}$$

$$\partial_\tau v_2 - i\zeta v_2 = -q_1^* v_1 \tag{5.7b}$$

$$\partial_\tau v_3 - i\zeta v_3 = -q_2^* v_1, \tag{5.7c}$$

which have been reported to support vector Bright-Dark Soliton, Dark-Dark Soliton and Rogue-Waves [86].

Clearly, there is a multitude of nonlinear systems that support *RW* or Solitonic excitations that share similarities with *RW*. They all suggest that nonlinear processes play a role in the formation and dynamics of *RW*. A question arises though on the role of noise and fluctuations on the formation of *RW*, as suggested by the early explanations of oceanic *RW*. This last aspect will be investigated in the following sections.

5.2 Noise, Coincidences and Rogue-Waves

The previous section discussed how particular solutions of the *CGLE* exhibit phenomenology similar to RW. This suggests that *RW* can constitute unstable nonlinear excitations [95]. However, this is not the only candidate explanation for *RW*.

Another possible interpretation does not even require the existence of nonlinear effects. For example, a set of linear waves with different frequencies can overlap momentarily at a given position, interfere constructively and then break away. This sort of processes has been identified in the field of quantum chaos as waves propagate in a quantum stadium and quantum corrals [19] with specific shapes [96].

To illustrate this hypothesis, consider a closed domain containing a large number of strongly localized wave packets, which for sake of simplicity are such that they all have the same phase at the maximum of amplitude. Also assume that the boundaries of the domain are perfectly reflective and that there is no dissipative or diffractive processes. Furthermore, all the waves are randomly distributed throughout the domain, constituting what could be described as noise. Then, if these wave packages obey a linear equation of propagation, such as the ordinary Schrödinger equation, they do not interact and the system can be considered as an ideal gas of waves.

Now, we divide the domain into little cells of size comparable to the width of the wave package and compute the probability of finding x of them simultaneously at a given cell. This probability is approximately given by [97, 98]

$$P(x) = C_n^N p^n (1-p)^{N-n}, \tag{5.8}$$

where N is the total number of wave packages and p is the probability of a given wave-package to be in a specific cell.

Since the wave-packages all have the same phase at their center, then the probability of having a wave with an amplitude n times than the average coincides with $P(n)$, basically a binomial distribution.

This very simple model developed only to illustrate how coincidence may produce similar effects to *RW* even in linear systems can be easily improved to become more realistic. This type of events is studied in Extreme Value Theory [99], a branch of statistics that investigates extreme deviations from the mean of the probability distributions.

One interesting prediction of this theory is that the distribution of extreme events can only converge to one of three possible distributions: (i) the Gumbel distribution [100]; (ii) the Fréchet distribution [101]; or (iii) the Weibull distribution [102]. This theorem is known as the Extreme Value Theorem or the Fisher–Tippett–Gnedenko Theorem [103].

Finally, it should be noticed that despite this discussion assumed that the dynamics of the waves is linear, this is not a requirement. Nonlinear behavior certainly introduces a more complex phenomenology and allows for waves to interact, exchange energy and collide.

5.3 Nonlinear Wave Interactions

Another explanation for the formation of RW has been attributed to nonlinear coupling between waves. The idea is that the nonlinear effects can introduce effective interaction between wave packages that can result in the momentary concentration of energy in one of them. As illustration of this type of processes, consider a nonlinear medium governed by the *NLSE* [43]

$$i\frac{\partial\psi}{\partial\xi}+\frac{1}{2}\frac{\partial^2\psi}{\partial\tau^2}+N^2|\psi|^2\psi=0, \tag{5.9}$$

and assuming that the wave can be written as

$$\psi(\xi,\tau)=\sum_{n=-N/2}^{N/2}\phi_n(\xi,\tau)\,\mathrm{e}^{i(k_n\xi-\omega_k\xi)}. \tag{5.10}$$

Then, replacing this in the *NLSE* of equation (5.9) and considering the *SVEA*, we obtain the following envelope equation for each wave package

$$i\left(\partial_\xi+2\omega_n\partial_\tau\right)\phi_n=-N^2\mathcal{F}_n, \tag{5.11}$$

where $\mathcal{F}_n$ is the nonlinear coupling between waves and given by

$$\mathcal{F}_n = \phi_0^* \phi_0 \left[\phi_{n-1} e^{i\Delta^+ \tau} + \phi_{n+1} e^{i\Delta^- \tau} \right], \tag{5.12}$$

where $\Delta^\pm$ are the phase mismatch and given by

$$\Delta^\pm = \mp k_0 \pm k_1 + k_{n\mp 1} - k_n. \tag{5.13}$$

When writing the nonlinear coupling, we are taking into account several assumptions:

(i) the nonlinear terms proportional to $|\phi_m|^2 \phi_n$ with $m \neq 0$ have been neglected since we are considering that all wave packages are sufficiently weak not to produce any noticeable self or induced phase modulation;

(ii) ϕ_0 represents an uniform background on top of which all other wave packages exists and $|\phi_0| \gg |\phi_m|$ for $m \neq 0$;

(iii) ϕ_0 remains approximately constant.

Then, we can write for $\Delta^\pm \approx 0$ that

$$\frac{d}{d\eta} \phi_n = i\mathcal{W} \left[\phi_{n-1} + \phi_{n+1} \right], \tag{5.14}$$

with

$$\tfrac{d}{d\eta} \approx \left[\partial_\xi + 2\omega_n \partial_\tau \right] \tag{5.15}$$

$$\mathcal{W} = N^2 |\phi_0|^2. \tag{5.16}$$

Using the following transformations

$$\phi_n = (-1)^{s/2} A_n \tag{5.17}$$

$$z = 2\mathcal{W}\eta, \tag{5.18}$$

it is possible to rewrite equation (5.14) in a way which is identical to the recurrence relation for the Bessel functions $\mathcal{J}_n(z)$,

$$2\frac{d}{dz} A_n = A_{n-1} - A_{n+1} \tag{5.19}$$

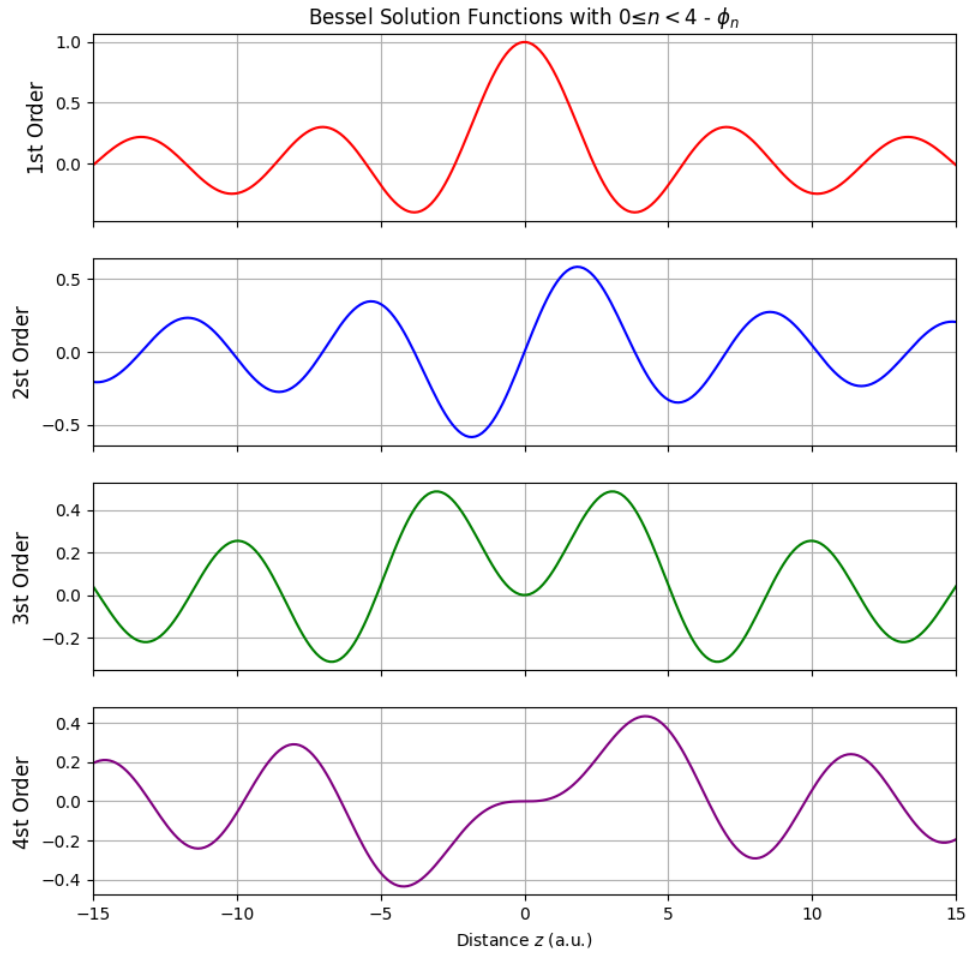

FIGURE 5.4: Representation of the first 4 orders of Bessel Functions that are solutions of equation (5.19). As we can see, only for $n = 0$ we have a non-null value of the function $A_n(z)$. Amplitude values are normalized.

which has the solution

$$A_n(z) = A\mathcal{J}_n(|z|) + A'\mathcal{J}_{n-1}(|z|) \tag{5.20}$$

Assuming that the whole energy is concentrated in the wave package ϕ_n at $z = 0$, we obtain the following values of A_n at $z = 0$ as

$$A_0(0) = A \quad , \quad A_1(0) = A' \quad , \quad A_{n\neq 0,1}(0) = 0, \tag{5.21}$$

since $\mathcal{J}_0(0) = 1$ and $\mathcal{J}_n(0) = 0$, for $n \neq 0$.

A representation of this solution is presented in figure 5.4, where it is possible to verify that the energy initially distributed by all the wave packages gets concentrated in ϕ_1 at $z = 0$ and then returned back to their original wave packages. Furthermore, using the fundamental proprieties of the Bessel functions, we can obtain

$$\sum_{+\infty}^{n=-\infty} |A_n(z)|^2 = A^2 + A'^2 = contant, \tag{5.22}$$

implying the conservation of energy during this nonlinear interaction.

Another process that can exist in nonlinear wave interaction is sometimes called Modulation Instability, which instead of considering the interaction and energy transference between different waves, looks at the evolution of a single wave on top of the plateau. In this case one may consider that the dynamical equation for the propagation is simply

$$\frac{\partial \psi}{\partial \xi} + I\beta_2 \frac{\partial^2 \psi}{\partial \tau^2} + i\gamma P\psi = 0, \tag{5.23}$$

where $P = |\psi|^2 \approx |\psi_0|^2$.

Now assuming a small perturbation on the wave package of the form $\phi \approx \phi_0 + \epsilon(\xi, \tau)$, we obtain the following equation for the perturbation

$$\frac{\partial \epsilon}{\partial \xi} + I\beta_2 \frac{\partial^2 \epsilon}{\partial \tau^2} + i\gamma P(\epsilon + \epsilon^*) = 0, \tag{5.24}$$

whose solutions are plane waves satisfying the dispersion relation

$$k_m = \pm\sqrt{\beta_2^2\omega_m^4 + 2\gamma P\beta_2\omega_m^2}. \tag{5.25}$$

This dispersion relation and properties of the perturbation on the initial wave package strongly dependent on the sign of the term within the square root. When this quantity is positive, the wavenumber is real, resulting in simple oscillations around the unperturbed solution, which remains stable. On the other hand, when such quantity is negative, the wavenumber is imaginary, corresponding to exponential growth and thus to an instability. This example shows how perturbation to stable solution, whether they are coherent in nature or simply noise, can grown and eventually result in a strong excitation, such as Rogue Waves.

The simple models presented in this and the previous section illustrate two of the hypothesis behind the formation of *RW*s. Unfortunately, the studies on this topic are not conclusive and the real mechanism behind *RW* is still illusive, despite this being nowadays a very hot topic in nonlinear physics.

The lack in a good understanding of *RW*s can be justified by the difficulty in obtaining good and extensive experimental data. There is a big limitation in performing simulations for sufficiently large systems and including all the effects and phenomena that exists in

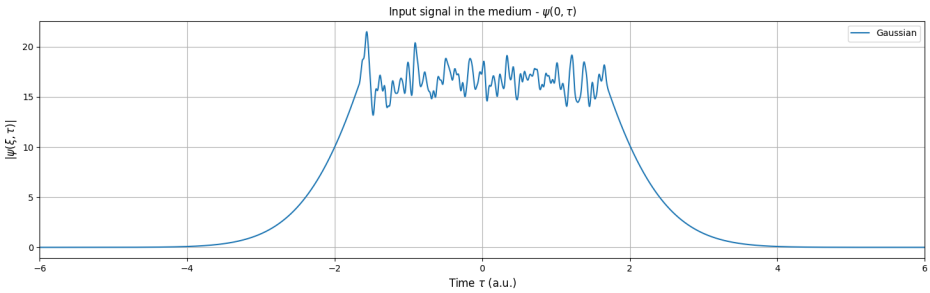

FIGURE 5.5: Profile of the input signal. The random generation is made with pseudo-random numerical generators following the Gaussian distribution from -1 to 1.

Nature, and that can be taking part in the generation of *RW*s. As described, these ingredients may include nonlinear processes but also dissipation and gain. Therefore, in the next section we present some numerical work that aims to clarify some aspects of *RW*.

5.4 Simulation of Rogue-Waves with the *CGLE*

The *CGLE* of equation (5.26) constitutes an ideal model to investigate the generation of RW in nonlinear dissipative systems.

$$i\partial_\tau\psi + (\zeta - i\beta)\,\partial^2_\xi\psi + (\alpha - i\gamma)\,\psi + (\eta - i\varepsilon)\,|\psi|^2\psi + (\nu - i\mu)\,|\psi|^4\psi = 0 \tag{5.26}$$

This equation incorporates both the gain and dissipation effects discussed in Chapter 4 with a different type of nonlinearity, namely a cubic-quintic nonlinearity that combines focusing and defocussing terms. Thus, it joins the conditions for the formation of *RW* described in the literature [84, 86] with the possibility of supporting both Bright and Dark Soliton-like excitations. Therefore, it can in principle support the type of nonlinear excitation described in section 5.1 that resemble qualitatively *RW*. This model can also support nonlinear interactions between waves that can result in the energy transference processes described in section 5.3, as well as, the constructive wave coincidence depicted in section 5.2.

The simulations consider a $(1+1)$-dimensional system where the initial conditions correspond to a central plateau that decays at the edges with an exponentially decaying dependency. On top of this signal we have added noise resulting in a final intensity profile illustrated in figure 5.5.

The parameters of the *CGLE* used correspond to $\zeta = -1.35$; $\nu = -2.00 \times 10^{-3}$, $\gamma = -8.00 \times 10^{-2}$; $\beta = 0.180$; $\varepsilon = 4.00 \times 10^{-2}$; $\mu = 2.50 \times 10^{-5}$ and lastly $\eta = 1.00$. The noise

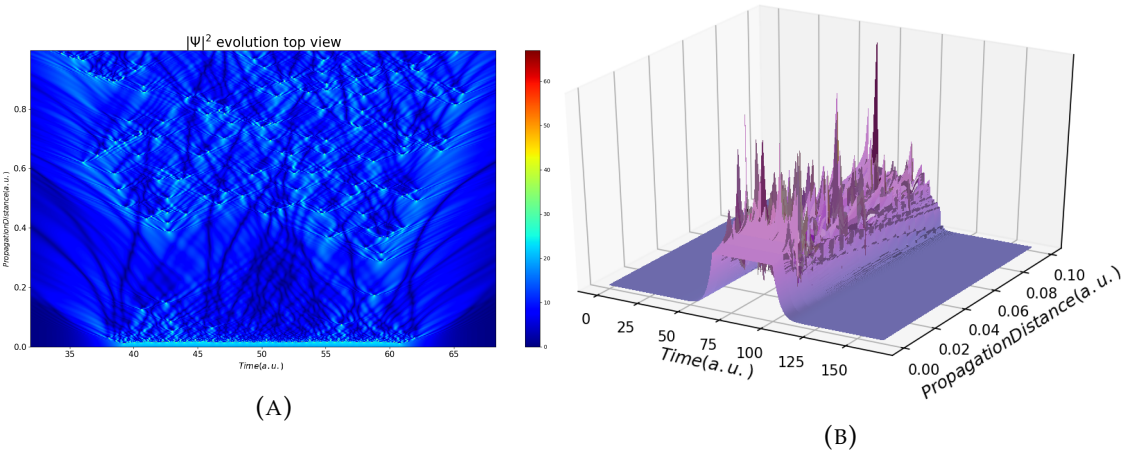

(A) (B)

FIGURE 5.6: *(A)* Output of the simulation using *GPGPU* Supercomputing developed solver for the indicated medium. We observe various spikes and changes in the direction of Dark Solitons. In *(B)* we present a 3D visualization of a typical outcome of simulations. Observe the well confinement of the solution to the designated pedestal section. There also is an higher activity generation of *RW* at the start than in the rest.

component of the initial conditions follow several distributions in order to investigate the impact of the noise in the generation of *RW*s. This attends the idea discussed in the literature that the amplitude fluctuations produced by the noise constitute the seed for the *RW* [13].

Another important aspect of the simulations is that the use of *GPGPU* Supercomputing allows to consider large systems with very thin resolution, in particular the simulations considered a discretization of the simulating domain into 2^{18}. This allows to simulate the generation of many *RW*s simultaneously with sufficient resolution to discriminate with much detail the structure of each *RW*.

The typical results of the simulation are shown in figure 5.6a and 5.6b, where it is possible to observe the generation of both spikes and depressions in the amplitude of the pedestal, that can be identified as Bright and Dark nonlinear excitations, similar to their Solitonic counterparts.

The hight resolution of the calculations provided by our *GPGPU* Supercomputing solver has another important advantage regarding the study of *RW*s dynamics. It allows us to execute such high zoom-in that we can evaluate individually each spike without losing information about the whole system (see figure 5.7).

There is a qualitative difference between the Dark and Bright excitations: while the dark excitations seem to exist and propagate for long times (on the order of the simulation itself), the Bright excitations are formed and disappear very fast, constituting the candidates for *RW*.

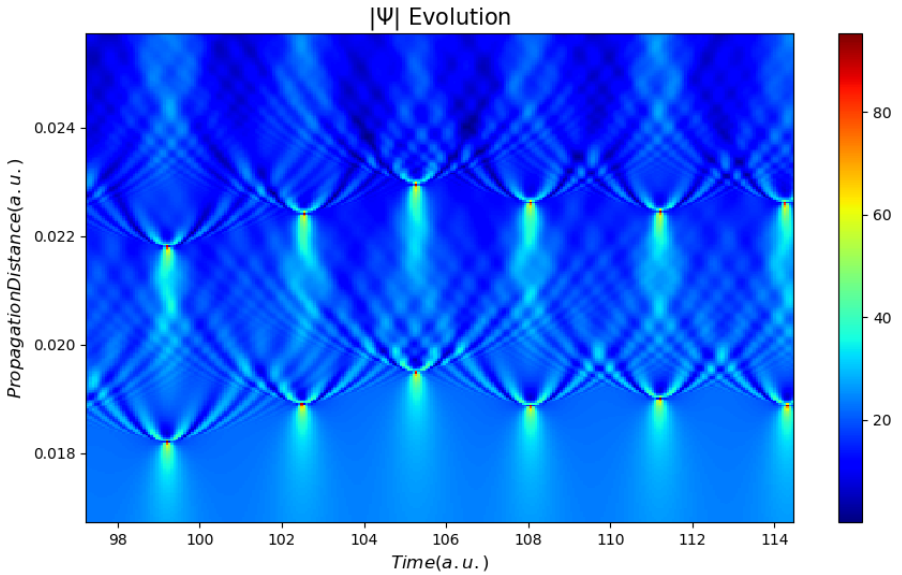

FIGURE 5.7: Representation of the detail obtained when we zoom-in to individually evaluate each formed spike This level of detail is possible because the high resolution provided by the *GPGPU* Supercomputing.

In the following section we will explore the dependency of RW on the initial noise and discuss how this is related to the mechanism of formation of RW discussed in previous sections.

5.5 Statistical Analysis of Rogue-Waves

In sections 5.1 to 5.4, we have discussed different candidate mechanisms for the generation of *RW*. In all of them it is assumed the preexistence of wave packages in the system that may work as seeds for *RW*. Whether these seeds are preexisting Solitons, and ideal gas of waves, or trains of waves coupled nonlinearly, we expect that the proprieties of these seed waves should in one way or another influence the nature and proprieties of the generated *RW*. Having this in mind, we propose the following numerical experiment, where we initialize the simulation with noise following different statistical distribution and investigate the difference in the number and amplitude of the *RW* generated (see figure 5.8).

In particular, we consider random noise that follows the Gaussian, Uniform, Lorentzian and Logistic Probability Distribution Function (*PDF*). For each *PDF* we generated 2600 initial conditions and performed the simulations. In this initial study, despite the noise being generated from different distributions, the level of noise (measured as a fraction of

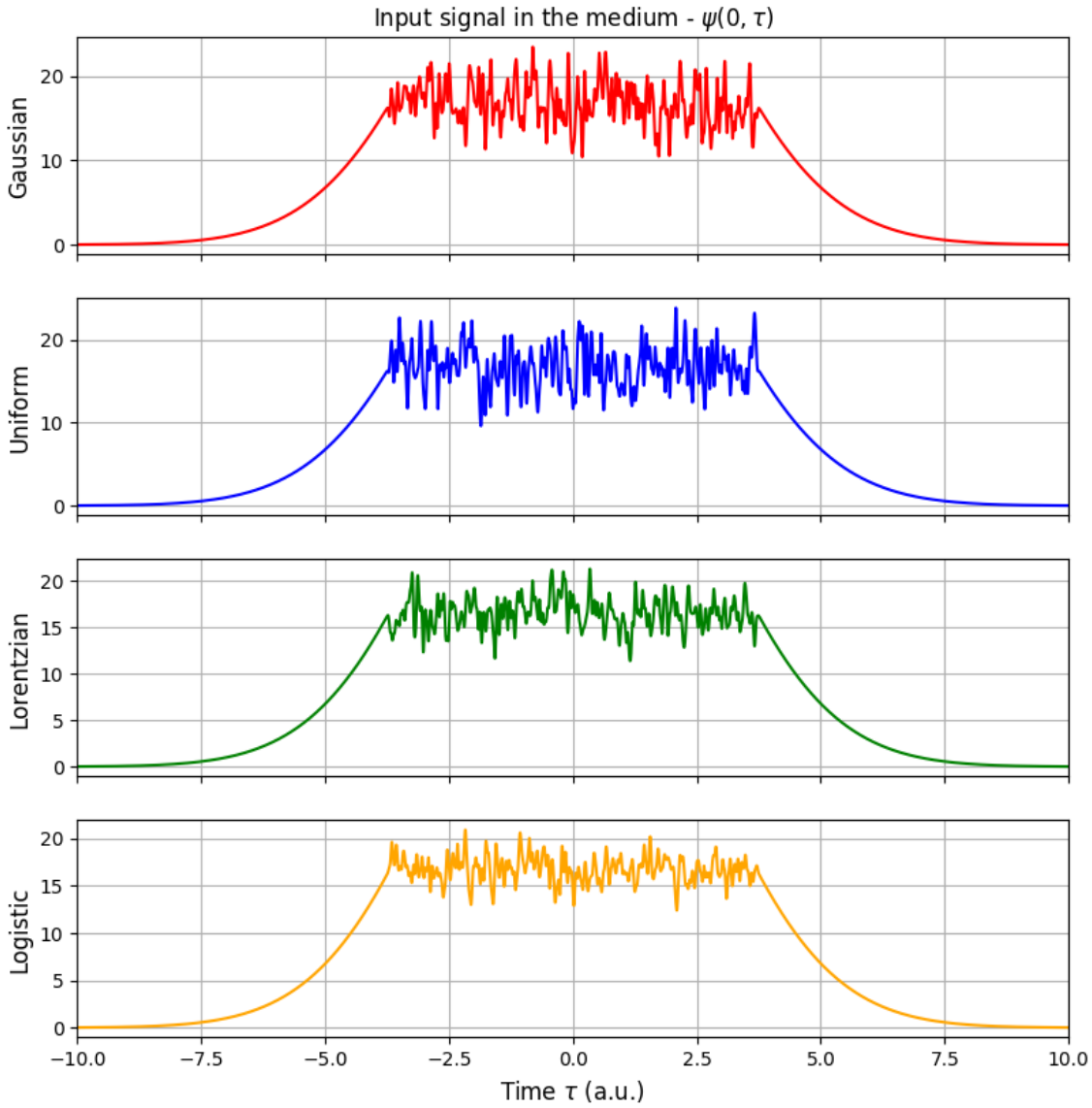

FIGURE 5.8: The different signals generated throughout Gaussian, Uniform, Lorentzian and Logistic probabilistic distributions. Due the noise nature of the simulations, different runs lead to different signals but we cannot visually distinguish between one another.

the amplitude of the pedestal) remains constant. In each simulation we used a *Python* script to detect the peak amplitudes and number of each Bright excitation (which are interpreted as *RW*) and from this computed the statistical proprieties of the *RW* population. In particular, each simulation resulted in about 28000 *RW* spikes and it was possible to calculate the statistical distribution corresponding to the frequency of occurrence of each *RW* amplitude, as shown in figure 5.9.

Remarkably, the peak amplitude distribution for each type of noise is very much alike. The mean peak amplitude for all cases is about 31.5, with variability of about 1%. This

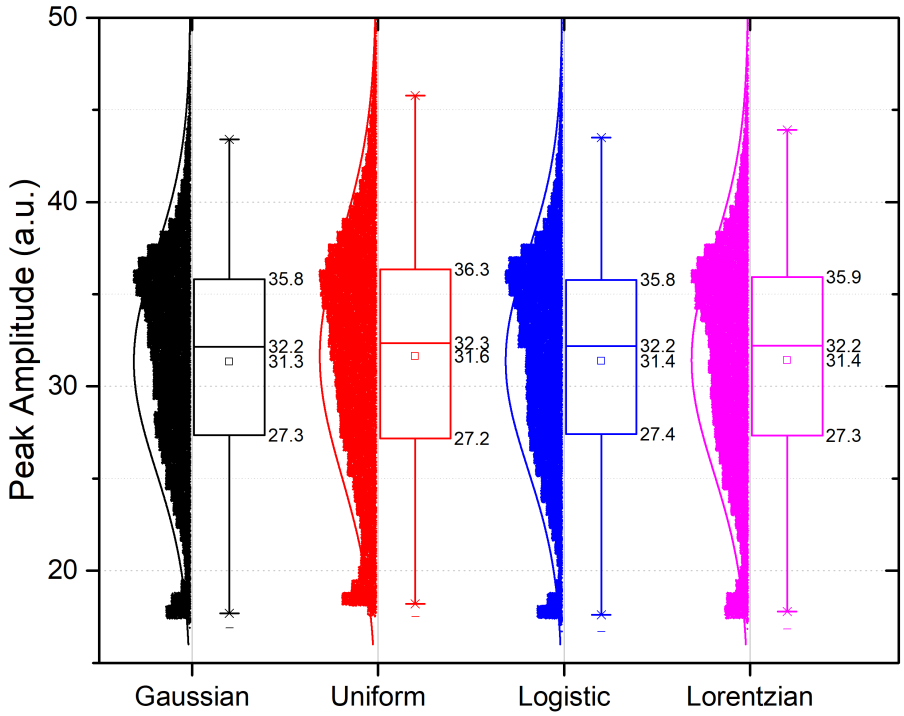

FIGURE 5.9: Statistical representation in the form of Box Plot of how the various distributions of the random noise added to a baseline affect the amplitude of *RW*. The datasets have around 28000 each.

raises the question of how can a noise generated by such a broad *PDF* band like the Uniform have the same outcome as the one generated by a narrow one such the Lorentzian? And even the behavior regarding the quartiles is strangely similar. This can even lead one to think that the initial conditions have no impact on the *RW*s proprieties. Caution is necessary when evaluating these results: the mathematical description explicitly shows that there is a very important dependence on the initial conditions, even with high-order nonlinear effects.

Despite these counterintuitive results, they do not demonstrate conclusively that *RW* do not depend on the initial conditions, but only that the asymptotic distribution of *RW* does not depend on the initial distribution of the noise. Therefore, in a second numerical experiment we explored the impact of the level or amplitude of the noise in the *RW*. In particular, we selected the Gaussian distribution to generate the noise and repeated a large number of simulations for each level of amplitude.

We expected the level of noise to have impact on the proprieties of the *RW* population, specially when it surpasses the limit of validity of the perturbative approach and we fall into the extreme regime of nonlinear optics and the results detach from the rest. However, and again, the results shown in figure 5.10 are surprising. First, we found no significant

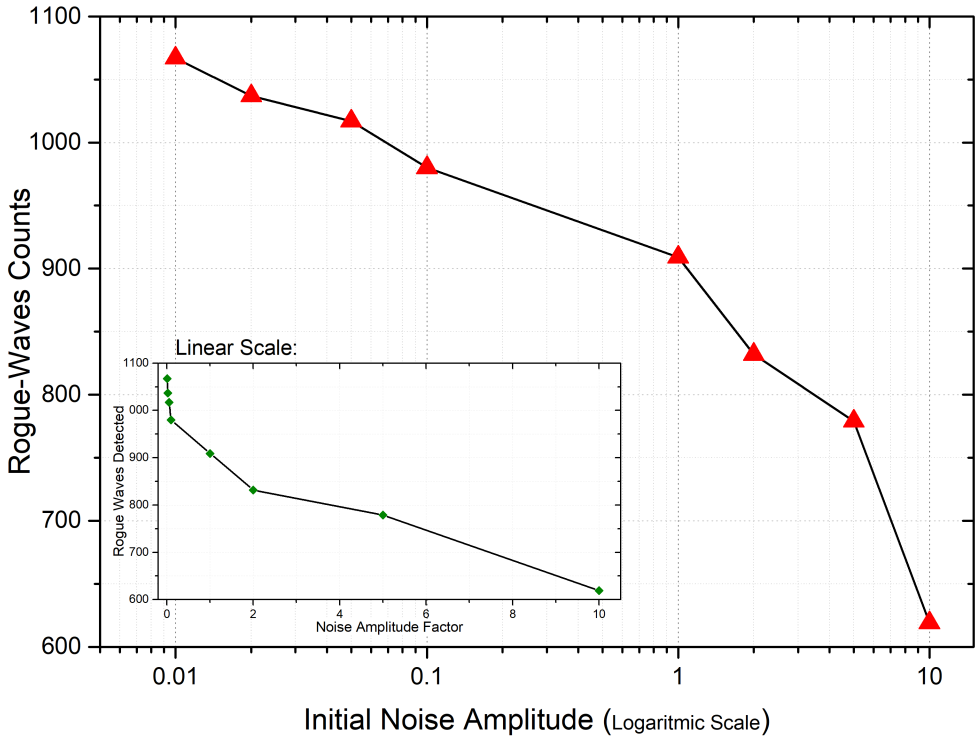

FIGURE 5.10: Graphical representation of the calculated results of the initial amplitude of the noise and the total number of spike *RW* identified over the same distance.

change in the amplitude of the spikes. But the most mysterious result was that the higher the level of noise the smaller was the number of *RW* detected. Indeed, figure 5.10 shows that the number of RW and the level of noise follows a negative power law. In other words, it seems that the noise has an inhibition effect on the *RW*.

These results are quite puzzling: they suggest that the relation between noise and RW is not trivial and that a special mechanism exists like in the case of extreme events and constructive coincidences discussed in section 5.2, the final distribution of RW does not depend on the initial statistics of noise, instead it seems determined by the dynamical mechanics or processes supported by the *CGLE*. Indeed, the asymptotic distribution of RW is none of the three predicted by the Theorem of Extreme Value, suggesting that RW are not the result of independent processes but rather from the combination of some interconnected players or excitations.

On the other hand, such excitations do not appear to be random noise initially introduced in the system. In fact, noise kills RW, suggesting that these excitations must have an inherit coherence between themselves, just like in the case of nonlinear coupling proposed in section 5.3 of of the Solitons described in section 5.1.

At the end of this study we are left with more questions than answers as often is the case in Science. Clearly much work must follow these counterintuitive results.

5.6 Conclusion

In conclusion, we started by describing the main Breathers that are solution of the *NLSE* and in some extent to the *CGLE*. These are very important since they provide insight on the subject of Breathers and we did evaluate how sensitive the equation is to its parameters and how it can change the overall proprieties of the breather. In nonlinear media we studied, again, the *CGLE* and proposed two interesting explanations of the phenomena. One related to the application of the Extreme Events Theorem to modeling systems that acquire Rogue-Waves and the other associated with the coherent coincidence of wave to interfere in a constructive fashion in a short period. A complete quantitative description of this behavior is still unexplained.

The performed simulations show that we can simulate how *RW* appear and behave in these media. The provided simulations are of great resolution and allows us to zoom in to an extent that we can evaluate the dynamics of the spike breaking after its maximum. We ended up intrigued with these spikes and how they are influenced by the input signal. Since we had at our hand a tool that allows very fast calculations we studied how the initial optical field influences the proprieties of *RW*, starting by changing the probabilistic distribution of the random profile on top of the pedestal and found that it has no significant impact neither in the amplitude of the *RW* nor in the number of *RW* that appear.

Driven by this curiosity of the dynamics of *RW* we evaluated if the random noise amplitude effects the long run proprieties. We sticked to the Gaussian random noise because it is one of the most found in nature. After thousands of simulations discovered that the noise initial amplitude has, in fact, an important consequence in the total number of *RW* identified. In the regime where the perturbative approach is valid we discovered a logarithmic dependence on the initial noise amplitude, with higher number of spikes with lower noise input, which is very counterintuitive.

Chapter 6

Conclusions

Over the course of this thesis we studied many important phenomena in Nonlinear Optics, from balanced Dissipative Soliton solutions in real open systems with dispersion and nonlinearities to descriptions that account for both gain and losses. We intended to study how the generation of both stable and unstable excitations propagates and evaluate its dynamics proprieties. With the vast literature available regarding Nonlinear Optics and open systems we were able to develop a numerical system to validate and evaluate the hardware proprieties.

Moreover, the process of improvement lead us to implement the Symmetric Split-Step Fourier Method in *GPGPU* Supercomputing in order to take advantage of Graphics Cards and their high core-counts. This solver is capable to calculate very complex operations, namely matrix multiplication and Fast Fourier Transforms. The supercomputing solver was written in *C++* using the *ArrayFire* library and is capable to simulate the propagation of $(1+1)$-dimensional optical pulse in a nonlinear system described by the *CGLE*. The main structure is based in an inner kernel that was optimized to performs calculations and the remaining non-kernel sections detached. This allows a great modularity to add/remove/work on parameters that describes the solution as well as to manipulate the Soliton stability condition factors. The benchmarks of the *GPGPU* Supercomputing solver reinforced what was predicted. Against single core operation, we obtained a *SpeedUp* of around 55 using a *GTX Titan* with *CUDA* framework by means of *ArrayFire*. When using mainstream desktop hardware we observed a good improvement, with 30 times less time required to simulate the propagation dynamics of an example physical nonlinear light-matter interaction system. Lower-end *GPGPU*s also provide a reduction of runtime, with

*SpeedUp*s lower than 10. In the case of CPU operation in multi-thread the improvement range of *GPGPU*s is reduced but we still achieved a maximum *SpeedUp* of 3.7.

We proceeded by studying of Dissipative Optical Solitons in atomic gases in a system with coherent pump-probe to manipulate the populations to the desired arrangement described by the Complex Cubic-Quintic Ginzburg-Landau Equation. Furthermore and with the *GPGPU* Supercomputing solver developed we used it to simulate open dissipative systems and evaluate how the before solutions behave in the presence of gain and losses. As expected we observe Solitons that were solutions of the Nonlinear Schrödinger Equation lose their validity and complex adjustments are required to regain balanced propagation. Next was studied stability conditions, namely the specific case where the background instability lead to the annihilation of the stable Solitonic solution.

Lastly we decided to study Rogue-Waves and their process with the statistical analysis. Such phenomena are important in Science (also beyond Physics, such as in Oceanography) and yet much is unknown. A complete quantitative description of this behavior is still unexplained. In this thesis we proposed the application of the Extreme Events Theorem to modeling systems that acquire Rogue-Waves by the Complex Cubic-Quintic Ginzburg-Landau Equation. We were able to observe Rogue-Waves formation in a nonlinear open system with very fine detail due the high resolution possible. We proceeded to study how the initial noise affects the propagation characteristics and dynamics of Rogue-Waves. This was possible because our *GPGPU* Supercomputing solver could construct large amounts of datasets necessary to arrive at trustworthy statistical results. We concluded that the Probabilistic Distribution Function of the random noise of the background has no significant effects on neither the proprieties nor the amount of Rogue-Waves generated. However, the amplitude input optical noise leads to a counterintuitive results, where we observe that the lower the noise the higher the number of Rogue-Waves observed. This suggests that none of the presented description models is capable to completely describe the phenomenon. The results seem to be a complex combination of proprieties of the various pulse shapes and breathers. This validates the fact that Rogue-Waves are a very complex and are yet a field with many unknown answers and equations.

The Complex Cubic-Quintic Ginzburg-Landau Equation is capable to provide a very large description of real nonlinear systems, with many types of nonlinearities, dispersion/diffraction, gain and losses. We used our *GPGPU* Supercomputing solver to trade complexity with an higher accuracy of solutions. In this thesis we crossed from stable

(Dissipative Solitons) to chaotic unstable (Rogue-Waves) open systems. For these reasons we conclude that the work of this thesis constitutes a good testbed to further develop/study the dynamical effects of both types of the presented Case Studies. Much work is still to be performed.

The resulting outputs of this thesis are:

- *1* submitted article in scientific journal;
- *1* inproceedings article in conference;
- *9* oral presentations, of which *3* as a speaker;
- *21* poster presentations, of which *5* as first author.

The author also attended *4* conferences, of which *2* were international.

6.1 Future Work

Nonlinear optical propagation is an area with enormous potential to provide alternatives to some optical systems that require maintenance, such as optical amplifiers: if the propagation with nonlinear optical fibers could be build in and applied, stable pulse signals could be provided in an unchanged light pulse that would arrive at the end without the need of an intermediate amplifier which allows faster communication speeds.

Another important application for our *GPGPU* Supercomputing solver is related with the recent expansion of Nonlinear Photonics and its potential applications in micro/nanofabrication. Simulate very complex systems to gain information about how it behaves when considering energy dissipation at specific wavelengths can provide new important insight. Nevertheless, this specific work would require more time and resources to understand advanced Nonlinear Photonics and programming equations or methods to *GPGPU* Supercomputing.

The continuous development of the *GPGPU* Supercomputing solver and its kernel to simulate $(2+1)$-dimensional nonlinear light propagation can provide very interesting studies in Vortex systems and $2D$ Soliton solutions. The ability to study these physical systems is very important and is slowly becoming a hot topic, mainly in what concerns Optical Vortexes.

Rogue-Waves were identified and statistical analysis was performed. However other types of proprieties of the noise can have interesting impact on the long run proprieties. This study is important to develop a stronger knowledge regarding Extreme Events. These are yet a very recent topic but laser cavities and Random Lasers systems can take advantage of more robust information. Also, the ability to simulate the propagation dynamics of a specific input signal provides interesting insight about the system. Nevertheless, scientific progress must be done first to latter open the doors for its world-impact [1]...

[1] Reminder: when Quantum Mechanics was born nobody could predict the impact it would take in transistor manufacturing and allow the construction of the *GPGPU* used to do these very complex simulations. Quantum Mechanics changed the world in a way that nobody could predict

Appendix A

From Maxwell Equations to the Wave Equation

The foundations of Classical Electromagnetism are well known and depicted by the famous Maxwell's Equations. In the form of partial differential equations and in the formulation of International System of Units (*SI*), they are presented as

$$\nabla \cdot \mathbf{E} = \frac{\rho}{\varepsilon_0} \tag{A.1a}$$

$$\nabla \cdot \mathbf{B} = 0 \tag{A.1b}$$

$$\nabla \times \mathbf{E} = -\frac{\partial \mathbf{B}}{\partial t} \tag{A.1c}$$

$$\nabla \times \mathbf{B} = \mu_0 \left(\mathbf{J} + \varepsilon_0 \frac{\partial \mathbf{E}}{\partial t} \right) \tag{A.1d}$$

Considering the Faraday's Law, we take the curl of both sides of the equation,

$$\nabla \times \nabla \times \mathbf{E} = -\nabla \times \frac{\partial \mathbf{B}}{\partial t}$$

which allows us to use the following vector identity

$$\nabla \times \nabla \times \mathbf{A} = \nabla \cdot (\nabla \cdot \mathbf{A}) - \nabla^2 \mathbf{A}$$

With this vectorial identity, we develop and use the Ampere-Maxwell Law $\nabla \times \mathbf{B} = \mu_0 \left(\mathbf{J} + \varepsilon_0 \frac{\partial \mathbf{E}}{\partial t} \right)$ to proceed

$$\nabla \cdot (\nabla \cdot \mathbf{E}) - \nabla^2 \mathbf{E} = -\nabla \times \tfrac{\partial \mathbf{B}}{\partial t} \tag{A.2a}$$

$$\nabla \cdot (\nabla \cdot \mathbf{E}) - \nabla^2 \mathbf{E} = -\tfrac{\partial}{\partial t} (\nabla \times \mathbf{B}) \tag{A.2b}$$

$$\nabla \cdot (\nabla \cdot \mathbf{E}) - \nabla^2 \mathbf{E} = -\varepsilon \tfrac{\partial}{\partial t} \left(\mathbf{J} + \mu \tfrac{\partial \mathbf{E}}{\partial t} \right) \tag{A.2c}$$

We now assume that the current density $\mathbf{J}$ is equal to zero for all times, meaning that there is no allocation or generation of electrical charges in our time treatment. This transforms the previous equation to

$$\nabla \cdot (\nabla \cdot \mathbf{E}) - \nabla^2 \mathbf{E} = -\varepsilon \mu \frac{\partial^2 \mathbf{E}}{\partial t^2}$$

This is an important point to consider. Since we assumed that there are no charges variations, the net electric charge is zero ($\nabla \cdot \mathbf{E} = \frac{\rho}{\varepsilon_0} \to 0$). And so the divergence of a non-vectorial non-changing quantity is zero.

Knowing that the product $\mu\varepsilon$ gives the inverse squared speed velocity $1/c^2$,

$$\nabla^2 \mathbf{E} = \mu \varepsilon \frac{\partial^2 \mathbf{E}}{\partial t^2} \tag{A.3a}$$

$$\nabla^2 \mathbf{E} = \frac{1}{c^2} \frac{\partial^2 \mathbf{E}}{\partial t^2} \tag{A.3b}$$

The final result - equation A.3b - is the well known Wave Equation. This outcome is important for numerous reasons, such that this developed directly from Maxwell's Equation by assuming common physical scenarios and so it is very general and with little loss of generality. But more importantly, it assures us that a wave description of Classical Electromagnetism (and Optics) is present from the very nature of the primordial equations A.1.

In the context of this thesis, we worked with nonmetallic materials, so that we have ($\varepsilon_r > 1$ and $\mu = 1$). Also, if we assume that the medium has a polarization response to some applied electric field, an extra second order temporal differentiation appears, resulting in the following mathematical description.

$$\nabla^2 \mathbf{E} - \frac{1}{c^2} \frac{\partial^2 \mathbf{E}}{\partial t^2} = \frac{1}{\varepsilon_0 c^2} \frac{\partial^2 \mathbf{P}}{\partial t^2}$$

Bibliography

[1] G. New, *Introduction to nonlinear optics* (Cambridge University Press, 2011).

[2] W. L. Kath, *Making waves: solitons and their optical applications*, Siam News (1998).

[3] S. Trillo and W. Torruellas, *Spatial solitons*, Vol. 82 (Springer, 2013).

[4] D. Peregrine, *Water waves, nonlinear Schrödinger equations and their solutions*, The ANZIAM Journal **25**, 16 (1983).

[5] E. Lucas, M. Karpov, H. Guo, M. Gorodetsky, and T. Kippenberg, *Breathing dissipative solitons in optical microresonators*, Nature communications **8**, 736 (2017).

[6] A. H. Safavi-Naeini, T. M. Alegre, J. Chan, M. Eichenfield, *et al.*, *Electromagnetically induced transparency and slow light with optomechanics*, Nature **472**, 69 (2011).

[7] P. Grelu and N. Akhmediev, *Dissipative solitons for mode-locked lasers*, Nature Photonics **6**, 84 (2012).

[8] M. J. Ablowitz, M. Ablowitz, P. Clarkson, and P. A. Clarkson, *Solitons, nonlinear evolution equations and inverse scattering*, Vol. 149 (Cambridge university press, 1991).

[9] A. Maimistov, *Evolution of solitary waves which are approximately solitons of a nonlinear Schrödinger equation*, Soviet Journal of Experimental and Theoretical Physics **77**, 727 (1993).

[10] E. Falcão-Filho, C. B. de Araújo, and J. Rodrigues Jr, *High-order nonlinearities of aqueous colloids containing silver nanoparticles*, JOSA B **24**, 2948 (2007).

[11] J. Soto-Crespo, N. Akhmediev, V. Afanasjev, and S. Wabnitz, *Pulse solutions of the cubic-quintic complex Ginzburg-Landau equation in the case of normal dispersion*, Physical Review E **55**, 4783 (1997).

[12] A. Hasegawa and Y. Kodama, *Solitons in optical communications*, 7 (Oxford University Press, USA, 1995).

[13] J. M. Dudley, F. Dias, M. Erkintalo, and G. Genty, *Instabilities, breathers and rogue waves in optics*, Nature Photonics **8**, 755 (2014).

[14] N. Akhmediev, J. M. Dudley, D. Solli, and S. Turitsyn, *Recent progress in investigating optical rogue waves*, Journal of Optics **15**, 060201 (2013).

[15] D. Solli, C. Ropers, P. Koonath, and B. Jalali, *Optical rogue waves*, Nature **450**, 1054 (2007).

[16] N. Veretenov and M. Tlidi, *Dissipative light bullets in an optical parametric oscillator*, Physical Review A **80**, 023822 (2009).

[17] J. Borhanian, *Dissipative ion-acoustic solitary and shock waves in a plasma with superthermal electrons*, Plasma Physics and Controlled Fusion **55**, 105012 (2013).

[18] V. Skarka and N. Aleksić, *Stability criterion for dissipative soliton solutions of the one-, two-, and three-dimensional complex cubic-quintic Ginzburg-Landau equations*, Physical review letters **96**, 013903 (2006).

[19] G. B. Lemos, R. M. Gomes, S. P. Walborn, P. H. S. Ribeiro, and F. Toscano, *Experimental observation of quantum chaos in a beam of light*, Nature communications **3**, 1211 (2012).

[20] F. Baronio, B. Frisquet, S. Chen, G. Millot, S. Wabnitz, and B. Kibler, *Observation of a group of dark rogue waves in a telecommunication optical fiber*, Physical Review A **97**, 013852 (2018).

[21] W. Chang, J. M. Soto-Crespo, P. Vouzas, and N. Akhmediev, *Spiny solitons and noise-like pulses*, JOSA B **32**, 1377 (2015).

[22] T. H. Maiman *et al.*, *Stimulated optical radiation in ruby*, (1960).

[23] R. W. Boyd, *Nonlinear optics* (Elsevier, 2003).

[24] N. Akhmediev, J. M. Soto-Crespo, and P. Grelu, *Roadmap to ultra-short record high-energy pulses out of laser oscillators*, Physics Letters A **372**, 3124 (2008).

[25] e. P. Franken, A. E. Hill, C. e. Peters, and G. Weinreich, *Generation of optical harmonics*, Physical Review Letters **7**, 118 (1961).

[26] T. Higo, H. Man, D. B. Gopman, L. Wu, *et al.*, *Large magneto-optical Kerr effect and imaging of magnetic octupole domains in an antiferromagnetic metal*, Nature photonics **12**, 73 (2018).

[27] A. Rybin, I. Vadeiko, and A. Bishop, *Theory of slow-light solitons*, Physical Review E **72**, 026613 (2005).

[28] M. Fox, *Optical properties of solids. Oxford master series in condensed matter physics*, Oxf. Univ. Press NY , 305 (2001).

[29] T. D. Ferreira, N. A. Silva, and A. Guerreiro, *Superfluidity of light in nematic liquid crystals*, Physical Review A **98**, 023825 (2018).

[30] N. M. A. Silva, *GASE: a high performance solver for the Generalized Nonlinear Schrödinger equation based on heterogeneous computing*, (2013).

[31] G. Agrawal, *Applications of nonlinear fiber optics* (Academic press, 2001).

[32] Y. S. Kivshar and G. Agrawal, *Optical solitons: from fibers to photonic crystals* (Academic press, 2003).

[33] E. Hecht, *Optics* (Pearson Education, 2016).

[34] M. Born, E. Wolf, A. B. Bhatia, *et al.*, *Principles of optics: electromagnetic theory of propagation, interference and diffraction of light*, Vol. 7 (Cambridge university press Cambridge, 1999).

[35] V. E. Zakharov, in *Solitons* (Springer, 1980) pp. 243–285.

[36] J. R. Ray and J. L. Reid, *Noether's theorem, time-dependent invariants and nonlinear equations of motion*, Journal of Mathematical Physics **20**, 2054 (1979).

[37] A. Ankiewicz and N. Akhmediev, *Dissipative Solitons: From Optics to Biology and Medicine* (Springer, 2008).

[38] N. J. Zabusky and M. D. Kruskal, *Interaction of" solitons" in a collisionless plasma and the recurrence of initial states*, Physical review letters **15**, 240 (1965).

[39] J. S. Russell, in *14th meeting of the British Association for the Advancement of Science*, Vol. 311 (1844) p. 1844.

[40] J. R. Taylor, *Optical solitons: theory and experiment*, Vol. 10 (Cambridge University Press, 1992).

[41] P. G. Drazin and R. S. Johnson, *Solitons: an introduction*, Vol. 2 (Cambridge university press, 1989).

[42] C. Gu, *Soliton theory and its applications* (Springer Science & Business Media, 2013).

[43] N. N. Akhmediev and A. Ankiewicz, *Solitons: nonlinear pulses and beams* (Chapman & Hall, 1997).

[44] T. Miwa, M. Jimbo, and E. Date, "Mathematics of solitons," (1999).

[45] A. Boardman, P. Bontemps, T. Koutoupes, and K. Xie, in *Beam Shaping and Control with Nonlinear Optics* (Springer, 2002) pp. 183–228.

[46] C. Dorrer, *Chromatic dispersion characterization by direct instantaneous frequency measurement*, Optics letters **29**, 204 (2004).

[47] D. Payne and A. Hartog, *Determination of the wavelength of zero material dispersion in optical fibres by pulse-delay measurements*, Electronics Letters **13**, 627 (1977).

[48] W. Liang-Liang, Q. Cun, D. Chao-Qing, and Z. Jiefang, *Analytical soliton solutions for the general nonlinear Schrödinger equation including linear and nonlinear gain (loss) with varying coefficients*, Optics Communications **283**, 4372 (2010).

[49] L.-G. Huang, L.-H. Pang, P. Wong, Y.-Q. Li, S.-Y. Bai, M. Lei, and W.-J. Liu, *Analytic soliton solutions of cubic-quintic Ginzburg-Landau equation with variable nonlinearity and spectral filtering in fiber lasers*, Annalen der Physik **528**, 493 (2016).

[50] M. Scalora, M. S. Syrchin, N. Akozbek, E. Y. Poliakov, *et al.*, *Generalized nonlinear Schrödinger equation for dispersive susceptibility and permeability: application to negative index materials*, Physical review letters **95**, 013902 (2005).

[51] Y. Zhang, H.-x. Xu, C.-z. Yao, and X.-n. Cai, *A class of exact solutions of the generalized nonlinear Schrödinger equation*, Reports on Mathematical Physics **63**, 427 (2009).

[52] D. Jia, J. Chen, Y. Yan, H. Zhang, T. Liu, and Y. Zhang, *A self-healing evaluation model for dedicated protection optical fiber sensor networks using All-terminal reliability function*, Optical Fiber Technology **39**, 49 (2017).

[53] J. He, Z. Zhou, and J. Ou, in *OFS2012 22nd International Conference on Optical Fiber Sensors*, Vol. 8421 (International Society for Optics and Photonics, 2012) p. 8421BH.

[54] R. Chiao, *RY Chiao, E. Garmire, and CH Townes, Phys. Rev. Lett. 13, 479 (1964).*, Phys. Rev. Lett. **13**, 479 (1964).

[55] T. J. Buckholtz, *Models for physics of the very small and very large* (Springer, 2016).

[56] G. Malpuech and D. Solnyshkov, *Bose Einstein condensation and superfluidity in an open system: theory*, arXiv preprint arXiv:0911.0807 (2009).

[57] G.-J. Lee, in *Applications of High-Tc Superconductivity* (InTech, 2011).

[58] Y. S. Kivshar and B. A. Malomed, *Dynamics of solitons in nearly integrable systems*, Reviews of Modern Physics **61**, 763 (1989).

[59] T. A. Nguyen, *Intel to AMD: Your x86 License Expires in 60 Days*, tom's HARDWARE (2009).

[60] P. Schmid, *The New Generation Is Here: Celeron 2.0 GHz, with 0.13 um*, tom's HARDWARE (2002).

[61] ReliaSoft, "Single-thread vs. multi-thread," (2017).

[62] M. D. Hill and M. R. Marty, *Amdahl's law in the multicore era*, Computer **41** (2008).

[63] V. M. Pérez-Garcıa and X.-y. Liu, *Numerical methods for the simulation of trapped nonlinear Schrödinger systems*, Applied Mathematics and Computation **144**, 215 (2003).

[64] R. M. Caplan, *Study of vortex ring dynamics in the nonlinear Schrödinger equation utilizing GPU-accelerated high-order compact numerical integrators*, (2012).

[65] C. S. Gardner, J. M. Greene, M. D. Kruskal, and R. M. Miura, *Method for solving the Korteweg-deVries equation*, Physical review letters **19**, 1095 (1967).

[66] D. Novoa, B. A. Malomed, H. Michinel, and V. M. Perez-Garcia, *Supersolitons: solitonic excitations in atomic soliton chains*, Physical review letters **101**, 144101 (2008).

[67] D. Goldman and L. Sirovich, *A novel method for simulating the complex Ginzburg-Landau equation*, Quarterly of applied mathematics **53**, 315 (1995).

[68] C. Liu, Y. Y. Li, M. Gao, Z. Wang, Z. Dai, and C. Wang, *Rogue wave solutions of the nonlinear Schrödinger equation with variable coefficients*, Pramana **85**, 1063 (2015).

[69] V. Ginzburg, *Superconductivity and superfluidity (what is done and what is not done)*, Uspekhi Fizicheskikh Nauk **167**, 429 (1997).

[70] I. S. Aranson and L. Kramer, *The world of the complex Ginzburg-Landau equation*, Reviews of Modern Physics **74**, 99 (2002).

[71] M. Facão, S. Rodrigues, and M. I. Carvalho, *Temporal dissipative solitons in a three-level atomic medium confined in a photonic-band-gap fiber*, Physical Review A **91**, 013828 (2015).

[72] S. L. McCall and E. L. Hahn, *Self-induced transparency by pulsed coherent light*, Physical Review Letters **18**, 908 (1967).

[73] A. Biswas, *Temporal 1-soliton solution of the complex Ginzburg-Landau equation with power law nonlinearity*, Progress in Electromagnetics Research **96**, 1 (2009).

[74] N. Akhmediev and A. Ankiewicz, in *Dissipative solitons* (Springer, 2005) pp. 1–17.

[75] N. A. Silva, *Slow-light dissipative solitons in an atomic medium in a waveguide assisted by an incoherent pumping feld*, Physical Review A .

[76] J. P. C. Costa, *Development of a solver of the Maxwell-Bloch equations with GPGPUs*, (2017).

[77] G. Huang, L. Deng, and M. Payne, *Dynamics of ultraslow optical solitons in a cold three-state atomic system*, Physical Review E **72**, 016617 (2005).

[78] N. R. Pereira, *NONLINER SCHRODINGER EQUATION INCLUDING GROWTH AND DAMPING*, (1977).

[79] N. Akhmediev, V. Afanasjev, and J. Soto-Crespo, *Singularities and special soliton solutions of the cubic-quintic complex Ginzburg-Landau equation*, Physical Review E **53**, 1190 (1996).

[80] H. A. Haus and W. S. Wong, *Solitons in optical communications*, Reviews of modern physics **68**, 423 (1996).

[81] J. R. Apel, J. R. Holbrook, A. K. Liu, and J. J. Tsai, *The Sulu Sea internal soliton experiment*, Journal of Physical Oceanography **15**, 1625 (1985).

[82] A. Mathis, L. Froehly, S. Toenger, F. Dias, G. Genty, and J. M. Dudley, *Caustics and rogue waves in an optical sea*, Scientific reports **5**, 12822 (2015).

[83] C. Fochesato, S. Grilli, and F. Dias, *Numerical modeling of extreme rogue waves generated by directional energy focusing*, Wave Motion **44**, 395 (2007).

[84] J. M. Dudley, G. Genty, F. Dias, B. Kibler, and N. Akhmediev, *Modulation instability, Akhmediev Breathers and continuous wave supercontinuum generation*, Optics express **17**, 21497 (2009).

[85] N. Akhmediev and V. Korneev, *Modulation instability and periodic solutions of the nonlinear Schrödinger equation*, Theoretical and Mathematical Physics **69**, 1089 (1986).

[86] F. Baronio, M. Conforti, A. Degasperis, S. Lombardo, M. Onorato, and S. Wabnitz, *Vector rogue waves and baseband modulation instability in the defocusing regime*, Physical review letters **113**, 034101 (2014).

[87] C. Conti, M. Peccianti, and G. Assanto, *Spatial solitons and modulational instability in the presence of large birefringence: The case of highly nonlocal liquid crystals*, Physical Review E **72**, 066614 (2005).

[88] B. Kibler, J. Fatome, C. Finot, G. Millot, *et al.*, *The Peregrine soliton in nonlinear fibre optics*, Nature Physics **6**, 790 (2010).

[89] B. Kibler, J. Fatome, C. Finot, G. Millot, *et al.*, *Observation of Kuznetsov-Ma soliton dynamics in optical fibre*, Scientific reports **2**, 463 (2012).

[90] L.-C. Zhao, L. Ling, and Z.-Y. Yang, *Mechanism of Kuznetsov-Ma breathers*, Physical Review E **97**, 022218 (2018).

[91] Z.-D. Li, X. Wu, Q.-Y. Li, and P. He, *Kuznetsov–Ma soliton and Akhmediev breather of higher-order nonlinear Schrödinger equation*, Chinese Physics B **25**, 010507 (2015).

[92] A. Chowdury, D. Kedziora, A. Ankiewicz, and N. Akhmediev, *Breather solutions of the integrable quintic nonlinear Schrödinger equation and their interactions*, Physical Review E **91**, 022919 (2015).

[93] R. Radhakrishnan and M. Lakshmanan, *Bright and dark soliton solutions to coupled nonlinear Schrodinger equations*, Journal of Physics A: Mathematical and General **28**, 2683 (1995).

[94] D. Kaup and B. Malomed, *Soliton trapping and daughter waves in the Manakov model*, Physical Review A **48**, 599 (1993).

[95] D. S. Wiersma, *The physics and applications of random lasers*, Nature physics **4**, 359 (2008).

[96] E. Heller, M. Crommie, C. Lutz, and D. Eigler, *Scattering and absorption of surface electron waves in quantum corrals*, Nature **369**, 464 (1994).

[97] K. B. Dysthe, *Modelling a" Rogue Wave"-Speculations or a realistic possibility*, Rogues Waves 2000 , 255 (2001).

[98] M. Christou and K. Ewans, *Field measurements of rogue water waves*, Journal of Physical Oceanography **44**, 2317 (2014).

[99] Y. Bensalah *et al.*, *Steps in applying extreme value theory to finance: a review* (Citeseer, 2000).

[100] E. C. Pinheiro and S. L. Ferrari, *A comparative review of generalizations of the Gumbel extreme value distribution with an application to wind speed data*, Journal of Statistical Computation and Simulation **86**, 2241 (2016).

[101] C. J. Tablada and G. M. Cordeiro, *The modified Fréchet distribution and its properties*, Communications in Statistics-Theory and Methods **46**, 10617 (2017).

[102] S. J. Almalki and S. Nadarajah, *Modifications of the Weibull distribution: a review*, Reliability Engineering & System Safety **124**, 32 (2014).

[103] E. Castillo, *Extreme value theory in engineering* (Elsevier, 2012).